NTNU – Trondheim
Norwegian University of
Science and Technology

Compression Capacity of Timber Sills Loaded Perpendicular to the Grain

Ultimate Limit State (ULS) and Serviceability
Limit State (SLS)

Joakim Brendjord Troller

Civil and Environmental Engineering
Submission date: June 2014
Supervisor: Kjell A Malo, KT

Norwegian University of Science and Technology
Department of Structural Engineering

Department of Structural Engineering
Faculty of Engineering Science and Technology
NTNU- Norwegian University of Science and Technology

ACCESSIBILITY

OPEN

MASTER THESIS 2014

SUBJECT AREA:	DATE ISSUED:	NO. OF PAGES:
TIMBER ENGENEERING	14 JANUARY 2014	4 + 14 + 129

TITLE:

Compression Capacity of Timber Sills Loaded Perpendicular to the Grain
Ultimate Limit State (ULS) and Serviceability Limit State (SLS)

BY:

Joakim Brendjord Troller

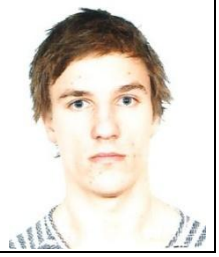

SUMMARY:

The purpose of this thesis is to derive a new model to calculate the compression capacity of timber loaded perpendicular to the grain in Ultimate Limit State (ULS). The different parameters included in the capacity formulas, were found/discovered through various compression tests conducted at the Department of Structural Engineering (KT) during the spring of 2014. Some of the parameters have been determined directly from data collected from the compression machine, while others required the usage of optical measuring techniques.

Two different models for calculation the compression capacity perpendicular to the grain were derived in this thesis. The first model is based on the strain field generated in the wood, and the second on the total energy required to reach a defined fracture criterion.

The two models give some variation in the carrying capacity, compared to the values calculated with the current regulations in Eurocode 5 part 1-1. For smaller loading lengths the current regulations gives a capacity that is quite high, compared to the new models derived in this thesis. This is because the current model has rules that allows the applied load to be distributed over an effective area, which can lead to a carrying surface that is twice the size of the actual loading surface. When the loading length increases, the new models will stabilize towards values of the capacity that is similar or larger to the ones found with the current regulations.

A model has also been derived for calculating in Serviceability Limit State (SLS), which provides the opportunity to determine the desired deformations in a connection based on our own preferences.

SUPERVISOR: Kjell Arne Malo
CARRIED OUT AT: Department of Structural Engineering, NTNU

NORWEGIAN UNIVERSITY OF SCIENCE AND TECHNOLOGY
DEPARTMENT OF STRUCTURAL ENGINEERING

MASTER THESIS 2014

for

Joakim Brendjord Troller

Compression Capacity of Timber Loaded Perpendicular to the Grain

(Modell for trykkbelastning normalt på fiberretning)

Eurocode 5 has a model for calculating the compression capacity of timber loaded perpendicular to the grain. This should be controlled in Ultimate Limit State (ULS), and the rules imply that the traditional building methods here in Norway do not have satisfactory strength. This in spite of almost no records of damages or problems with compression perpendicular to the grain in the millions of connections made in the traditional way. It is therefore a reason to believe that the calculation methods in Eurocode 5, are not satisfactory for these types of connections. A large database with results from research conducted over the years is available, but it lacks a consistent and accurate capacity model for this type of loading. The task is to develop a method or a foundation for a new capacity model.

The candidate may agree with supervisors to pay particular attention to specific parts of the investigation, or to include other aspects than those already mentioned.

The thesis is to be organized as a research report, recognizing the guidelines provided by the Department of Structural Engineering.

Supervisor: Kjell Arne Malo

This report is to be handed in no later than 10 June 2014

Preface

This is a master thesis written as a final paper for a 5-year study to become a Civil Engineer at the Norwegian University of Science and Technology (NTNU). The paper was written during the spring of 2014, on behalf of the Department of Structural Engineering (KT), and suggested by Kjell Arne Malo, a professor at the university.

The main purpose of the thesis is to derive new calculation models that will give more accurate results compared to the ones calculated with the current regulations. This will be done by analysing existing method, do own assumptions and verify different approaches by conducting laboratory tests. All tests were conducted at the Department of Structural Engineering during the spring of 2014, from the period of March to April. At the department all the needed equipment, software and test material was available.

I would like to thank Kjell Arne Malo for his help and guidance during the period working with this thesis. His expertise in the field of material properties of timber has been a great help in my research to create a new calculation model.

I would also like to thank Paal Rike, Chief Engineer at the Department of Structural Engineering, for helping with the execution of the laboratory tests, as well as guidance in the usage of the analysis software.

Trondheim, June 2, 2014

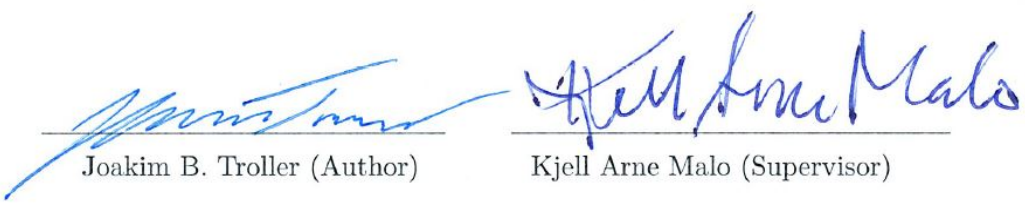

Joakim B. Troller (Author) Kjell Arne Malo (Supervisor)

Introduction

With the current model defined in Eurocode 5, used to calculate the bearing capacity of timber loaded in compression perpendicular to the grain, the traditional Norwegian building method does not satisfy the requirements. It has not been registered major problems or faults with these types of connections, and it is therefore a reason to believe that the current rules are not satisfactory when it comes to this type of connections.

The current method used to calculate the capacity of the timber, does not in a satisfactory way separate between configurations and geometrical differences. This leads to a model that in some cases describes the behaviour and capacity in an accurate way, but other times gives very conservative results. With the current regulations given in Eurocode 5, there are not many parameters that can be changed to account for these effects, and this may be the reason why the rules do not comply with what is found to be satisfying building methods here in Norway.

When a material is loaded in compression perpendicular to the grain, a natural way to define the capacity is to choose limitations of the deformation underneath the loading area. It is not desirable to get deformations in the range where the system gets unstable, with askew and damaged components. It is therefore necessary to define complying rules that prevent these types of effects. With the current regulations, there are not clearly defined calculation methods that separates Serviceability Limit State (SLS) and Ultimate Limit State (ULS). These are two different concepts that should be treated separately, not mixed into one calculation model, the way it is given in the Eurocode. What is defined as unfortunate deformations, varies from person to person, and will depend on the location of the connection. A farm owner will most likely allow a greater deformation in his barn, that he would do in his own house, and rules and calculation methods should therefore be defined that take individual circumstances into consideration.

The main purpose of this study, is to develop new models to calculate the compression capacity of sills loaded perpendicular to the grain. The study aims to further our understanding of the different effects contributing to the total bearing strength, and to get an overview of the material behaviour with this type of loading. Much study has been conducted in this field, but a more accurate and suitable model that takes different system configurations into account, should be derived. It is also a goal to develop separate calculation methods for Serviceability Limit State and Ultimate Limit State.

Abstract

This study will introduce two new models for calculating the compression capacity of wood loaded perpendicular to the grain. In the first model (Model 1), the different mechanical phenomena that are decisive for the total bearing capacity are modelled separately, by introducing an additional parameter to the ordinary compressive strength based on a mathematical model and equilibrium considerations. The second model (Model 2) is a purely empirical formula, where different generated factors are multiplied with the pure compressive strength to account for the capacity increase for various load situations and cross-sectional geometries. It is mainly the amount/length of untouched timber on the side of the loading area, that is decisive for the magnitude of the additional capacities, and in the last model this will be included by adding a factor k_1, which is found on the basis of energy considerations. In the first model, this is taken into account by an additional part, $f_{H,90}$. This factor is based on equilibrium considerations of a *rope system*, where the increase in capacity is based on strain concentrations generated on the side of the loading area.

Some disadvantages with the existing calculation model given in Eurocode 5 part 1-1, is that the capacity changes heavily dependent on the choice of loading configuration. For smaller loading lengths the compression capacity will become quite high, as a result of the definition of the permitted distribution of the applied load in the wood. As the length increases, the formula gives increasingly conservative results.

In the model based on energy (Model 2), the additional capacity from the load distribution in the wood is taken directly into the energy calculations. This obviates the need to account for an effective loading area in the capacity calculations, the way it is done with the current regulations. The model based on strains (Model 1), uses the same definition of the increased loading length as given in Eurocode 5, but the carrying capacity is regulated by additional parameters, which has conditions and factors implemented in the formula that takes the variation in load lengths into account. This will make the new calculation models stabilize towards values of the capacity that are somewhat lower for smaller loading lengths than the Eurocode 5 gives (approximately 25 % less for a loading length equal to 50 mm).

As the loading length increases (loading length equal to 90 mm), the total contribution that the current calculation model will get from the load being distributed over an effective area will be less significant. This will make Model 2 stabilize towards capabilities that are identical to the ones found with current regulations. Model 1 will take values that are 17% higher. By

increasing the loading length further (loading length equal to 150 mm), Model 2 provides higher capacities (approximately 16 %), while Model 1 will for smaller sill lengths get higher values, but stabilize at a capacity slightly lower than that the ones found with Eurocode 5.

By looking at the durability and strength of the new calculation models through constructed examples, the model based on energy (Model 2) provides more stable results than Model 1. The additional factor that accounts for the increase in capacity for different load situations and cross-sectional geometries in Model 1, is based on equilibrium in a *rope system* where the various parameters in the model are found by looking at the generated strain field in the wood. There are more uncertainties when it comes to the derivation of the parameters and validity of modelling the additional capacity in this way, compared to energy assumptions in Model 2. The empirical factors found through calculation of the total energy needed to get a certain deformation underneath the loading area in Model 2, are taken directly from the material behaviour, which provides more reliable and accurate results.

From the tests conducted in this study, we see a tendency for the rules determine the compressive strength to be quite conservative compared to what the material actually tolerates. The current regulations permits a plastic deformation of 1% (0.01h) of the height of a reference block with a fully loaded top surface. The curves describing the material behaviour found in this paper shows that no distinct failure mechanisms or visible cracks are generated before the deformation limit is tripled. Since the material behaviour quickly stabilizes when entering the plastic domain, the value of the strength will not increase significantly with a new deformation limit, but it will provide less conservative limits when boundaries in Serviceability Limit State are defined. The compressive strength, $f_{c,90}$, found in this thesis with the current regulations, is 15% larger than the one given in the documentation of the wood (Appendix C). This might be one reason why the current calculation model provides conservative values, and limits that the Norwegian building methods do not satisfy. By also allowing the custom limits derived in this thesis, the strength increases even further by 7%, which will provide a total increase of 22% of the compressive strength.

In this paper a model has been derived, which provides the opportunity to calculate in Serviceability Limit State. The model is based directly on the material behaviour of wood loaded perpendicular to the grain, and relies on defined limits of maximum allowed deformation underneath the loading area. The model is based on a predefined function Voce Law, which is a known function used extensively in the Material Mechanics to describe a ductile material behaviour, and provides a link between applied load and the corresponding deformation. The limits for the maximum allowable deformation is defined by conditions that do not violate the carrying capacity in Ultimate Limit State, which means that the values calculated in serviceability limit state will not provide a risk of system failure. The model gives an easy and convenient method to control and determine the deformation in a connection, based on how much is desired by the designer.

Sammendrag

Det har blitt introdusert to nye beregningsmodeller for å regne trykkapasiteten til tre på tvers av fiberretningen i denne masteroppgaven. I den første modellen (Modell 1) blir de forskjellige mekaniske fenomenene som er avgjørende for den totale bærekapasiteten modellert separat, ved å introdusere et tilleggsledd til den ordinære trykkfastheten som baserer seg på tøyningsfeltet og likevektsbetraktninger. Den andre modellen (Modell 2) er en ren empirisk formel, hvor det er generert faktorer som multipliseres med den rene trykkfastheten for å inkludere kapasitetsøkningen for ulike lastsituasjoner og tverrsnittsgeometrier. I stor grad er det mengden/lengden utørt trevirke på siden av lastområdet som er avgjørende for størrelsesordenen til tilleggskapasitetene, og i den siste modellen vil dette inkluderes i en faktor k_1, som er funnet på bakgrunn av energibetraktninger. I den første modellen blir dette inkludert i et tilleggsledd $f_{H,90}$, som baserer seg på likevektsbetraktninger av et *tausystem*, hvor økning i kapasitet finnes fra ulike verdier på tøyningskonsentrasjoner som genereres på siden av lastområdet.

En ulempe med den eksisterende beregningsmodellen slik som den står i Eurokode 5 del 1-1, er at den for små lastlengder gir en veldig høy kapasitet som følge av definisjonen på tillatt spredning av den påførte lasten, mens for større lastlengder kan gi noe konservative verdier. Dette har ført til at de tradisjonelle byggemetodene her i Norge ikke lengre tilfredsstiller de gjeldende kravene for slike forbindelser.

I modellen basert på energi (Modell 2), blir den økte bærekapasiteten som kommer av lastspredningen tatt direkte inn i energibetraktningene, noe som gjør at man unngår å måtte regne med et effektivt bærearealet slik som det gjøres i dagens reglement. I modellen basert på tøyning (Modell 1), benyttes den samme definisjonen på den økte bærelengden som gitt i Eurokode 5, men bæreevnen blir regulert av tilleggsleddet, som har betingelser og faktorer implementert i formelen som tar hensyn til variasjon i lastlengden. Dette fører til at de nye beregningsmodellene stabiliserer seg mot kapasiteter som er noe lavere for mindre lastlengder enn hva Eurokode 5 gjør (rundt 25% mindre for lastlengde lik 50 mm).

Etter hvert som lastlengden øker (lastlengde lik 90 mm), vil det totale bidraget som dagens modell får fra lastutbredelsen gjøre seg mindre gjeldende, og Modell 2 vil få kapasiteter som er identiske med de funnet med dagens reglement, mens Modell 1 vil legge seg noe høyere. For større lastlengder, vil Modell 2 gi en høyere kapasitet (rund 16%), mens Modell 1 stabiliserer seg på en verdi som er litt lavere enn den funnet med Eurokode 5.

Ved å se på holdbarheten og styrken til de nye beregningsmodellene gjennom konstruerte eksempler, ser man at Modell 2 gir noe mer stabile resultater enn Modell 1. Tilleggsleddet som tar hensyn til økningen i kapasitet for ulike lastsituasjoner og tverrsnittsgeometrier i Modell 1, er basert på likevekt av et *tausystem*, hvor de ulike parameterne i modellen er funnet ved å se på det genererte tøyningsfeltet i treet. Det er mer usikkerhet når det kommer til utledningen av parameterne, og gyldigheten ved å modellere tilleggskapasiteten på denne måten, i forhold til energibetraktingene i Modell 2. De empiriske faktorene funnet gjennom utregning av den totale energien som skal til for å få en bestemt deformasjon under lastområdet i Modell 2, er tatt direkte fra materialoppførselen, og gir dermed mer pålitelige og nøyaktigere resultater.

Fra tester gjennomført i denne masteroppgaven, kan man se tendenser til at reglementet som bestemmer trykkfastheten til tre belastet på tvers av fiberretningen, er noe konservativt i forhold hva materialet egentlig tåler. Det tillates i dag en plastisk deformasjon på 1% (0.01h) av høyden på en referansekloss med full belastet toppflate. Resultatene av materialoppførselen funnet i denne avhandlingen, viser at ingen markante bruddmekanismer eller synlige sprekker gjør seg gjeldende for en tredobling av denne deformasjonsgrensen. Siden materialoppførselen flater fort ut i det plastiske domenet, vil ikke verdien på fastheten øke betraktelig med et mindre konservativt deformasjonskriterium, men det er med på å gi mindre konservative grenser når det skal regnes i bruksgrensetilstand. Trykkfastheten, $f_{c,90}$, funnet i denne avhandlingen med det nåværende reglementet, er 15% høyere enn den gitt i material-dokumentasjonen (Appendix C), noe som kan være en av grunnene til at dagens beregningsmetode gir konservative kapasiteter, og grenser som de tradisjonelle norske byggemetodene ikke tilfredsstiller. Ved å i tillegg tillate de egendefinerte deformasjonsgrensene utledet i denne avhandlingen, vil fastheten kunne økes med enda 7%, som vil gi en total økning av trykkfastheten på 22%.

Det er utledet en kalkulasjonsmodell i denne avhandlingen, som gir mulighet for å regne i bruksgrensetilstand. Modellen tar direkte utgangspunkt i materialoppførselen til tre belastet i trykk på tvers av fiberretningen, og belager seg på tillatte grenser for maksimal deformasjon direkte under belastningsområdet. Modellen tar utgangspunkt i Voce Law, som er en kjent funksjon brukt mye i Materialmekanikken for å beskrive en duktil materialoppførsel, og gir en sammenheng mellom påført last og tilhørende deformasjoner. Grensene satt til tillatt maksimal deformasjon, er definert ut fra betingelser som ikke bryter med bærekapasiteten i bruddgrensetilstand, noe som gjør at verdiene beregnet i bruksgrensetilstand ikke gir fare for systemsvikt. Modellen gir en lett og hensiktsmessig metode for å kunne regulere deformasjoner i en forbindelse, ut i fra hvor mye som er ønsket av en konstruktør.

Terminology

Tests

Naming of the specimens

Luj-i	Test to find the effect of untouched timber on the side of the loading area. Where j defines the length of untouched timber in millimetre, and i the test number (See appendix A); j = 0; 30; 50; 70; 100; 150; 200; 250 [mm]
Rj-i	Test to find the effect of the height on the capacity. Where j defined the height, and i the test number (See appendix A); j = 30; 60; 90; 120; 150; 200 [mm]

Symbols (Lengths can be found in appendix A)

Lq	Loading length in the longitudinal direction for the applied compression force perpendicular to the grain
Lu	Length/Amount of untouched timber on the side of the loading area
L	Total length of the specimen
H	Cross-sectional height
B	Cross-sectional width
F	Applied compression force perpendicular to the grain

Existing calculation models

Symbols

$F_{c,90,max,est}$	Estimated compression capacity perpendicular to the grain (CEN-model)
$0.1F_{c,90,max,est}$	Point value in the linear domain on the load-deformation curve, used to define the fracture line (CEN-model)
$0.4F_{c,90,max,est}$	Point value in the linear domain on the load-deformation curve, used to define the fracture line (CEN-model)
$F_{c,90,max}$	Compressive strength perpendicular to the grain [N / kN]
$F_{c,90}$	Applied compression load perpendicular to the grain
$k_{c,90}$	Strength factor that takes the *Hammock effect* into account
A	Loading area
A_{ef}	Effective loading area

l_{ef}	Effective loading length
b	Cross-sectional width
Δl_i	Increased loading length on the side of he loading area
l_1	Distance between loads perpendicular to the grain
a_i	Length/Amount of untouched timber on the side of the loading area
$\sigma_{c,90}$	Compression stress perpendicular to the grain
$f_{c,90}$	Compressive strength perpendicular to the grain [MPa / N/mm^2]

New calculation models

Ultimate Limit State (ULS)

Model 1 (Based on strains)

$f_{H,90}$	Additional bearing capacity coming from the *Hammock effect*
S	Tension force generated from the strain concentrations on the side of the loading area
Δh	Total deformation underneath the loading area
q	Even distributed load perpendicular to the grain
$E_{s,\Theta}$	Modulus of elasticity in an angle Θ
$\varepsilon_{H,i}$	Strain concentrations on the side of the loading area
A_s	Area on the side of the loading surface that experiences the tension load
k_u	Load location factor
C	Defined parameter taking the loading length into account (Hammock Constant)

Model 2 (Based on energy)

E_j	Total energy calculated for a specimen with untouched timber length j
$f_j(\Delta)$	Function generated to describe the load-deformation curve for specimen j
$\Delta_{j,max}$	Maximum allowed deformation underneath the loading area for specimen j
x_0	Lower length limit for untouched timber
x_2	Upper length limit for untouched timber
k^l	Lower limit for the strength factor
k^u	Upper limit for the strength factor
k_1	Strength factor taking the amount of untouched timber into account
k_2	Height factor taking the cross-sectional height into account
$f_{c,90,j}$	Compression strength perpendicular to the grain for a cross-section with height j
$f_{c,90,ref}$	Compressive strength perpendicular to the grain for the reference case with cross-section height equal to 90 mm
h_{ref}	Reference height equal to 90 mm

Serviceability Limit State (SLS)

F	Load perpendicular to the grain [N]
C_1/C_2	Parameters in Voce Law used to describe the load-deformation curves
K/n	Parameters in Power Law used to describe the load-deformation curves
B	Parameter used to describe the linear domain of the load-deformation curve
Δ	Total deformation underneath the loading area
$\Delta_{j,max}$	Total deformation limit underneath the loading area
$\Delta_{j,el}$	Elastic deformation limit underneath the loading area
Δ_j^{el}	Elastic deformation for $L_u \leq x_2$
Δ_j^{pl}	Plastic deformation for $L_u > x_2$

Abbreviations

SLS	Serviceability Limit State
ULS	Ultimate Limit State
CEN	European Committee for Standardization
ASTM	American Society for Testing and Materials
LSM	Least Square Method

Used codes and literary texts

Eurocode 5 part 1-1 (EC5-1-1) (Norsk Standard NS-EN 1995-1-1: 2004+A1:2008+NA:2010)	*Eurocode 5: Design of timber structures - Part 1-1: General Common rules and rules for buildings*
Norsk Standard NS-EN 1194	Timber structures/Glue laminated timber - *Strength classes and determination of characteristic values*
Norsk Standard NS-EN 408:2010+A1:2012	Timber structures/Structural timber and glued laminated timber - *Determination of some physical and mechanical properties*
Practical design of timber structures to Eurocode 5	Written by Hans Larsen and Vahik Enjily

When new capacity models are introduced, the yellow sticker will be shown.

Contents

Chapter 1

Background

1.1 Purpose

This study aims to improve or/and replace the current model for calculating the compression capacity perpendicular to the grain. A new calculation model should take into account different system configurations, in respect to both load and geometry, and give the opportunity to calculate in both Serviceability Limit State and Ultimate Limit State.

An important part of the thesis is also to get a deeper understanding of mechanical phenomena that occurs during a load situation with compression perpendicular to the grain, and to determine what factors are important for the total capacity.

1.2 Methods

To verify the different calculation methods and the parameters presented in this thesis, compression tests were carries out in the laboratory at the Department of Structural Engineering. The tests were in full scale, and restricted to continuously supported timber sills loaded in the mid-span. To get accurate results in the determination of the parameters in the new models, and to get a good description of the behaviour of wood loaded in compression, it was performed advanced deformation analysis based on optical measuring techniques. This method provides an opportunity to describe the deformations, strains and stresses in the x-, y- and z-direction of the wood.

1.3 Limitations

The test set-up was restricted to continuously supported sills loaded with a compression force at the mid-point. To get an acceptable foundation to determine the parameters in the new models, a total number of 41 tests was conducted (Appendix A). Since this thesis has a weight of 30 units/student points, it was only conducted tests with this one set-up, due to the limitation in time.

There will also be some limitations with regards to the timber available for the compression tests, both for wood type and geometry. The type available is Norwegian CE L40C, which basically has the same properties as GL32c given in NS-EN 1194 [14]. The maximum available cross-sectional height is 150 mm. The compression machine that will be used during the tests is an INSTRON 5900 Series, which gives limitations to the specimens' lengths as well as the maximum compression force (100 kN).

The test specimens have been acclimatized in a climate room at the Department of Structural Engineering for the last 6 months, with constant temperature and relative humidity, with values of $20°C$ and 65%, respectively. The specimens tested during this thesis will therefore have the same climate properties, and differences in strength because of temperature and moisture content will not be tested.

1.4 Structure of the paper

At the beginning of the thesis, a summary of the existing calculation models will be presented, to get an overview of the theory and background for the regulations given in Eurocode 5. In the next chapters, the new models based on own assumptions and formulations will be derived, both for Ultimate Limit State (USL) and Serviceability Limit State (SLS). The theory behind the different parameters used to calculate the bearing capacity with the new models, will be described during the paper, and verified through the compression test conducted in the laboratory.

Further, an explanation of the various tests used to find the new parameters will be presented, together with the different test results. At the end of the paper, the new models will be discussed and compared with the existing regulations, and tested through various of generated examples. The test of the models and the calculation procedures will be included in the main paper, and serve as a contribution to the final conclusion.

All figures and illustrations in this thesis are the creation of the author, unless otherwise indicated.

Chapter 2

Theory

Because of its rich diversity and an easy access, timber has become a traditional building material in Norway. Over 80% of Norwegian households are built with timber [1], and in a world that is seeking towards cleaner construction materials, the demand for wood is likely to rise in the future. Global warming is today a major concern, and more and more companies are looking for environmentally friendly alternatives to replace their old construction methods, where steel and concrete have been dominating for the last decades.

2.1 Strength properties

Wood is a complex building material, because of its unique structure. The structure is built up from fibres and cells, which gives distinct properties in the different directions. Many factors are crucial for the bearing capacity of wood. Density, moisture content, load orientation, fibre orientation and the load period (creep), are all parameters that make up the total strength, and must be taken into account when deriving the capacity.

Because of its unique material structure, it is possible to find different symmetry planes in the wood, which gives it three main directions. This makes wood an orthogonal material. The main directions have large differences in their strength properties, and are oriented in the longitudinal- (L), radial- (R) and transverse (T) direction of the grain (Figure 2.1). The ratio between the strength properties for the different directions can be as large as a factor of nine. Mechanisms that are crucial for the bearing capacity are also varying with the orientation of the load, and is something that must be taken into account when creating capacity models for the different grain directions.

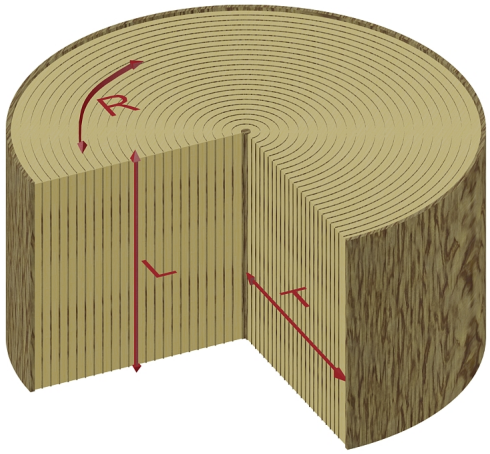

Figure 2.1: Main directions: Radial- (R), tangential- (T) and longitudinal (L) direction

Because of how the growth behaviour changes with varying climate conditions, wood with different strength properties will be formed during the year. This leads to a classification system that gives strength values dependent on which part of the log is being used. The class should always be documented on the timber, giving the buyer information about the properties that are expected of the wood. From various compression tests, different standards have been generated that give strength values for the different classes, both for construction- and glue laminated timber.

When timber is being loaded in compression, it will up to a certain limit behave linearly elastic, with non-permanent deformations, and the coherence between load and deformation can be described with Hooke's Law. When this limit is exceeded, the material will start to behave plastic, and permanent deformations will be generated. In this domain, the material can withstand even more load without any danger of sudden failing mechanisms, but the plastic non-reversible deformations will increase rapidly.

Knots in the wood is a crucial factor for the bearing capacity, and it makes the strength properties unpredictable. It breaks down the cell structure, and changes the directions of the grain. This is a phenomenon that can increase the compression capacity, but because of its randomness in the wood, it cannot be taken in to account when calculating the strength.

A more thorough description of the properties and structure of the wood can be found in literature written by Hans Larsen and Vanhik Enjily [2] and Eidvin Skaug [3].

Chapter 3

Existing calculation models

In this chapter, different approaches to define a fracture criterion will be presented, based on both allowed plastic deformation and total deformation. An overview of the existing models used to calculate the compression capacity for sills loaded perpendicular to the grain will be given, including the theory behind the method given in Eurocode 5 part 1-1.

3.1 Compressive strength

In order to calculate the bearing capacity for timber loaded perpendicular to the grain, capacity limits need to be defined. These limits do not necessarily result in a global fracture mechanism in the loaded part, but can give skew systems, that may lead to other failure mechanisms further up in the system

With the rules that apply today, the compressive strength is defined by a maximum allowed plastic deformation of a timber block loaded with a uniform compression force over the entire top surface. The maximum plastic deformation underneath the loaded area is set to a value of 0.01 times the height of the specimen, which equals a total strain of 1%. This method is called the CEN-model (European Committee for Standardization), and is one of several ways to define a fracture criterion. ASTM D143 (American Society for Testing and Materials) is a second model, that calculates the compressive strength by allowing certain amounts of total deformation, consisting of both a plastic and an elastic part.

3.1.1 CEN-Model

This model was developed in the early 90s, and defines the compressive strength from a limit to the plastic deformation under the loading area set to 0.01h. This gives a failure criterion that follows the curve of material behaviour (Figure 3.1). The specimens used to determine the strength, consists of a block with geometry 45x70x90 mm (bxhxl) for construction timber, and 45x70x180 (bxhxl) for glue-laminated timber. The entire top surface is uniformly loaded for both cases.

The compressive strength is calculated by an iteration process, where a maximum fraction value $F_{c,90,max,est}$ first needs to be estimated. From the load-deformation relation, found from the compression test on the timber block, two points are defined on the curve, $0.1F_{c,90,max,est}$ and $0.4F_{c,90,max,est}$. Through these two points, a straight line is drawn. This line is then shifted along the x-axis (deformation axis), until the allowed plastic deformation of 0.01h is reached. The intersection between the straight line, and the load-deformation curve, defines the compression strength $F_{c,90,max}$. If $F_{c,90,max}$ is within 5% of $F_{c,90,max,est}$, the estimated value can be used. If not, a new estimated value $F_{c,90,max,es}$ needs to be chosen, and the iteration process continues until the value of the strength is within the tolerance of 5% (Figure 3.1).

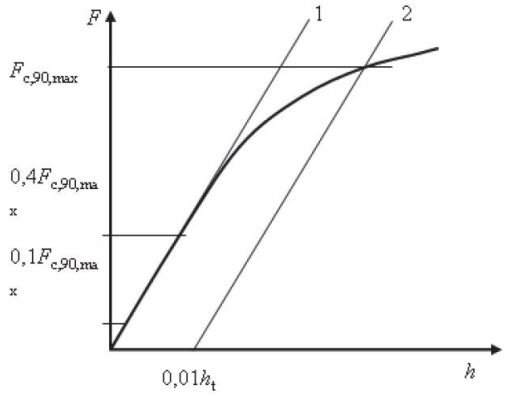

Figure 3.1: CEN-Model [12]

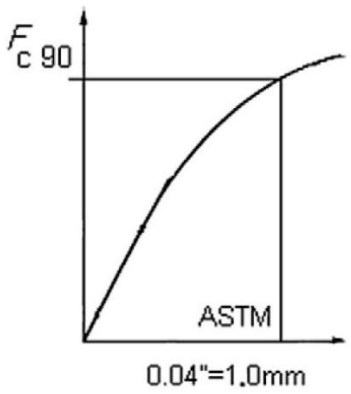

Figure 3.2: ASTM D143-Model [12]

3.1.2 ASTM D143-Model

The ASTM D143-model was used in the earlier calculation standards, and was presented in the 1920s. Unlike the CEN-model, which calculates the compressive strength from a timber block with uniform loading over the entire surface, ASTM uses sills with a point load in the middle. The geometry of the specimen is 51x51x150 mm (bxhxl), where the load is transferred to the wood trough a steel plate with dimensions equal to 51x51 mm.

The ASTM D143-model defines its strength from a limit of the total deformation underneath the loading area. This limit is often set to 1 mm (0.04'), which equals a total strain of 2%. The compressive strength is defined by the intersection between the allowed total deformation and the load-deformation curve found from the tests (Figure 3.2).

3.2 Compression capacity

Over the years, various methods of calculating the compression capacity perpendicular to the grain have been presented. Some of the methods have analytical backgrounds, while others use a more empirical approach.

The compression capacity depends on various factors and mechanical phenomena. With this type of loading, the bearing strength will depend on a pure compression capacity, defined from the limits given by the fracture criterion (Chapter 3.1), but also additional effects will be mobilized that increases the capacity. The magnitude of these additional effects, will vary with the amount of untouched timber on the side of the loading areal (i.e. distance from the load surface to the edge in the longitudinal direction)

By having untouched wood on the side of the loading, the applied force will be spread out in the width of the cross-section, which gives a bearing area that is larger than the loading surface. With the current regulations in the Eurocode 5, this spread is modelled linearly, which gives a simple calculation method to find the effective compressive length. This is of course a simplification, since the spread in reality becomes more complex.

Another effect, often refereed to as the *Hammock effect,* is generated when the fibres on the side of the loading area are being tilted because of the applied compression force. When the longitudinal fibres are tilted, concentrations of strains on the side of the loading surface will be generated, which will will give an additional bearing mechanism, leading to an increased total capacity of the system. The *Hammock effect* is taken into account in the existing models, by multiplying a factor k_c with the compressive strength found by the CEN-model.

A general expression often used to define the capacity of a section loaded in compression perpendicular to the grain, is shown in Equation 3.1, where the approaches in finding the various parameters separates the different existing models.

$$\frac{F_{c,90}}{A_{ef}} \leq k_c \cdot f_{c,90} \tag{3.1}$$

$F_{c,90}$	design load perpendicular to the grain
A_{ef}	effective area that carries the design load
$k_{c,90}$	factor that takes the *Hammock effect* into account
$f_{c,90}$	compressive strength

3.2.1 Calculation model *Madsen*

Madsen [10] defined a calculation model based on an empirical approach in the following way:

$$\frac{F_{c,90}}{l_{ef} \cdot b} \leq k_c \cdot f_{c,90} \tag{3.2}$$

The design load is taken by an area equal to the width, b, multiplied with an effective length l_{ef}. The effective length is larger than the loading length, because of the contributions from the untouched timber on the side. As early as 1983, Madsen performed simulations and compression tests that supported the theory of a load distributed over the cross-section. He concluded from his research that the maximal increase in the bearing length is restricted to a value of 1.5 times the height. To decide a value for the compressive strength, $f_{c,90}$, Madsen uses the ASTM-model (Chapter 3.1).

For the case of a continuously supported timber sill, Madsen defined the effective length as following:

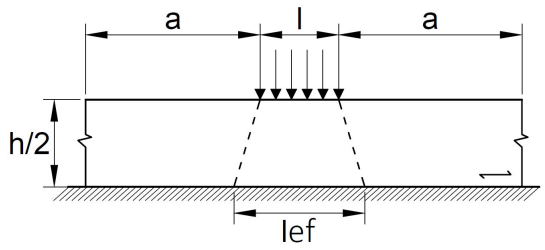

Figure 3.3: Load distribution: Mid-load

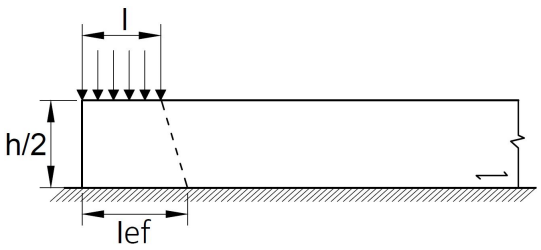

Figure 3.4: Load distribution: End-load

$$l_{ef} = l + \frac{h}{8} < 4l$$

$$l_{ef} = l + \frac{h}{3} < 2.5l$$

A documentation on how Madsen defined the factor k_c , that represents the additional bearing capacity from the *Hammock effect*, could not be found.

Summary:

- Empirical approach
- l_{ef} based on the height
- k_c unknown definition and background
- Uses the ASTM-model to define the compressive strength

3.2.2 Calculation model *Blass and Görlacher*

Blass and Görlacher [10] presented in 2004 a calculation method based on the theory derived by Madsen, and this is the model used in the current regulations in Eurocode 5. They concluded that the height was irrelevant for the capacity, and found from empirical approaches a maximal increase in bearing length equal to 30 mm, based on a scattering angle less than 45°. As a fracture criterion, Blass and Görlacher uses the CEN-model to determine the compressive strength.

$$\frac{F_{c,90}}{l_{ef} \cdot b} \leq k_{c,90} \cdot f_{c,90} \tag{3.3}$$

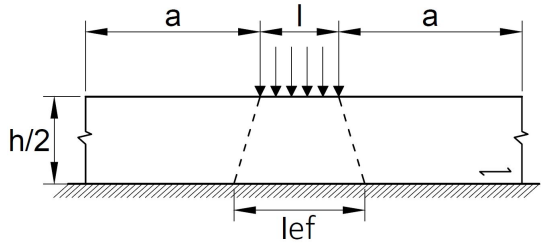

Figure 3.5: Load distribution: Mid-load

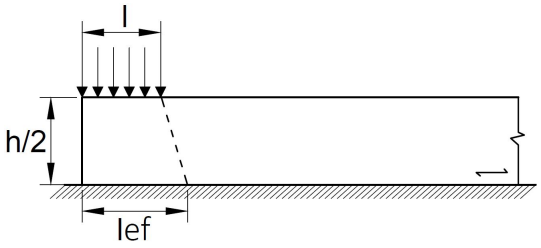

Figure 3.6: Load distribution: End-load

$$l_{ef} = l + 2 \cdot 30mm$$

$$l_{ef} = l + 30mm$$

The increase in bearing length is limited by the boundary conditions of the sill, and taken from the following equations:

$$l_{ef} = l + \sum_{i=1}^{2} \Delta l_i$$

$$\Delta l_i = min\{30mm; a_i; l; l_i/2\}$$

Blass and Görlacher separate between Serviceability- and Ultimate Limit State by changing the additional factor $k_{c,90}$, that is taking the *Hammock effect* into account. This factor varies with the load configurations and type of wood, and is found by an empirical approach.

	Ultimate (ULS)	Serviceability (SLS)	
Wood	Constructional/Glue laminated	Constructional	Glue laminated
$k_{c,90}$	1.0	1.25	1.5

Table 3.1: Strength factors to account for the *Hammock effect*

The reason for the factor being smaller for the constructional wood is related to the orientation of the annual rings.

Summary:

- Empirical approach based on research done by Madsen.
- Scattering angle less than 45°
- Maximum increase of the bearing length equal to 30 mm
- $k_{c,90}$ found empirical, and separates between Ultimate and Serviceability Limit State
- Uses the CEN-model to determine the compressive strength

3.2.3 Calculation model *Riberholt*

Riberholt defined a capacity model for continuously supported timber beams, by looking into test results found by Thorvald Pedersen at the Technical University of Denmark (DTU). He found the existing regulations, where an upper value for the plastic deformation was defined to 0.01 times the height, to be very conservative. Based on this, Riberholt defined a fracture criterion allowing a plastic deformation up to 0.1 times the height (i.e. 10 times larger than the existing limit).

Riberholt defined his capacity model the same way as both Madsen and Blass and Görlacher:

$$\frac{F_{c,90}}{l_{ef} \cdot b} \leq k_{c,90} \cdot f_{c,90} \tag{3.4}$$

By assuming a scattering angle of the stress equal to 1:1/3 ($\approx 20°$), Riberholt found an effective length equal to:

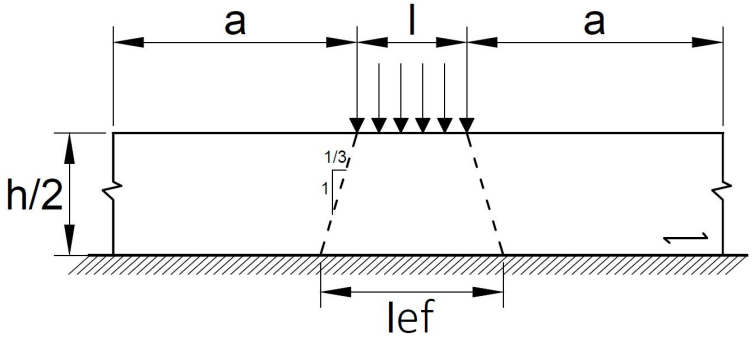

Figure 3.7: Load distribution: Mid-load

$$l_{ef} = l + \frac{2h}{3}$$

By an empirical approach, Riberholt defined an expression for the additional factor $k_{c,90}$, that both includes the loading and effective length.

$$k_{c,90} = 1.2 \leq (2.38 - \frac{l}{250} \cdot \sqrt{\frac{l_{ef}}{l}}) \leq 4.0 \tag{3.5}$$

Equation 3.5 is valid for a cross-section with height $h \leq 2b$, and a loading length less than the total length of the beam ($l < L$). By allowing a plastic deformation of 0.1h, the additional factor $k_{c,90}$ is put equal to 1.25.

Summary:

- Empirical approach
- Allows plastic deformations up to 0.1h (10 times higher than existing regulations)
- Scattering angle equal to 1:1/3 ($\approx 20°$)
- $k_{c,90}$ found empirical and valid for $h \leq 2b$ and $l < L$
- Uses the CEN-model to define the compressive strength

3.2.4 Calculation model *van Der Put*

Instead of looking into empirical approaches, van Der Put defined in 1988 a model based on equilibrium, and with a linear plastic material behaviour. This approach gives an exact model, since the boundary conditions is always satisfied, and the stresses always kept under the allowed fracture limits.

$$\frac{F_{c,90}}{l \cdot b} \leq k_{c,90} \cdot f_{c,90} \tag{3.6}$$

van Der Put separates between cases with small versus large deformations, and defines different scattering angles for the two cases. For deformations in the area around 3-4% of the height, the angle is equal to 1:1 ($= 45°$), while a load situation that results in a deformation equal to 10%, the scattering angle is increased to 1:1.5 ($\approx 56°$).

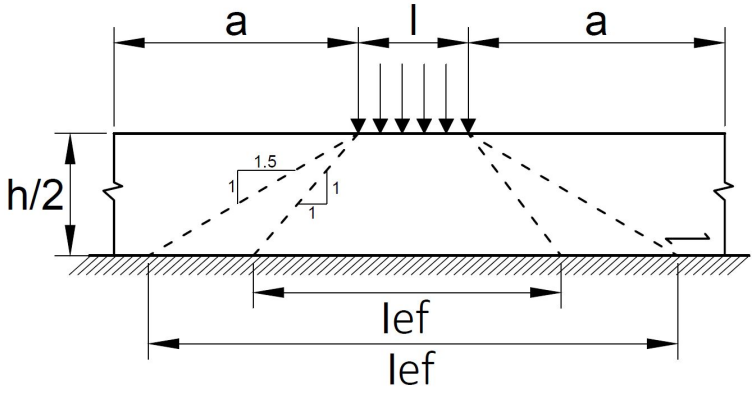

Figure 3.8: Load distribution: Mid-load

$$l_{ef(56°)} = l + 2 \cdot 1.5h = l + 3h$$

The maximum increase of the bearing length on both sides of the loading area, is taken from analytical approaches and found to be 1.5 times the height of the cross-section. This increase is limited by the boundary conditions of the sill, equal to the rules defined by Blass and Görlacher.

Instead of spreading the applied load over an effective area, the additional contribution to the bearing capacity is taken directly into the factor $k_{c,90}$, and found by analytical consideration equal to:

$$k_{c,90} = \mu \frac{A_{ef}}{A} = \mu \frac{l_{ef} \cdot b}{l \cdot b} = \mu \frac{l_{ef}}{l} \leq 5.0 \tag{3.7}$$

The factor μ, is found empirical and has it origin in tests done by Korin in 1990 [7], and accounts for the configuration of the compression block. The value is usually set equal to 1.0, which gives a lower limit of the capacity.

By using a scattering angle equal to 1:1.5, van Der Put defines an expression for the effective length $l_{ef} = l + 3h$, which leads to a final equation for the $k_{c,90}$ factor equal to:

$$k_{c,90} = \mu \frac{l_{ef}}{l} = \frac{l + 3h}{l} \tag{3.8}$$

The model derived by van Der Put gives more accurate result for the bearing capacity than the current model in Eurocode 5. It has therefore been suggested to replace the existing model during the next revision of the Eurocode. van Der Put's model is found to be more desirable, because of its ability to account for different systems, loading situations and cross-sectional geometries.

Summary:

- Model based on equilibrium
- Assumes a linear plastic material behaviour
- Scattering angle based on applied load

  1:1 ($\approx 45°$) for small deformations (3-4%)

  1:1.5 ($\approx 56°$) for larger deformations (10%)
- l_{ef} included in the expression for $k_{c,90}$
- $k_{c,90}$ found analytically
- Uses the CEN-model to define the compressive strength

3.2.5 Summary of the existing calculation models

Both Madsen, Blass og Görlacher and Riberholt defines calculation models based on empirical approaches, while van Der Put uses analytical assumptions based on equilibrium. They all support the theory of a strain field that is spreading over an effective length in the cross-section, which is limited by the amount of untouched timber on the side of the loading area. All the different models assume a linear spread of the stresses, where the differences in the value of the effective length, l_{ef}, lies in the definition of the scattering angle.

The current regulations defined in Eurocode 5 part 1-1, are taken from the model defined by Blass og Görlacher, but it has been suggested to replace the existing rules with the analytical approach defined by van Der Put at the next revision.

3.3 The effect of untouched timber

In 1939, Suenson performed compression tests on sills, where he varied the amount of untouched timber on the sides of the loading area [10]. These tests showed how the bearing capacity increases, as a result of the load being spread to nearby timber down the cross-section.

For *Case a*, which represents a cross-section with fully loaded top surface, it results in a uniform compression of the timber, that provides large deformations for relatively small changes in load. By increasing the amount of untouched timber, the stiffness and bearing capacity of the system increases, and the system needs more load to get the same deformations (Figure 3.9).

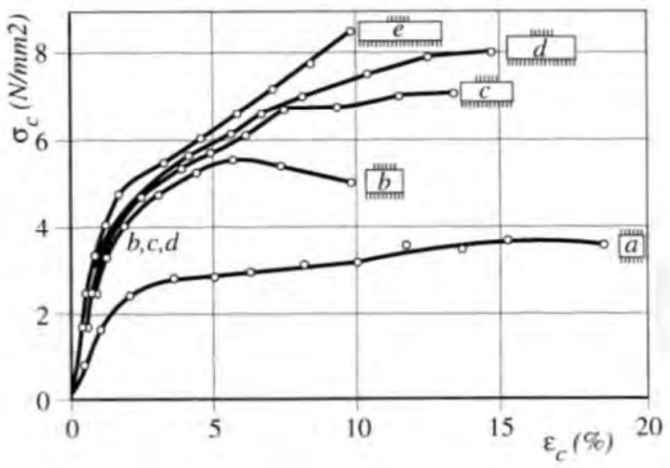

Figure 3.9: Differences in strength with various amount of untouched timber [10]

From the experiments made by Suenson, the capacities for the cases with an increased amount of untouched timber converges towards each other (Case c, d, e). This means that there will be limits for when increasing lengths no longer will provide extra contribution to the bearing capacity. The reason for this convergence, is a result of limitations in the total spread of the stresses in the wood. When exceeding this length, the wood will no longer feel any impact from the applied load.

Chapter 4

New calculation models

This chapter presents two new models for calculating the total capacity in Ultimate Limit State for continuously supported timber sills loaded perpendicular to the grain. The first model (Model 1), is based on describing the different mechanisms that contributes to the bearing capacity separately, while the second model (Model 2) uses energy to define the strength. This chapter will also present a model that gives the opportunity to calculate in Serviceability Limit State

4.1 Ultimate Limit State (ULS)

4.1.1 Earlier starting points

The existing calculation models are mainly based on empirical approaches, where the models have been adjusted and fitted to match the behaviour of a sill loaded in compression. Some of the models, including the current regulations, have been criticised for inaccurately representing the real capacity and behaviour of different load configurations. In some cases the calculation method provides good results for the capacity, but other times quite conservative values are found.

The models are often based on a calculation method where the load is spread out in the cross-section, and where the applied load is taken by an area larger than the actual loading surface. This results in a bearing capacity that is increasing with the amount of untouched wood on the side of the loading area, which stabilizes at a certain point when the limitations of the additional parameters is reached.

4.1.2 Model 1: Based on strains

The current model in Eurocode 5 part 1-1, has the following design:

$$\sigma_{c,90} \leq k_{c,90} \cdot f_{c,90} \tag{4.1}$$

where

$$\sigma_{c,90} = \frac{F_{c,90}}{l_{ef} \cdot b} \tag{4.2}$$

The pure compression capacity $f_{c,90}$, is found by a compression test on a timber block with a limit set to the plastic deformation (Chapter 3.1). This capacity is multiplied together with a factor $k_{c,90}$, that accounts for the increase in capacity coming from the *Hammock effect*. This factor is in the current model found empirical, and takes the boundary conditions and the type of wood into consideration.

In the current regulations in Eurocode 5, the design compression force $F_{c,90}$, is distributed over an effective area larger than the loading surface. The distribution is linearly increasing, and has a maximum value of $2 \cdot 30mm = 60mm$.

(For a deeper understanding and explanation of the current regulations, read Chapter 3.2.2)

With the new calculations method, it is desirable to model the various effects that makes up the total bearing capacity separately, giving a formula that is more suited to represent different loading configurations and geometrical systems. The existing model uses an empirical approach to quantify the additional capacity parameter, while the new model presented in the next chapter, will use equilibrium considerations to represent the same effect.

Design of the calculation model:

The following design is suggested for the new capacity model:

$$\sigma_{c,90} = f_{c,90} + f_{H,90} \tag{4.3}$$

where

$$\sigma_{c,90} = \frac{F_{c,90}}{A_{ef}} = \frac{F_{c,90}}{l_{ef} \cdot b} \tag{4.4}$$

$f_{c,90}$	compressive strength
$f_{H,90}$	strength coming from additional load carrying effects
$F_{c,90}$	applied compressive load perpendicular to the grain
A_{ef}	effective loading area
l_{ef}	effective loading length
b	cross-sectional width

The main difference between the new and the existing model, is that the empirical factor $k_{c,90}$, has been replaced by an additional part. This part represents the same effect, but is derived from the equilibrium of a mechanical system. It will consist of parameters that vary with the chosen design, making the model adaptable to multiple load cases. Figure 4.1 and 4.2 shows the different mechanisms that carries the applied load, $f_{c,90}$ and $f_{H,90}$, respectively.

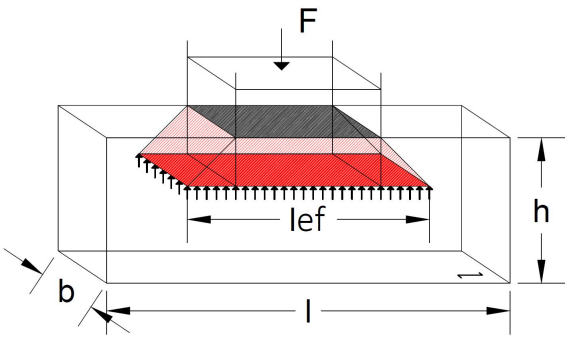

Figure 4.1: Pure compression capacity

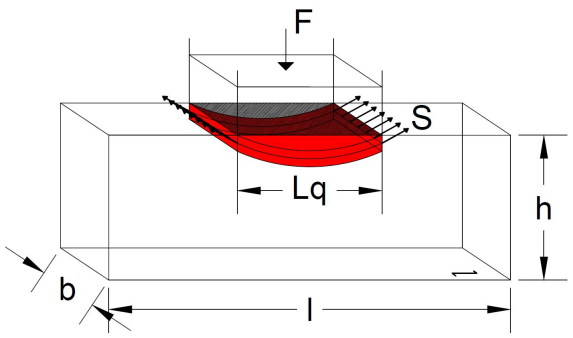

Figure 4.2: The Hammock Effect

Compressive strength:

This model depends on a predefined maximum allowed total deformation, which provides a starting point for deriving a fracture criterion. By looking at a fracture criterion defined on the basis of deformation consisting of both an elastic and a plastic part, the ASTM D143-model is used (Chapter 3.1). When this deformation is reached, the sill will by definition fail, and no longer have the ability to carry more load.

The size of the allowed deformation is largely involved in the determination of the total capacity of the timber. The ASTM-model uses a deformation limit equal to 1.0 mm underneath the loading area, which is found from compression tests on a timber sills with a point load in the mid-span. The new calculation method aims to determine the fracture limit from a reference block with a fully loaded top surface, and then add strength as the amount of untouched timber increases. This will lead to a fracture criterion that uses a combination of the ASTM- and CEN-model. The predefined maximum allowed total deformation of the reference block, will be determined by first using the CEN-model to calculate the compressive strength, then use the coherent total deformation as a fracture limit, which will provide a constant allowed deformation value (i.e. ASTM-model) (Figure 4.3).

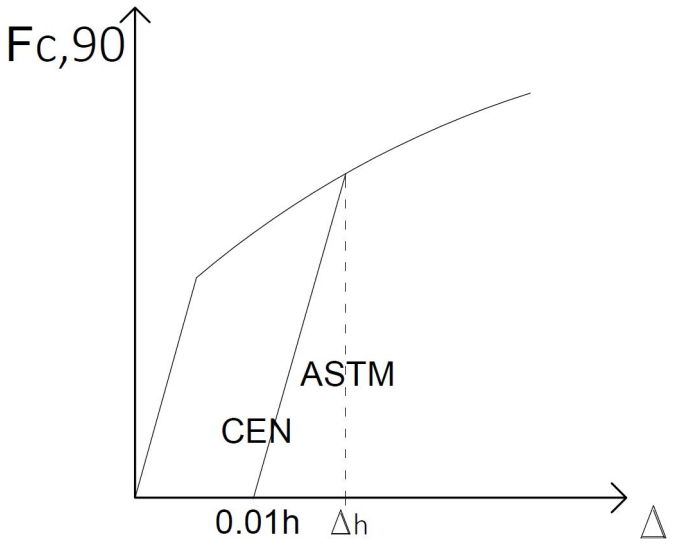

Figure 4.3: Combination of the ASTM D143-model and CEN-model

Load distribution:

In the same way as the existing regulations, the applied load is distributed along the cross-section, and carried by an effective area larger than the loading surface. This area is found by using the current regulations given in Eurocode 5 part 1.1.

$$l_{ef} = l + \sum_{i=1}^{2} \Delta l_i \tag{4.5}$$

$$\Delta l_i = min\{30mm; a_i; l; l_1/2\} \tag{4.6}$$

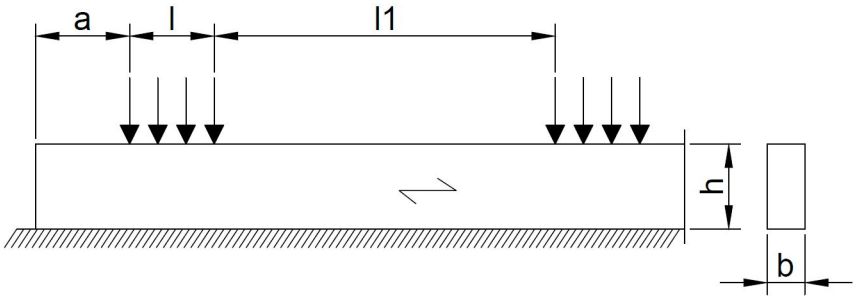

Figure 4.4: Lengths given with Eurocode 5 notation

The Hammock Effect:

When a sill is experiencing a concentrated compression force, the longitudinal fibres in the direction of the grain will start to tilt down on the side of the loading area, and create a *Hammock effect*. This effect produces large concentrations of strains on the side of the loading surface. Tests performed by Aldvis Hardeng [9] in 2011, clearly show these concentrations and how they vary with the amount of untouched timber. With a small amount of untouched timber (close to the reference block), these concentrations will not occur, and the capacity will only depend on the pure compressive strength. As the amount increases, the concentrations are getting larger, and at some point they will most likely stabilize and converge toward a limited value.

When the fibres are tilted on the side of the loading area, they will experience a tension force that will contribute to the bearing of the applied load. The size of this tension force is associated with the strain concentrations. This system can be modelled as a rope, with end-forces and an evenly distributed load that represents the loading area. Based on equilibrium considerations taken from the system shown in Figure 4.5, a formula for the end-load, S, can be derived [17].

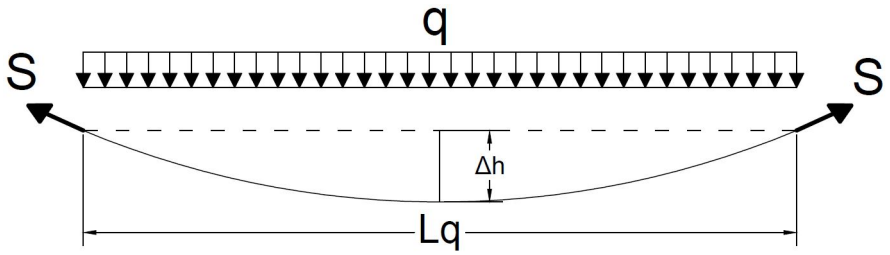

Figure 4.5: Mechanical system: Rope forces

$$S = \sqrt{(\frac{q \cdot L_q^2}{8 \cdot \Delta h})^2 + (\frac{q \cdot L_q}{2})^2} \tag{4.7}$$

From the mechanical system given in Figure 4.5, a value of the total deformation Δh, in the middle of the system needs to be defined, in order to say something about the magnitude of the tensile forces. By defining a fracture criterion based on the ASTM-model, a fixed value of the allowed deformation used in the formula can be defined.

By solving Equation 4.7 with respect to the evenly distributed load, q, an expression for the additional capacity for the system can be derived. Equation 4.8 gives a value of the extra load that can be put into the system, which is carried purely by the *Hammock effect*.

$$q = \frac{2 \cdot S}{L_q \cdot \sqrt{\frac{1}{16} \cdot (\frac{L_q}{\Delta h})^2 + 1}} \tag{4.8}$$

The tensile force, S, is determined by looking at the strain concentrations generated on the side of the loading area, and expressed in the following way:

$$S = E_{s,\Theta} \cdot \varepsilon_{H,j} \cdot A_s \tag{4.9}$$

$E_{s,\Theta}$	module of elasticity for wood in an angle Θ
$\varepsilon_{H,j}$	strain concentration on the side of the loading area
A_s	area that is effected by the tension force S

The expression for the tensile force is then inserted into Equation 4.8, which gives:

$$q = \frac{2 \cdot E_{s,\Theta} \cdot \varepsilon_{H,j} \cdot A_s}{L_q \cdot \sqrt{\frac{1}{16} \cdot (\frac{L_q}{\Delta h})^2 + 1}} \tag{4.10}$$

Definition of the effective tension area A_s:
The effective area that is experiencing the tensile force at the end of the loading surface needs to be defined. By looking at previous results from compression tests done by A. Hardeng [9], the effective area is found to be limited to the upper part of the timber section. From diagrams representing the strains in the y-direction over the entire specimen, the concentrations on the side of the loading area are found to decrease from the top of the cross-section, and become non-existing after a length of 10-20 mm. The tensile force will be uniform over the width of the cross-section, resulting in the following expression for the effective tension area.

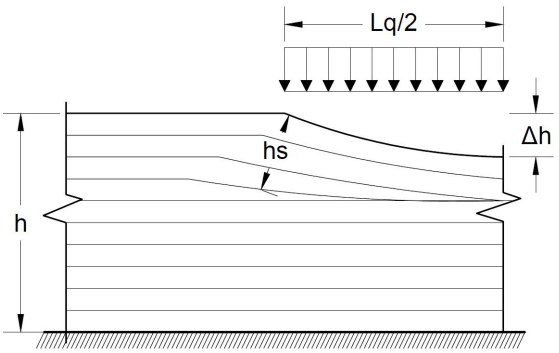

Figure 4.6: Effective tension height

$$A_s = b \cdot h_s \tag{4.11}$$

The *Hammock effect* is uniform over the entire width of the sill, which leads to an additional bearing capacity equal to

$$f_{H,90} = \frac{q}{b} \tag{4.12}$$

By inserting Equation 4.10 into Equation 4.12, it gives the following expression:

$$f_{H,90} = \frac{q}{b} = \frac{2 \cdot E_{s,\Theta} \cdot \varepsilon_{H,j} \cdot b \cdot h_s}{L_q \cdot b \cdot \sqrt{\frac{1}{16} \cdot (\frac{L_q}{\Delta h})^2 + 1}} = \frac{2 \cdot E_{s,\Theta} \cdot \varepsilon_{H,j} \cdot h_s}{L_q \cdot \sqrt{\frac{1}{16} \cdot (\frac{L_q}{\Delta h})^2 + 1}} \tag{4.13}$$

From Equation 4.13, b will disappear, and the *Hammock effect* becomes independent of the cross-sections width.

All the terms in the numerator are collected into one constant:

$$C = L_q \cdot \sqrt{\frac{1}{16} \cdot (\frac{L_q}{\Delta h})^2 + 1} \tag{4.14}$$

Which gives

$$f_{H,90} = \frac{2 \cdot E_{s,\Theta} \cdot \varepsilon_{H,j} \cdot h_s}{C} \tag{4.15}$$

The value of the constant C, is only dependent on the length of the loading area, and can either be determined by inserting values into Equation 4.14, or from Figure 4.7. Figure 4.7 is generated by putting the maximum allowed deformation $\Delta h = 2.72$ mm (This value will be derived in Chapter 7).

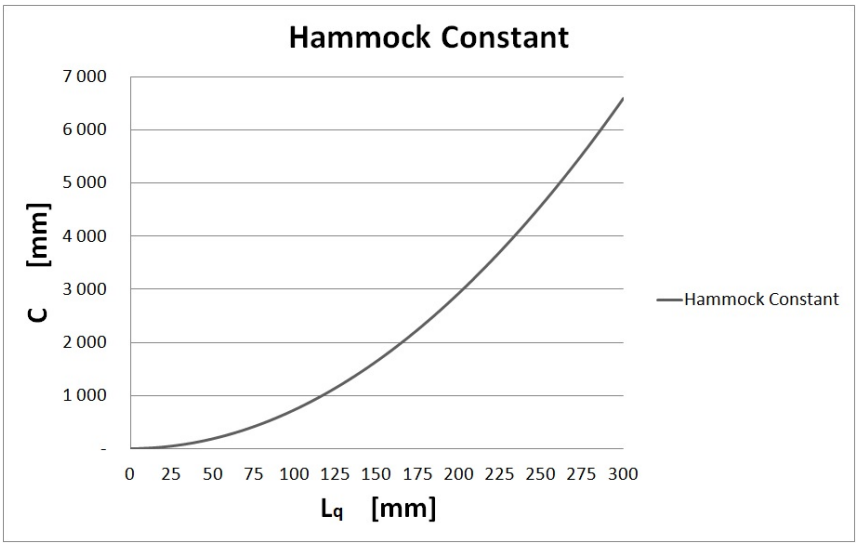

Figure 4.7: *The Hammock Constant*

Equation 4.15 gives an additional bearing capacity with contributions from both sides of the loading area (Figure 4.5). For cases with a load near the end of the sill, the contribution from one side will disappear. To account for this, the equation should be divided by a factor of two, which leads to a conservative approach when calculating the capacity for this type of configuration. Whether this procedure gives an exact representation of the capacity for an end-load, will not be tested in this master thesis, and should be verified by later studies.

The equation representing the *Hammock effect*, is divided into cases with untouched timber on one and two sides.

By adding a load location factor, k_u, a general expression that is valid for the two load cases is found:

$$f_{H,90} = \frac{k_u \cdot E_{s,\Theta} \cdot \varepsilon_{H,j} \cdot h_s}{C} \tag{4.16}$$

$$k_u = \begin{cases} 1 & \text{untouched timber on one side} \\ 2 & \text{untouched timber on two sides} \end{cases}$$

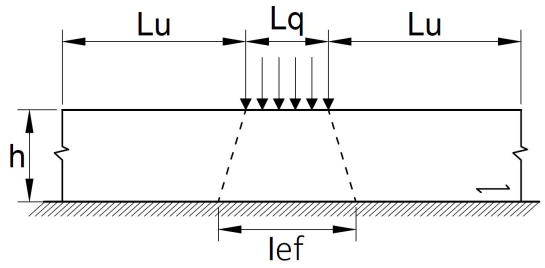

Figure 4.8: Untouched timber on two sides

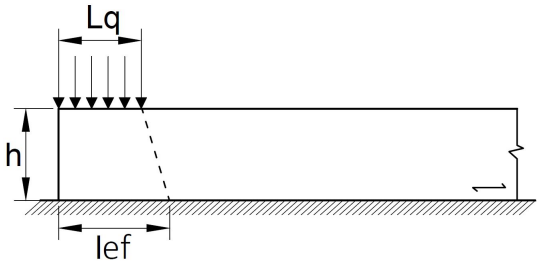

Figure 4.9: Untouched timber on one side

The value of the strain concentration, $\varepsilon_{H,j}$, varies with the amount of untouched timber, and determined by the chosen system configuration. By adding a small amount of untouched timber, the effect will not change drastically, and different domains with a fixed value for the parameter will be generated (Table 4.1).

Case	L_u **[mm]**	$\varepsilon_{H,j}$ [%]	**Effect**
0	$L_u \leq z_0$	0	No
1	$z_0 < L_u < z_2$	?	Partly
2	$Lu \geq z_2$	?	Full

Table 4.1: Strain concentrations for the different domains with untouched timber

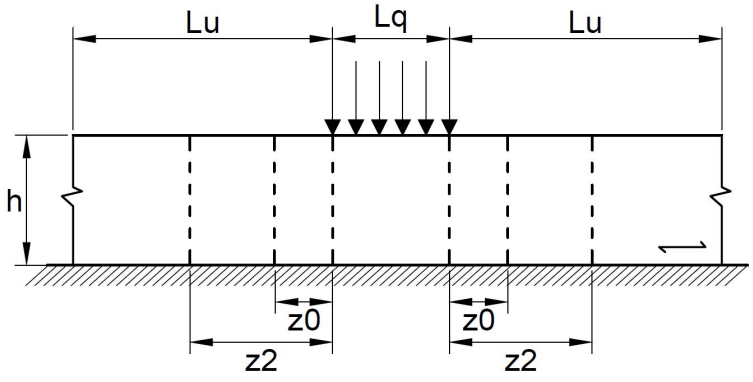

Figure 4.10: Boundary lengths for strain concentration values

By modelling the *Hammock effect* as a rope system with an evenly distributed load, as shown in Figure 4.5, the value of the capacity will increase towards infinity when the loading length, L_q, goes towards zero. To avoid this effect, a lower limit for the ratio between the loading length and the total deformation will be created.

$$\frac{L_q}{\Delta h} > 30 \tag{4.17}$$

This will prevent the additional strength, coming from the *Hammock effect*, from converging towards unrealistically high values for small loading lengths. The value of the limitation is determined by looking at the results from the tests of the calculation model conducted in the thesis.

Special case

For a loading case where the amount of untouched timber is enough to get *full effect* on one side, but only *partly* on the other, the smallest of the two values for the strain concentration will be used (Table 4.1). This leads to a conservative approach, that will ensure that the capacity is not being overestimated. The load location factor is kept equal to 2, since the system is getting contributions from two sides.

Module of elasticity

Since the fibres that are experiencing the tensile force are tilted on the side of the loading area, and defined by the strains in the y-direction, a most accurate size of the Module of Elasticity will be closer to the transverse value, $E_{90,mean}$, than the longitudinal, $E_{0,mean}$. This parameter will get the notation $E_{s,\Theta}$ and receive a value that is twice the size of $E_{0,mean}$, which equals approximately 800 kN/mm^2 for Norwegian CE L40C (Appendix C).

Summary:

- Uses equilibrium considerations to describe the additional compressive strengths from the *Hammock effect*
- The fracture limits is based on a given total deformation found by using both the ASTM- and CEN-model
- The effective length is calculated in the same way as the current regulations in Eurocode 5 part 1-1
- The height of the cross-section is not a factor in the calculation of the capacity
- The model is applicable for capacity control on continuously supported timber sills

Mark: By using the ASTM-model and a fixed value of the allowed deformation, the calculation model does not take the height of the cross-section into account, which results in equal deformation limits for small and large heights.

4.1.3 Model 2: Based on energy

Because of the complex strength properties and structure of the wood, a model based on strains can be difficult to define in an accurate way. Another approach to define a capacity model, is to look at the total energy that is required to reach a certain deformation of the system. Earlier research has shown how the bearing capacity depends on the amount of untouched timber on the side of the loading area. This means that it requires more energy to obtain the same deformation for longer sills than it does for shorter ones.

In order to calculate the bearing strength, boundaries for what is considered acceptable deformation must be defined. With the current regulations based on the CEN-model (Chapter 3.1), larger deformations are allowed for higher versus smaller cross-sections, as a result of a capacity limit defined in terms of a plastic deformation of 1% of the height (0.01h). As a result of this calculation method, there is reason to believe that the stiffness will vary with the chosen height of the section. A model should therefore have a design where a height factor is introduced, that account for these effects.

The CEN-model is chosen to define the compressive strength of the system. This gives, as mentioned earlier, the ability to create a model that takes the cross-section's height into account. To find the capacity, a given plastic deformation underneath the loading area needs to be defined.

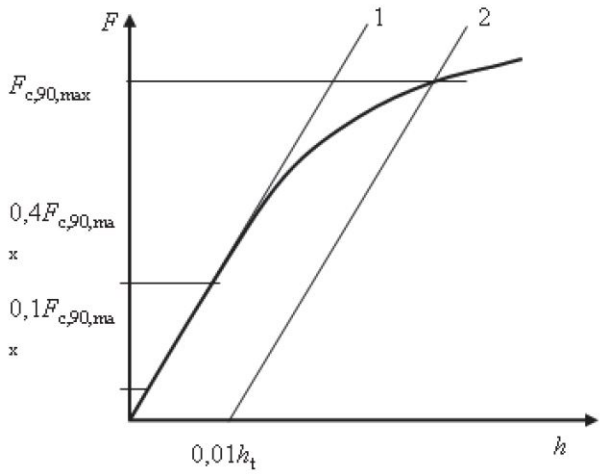

Figure 4.11: CEN-Model

The capacity of the various systems, is determined by looking at the total energy required to reach the given deformation limit. The total energy is calculated by looking at the area underneath the graph of the load-deformation curve. This area will get larger as the amount of untouched timber increases (Figure 4.12), because of a larger stiffness in the system (Gives a "higher" curve).

It is often beneficial to scale the different systems against a reference case, so factors independent of the chosen units are accumulated. The current rules in Eurocode 5 have been criticised, since some of the lengths in the calculation model require a specific unit (l_{ef} has maximum load distribution set to 2x30 mm). The different cases with various amount of untouched timber in the new model, will be scaled against the energy required to get a certain deformation of the reference block. This reference energy will get the notation E_0.

As written previously, a small increase in the amount of untouched timber on the side of the loading area, will not affect the system in any significant way. As a result of this, it will be defined domains dependent on the amount of untouched timber that have certain values.

As the amount of untouched timber increases, a limit will be reached where an additional length will not provide any more energy in the system. An upper limit must therefore also be defined, and this case will get the notation E_2.

Calculation of the energy:

Based on compression tests done with different amounts of untouched timber, plots showing the coherence between the applied compression force and the deformation for the different cases will be generated. By defining a value for the allowed plastic deformation, it will provide boundaries that limits the area underneath the graph, resulting in a restricted area that represents the total energy of the system. To calculate the energy, functions that represent the various load-deformation curves will be generated, which are then integrated with the boundary conditions given by the maximum deformation $\Delta_{max,j}$ (Figure 4.12). This will represent the overall energy that must be put into the system to obtain the allowed deformation limit.

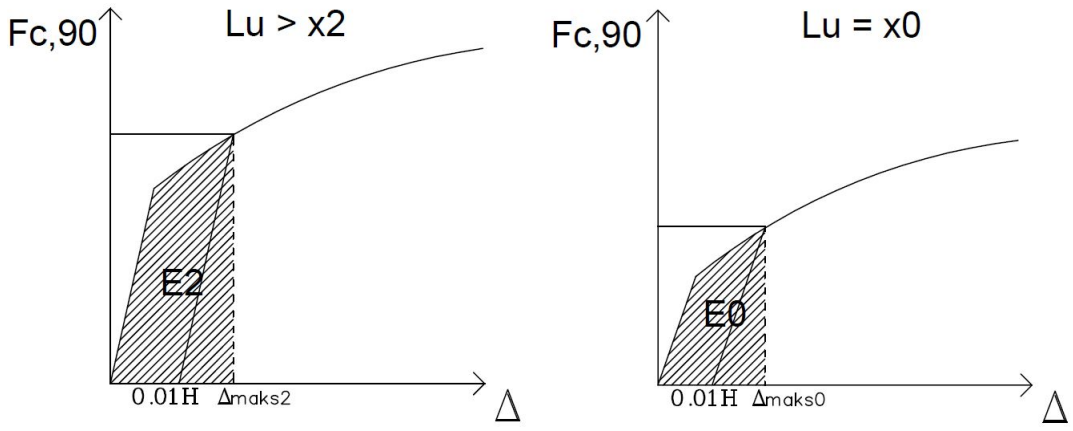

Figure 4.12: Total energy: Case E_2 and E_0

To calculate the total energy that is put into the systems for the different amount of untouched timber, the following mathematical approach is used:

$$E_j = \int_0^{\Delta_{max,j}} \mathrm{f_j}(\Delta)\mathrm{d}\Delta \tag{4.18}$$

$f_j(\Delta)$ generated function representing the load-deformation curve for specimen j
$\Delta_{max,j}$ deformation limit for specimen j

From the different compression tests, domains that will give certain values of the energy will be generated. For untouched timber lengths smaller than x_0, the total energy will be equal to the lower limit found for the reference block, E_0. With lengths larger than x_2, the energy will be equal to the upper limit E_2. In the intermediate state between the two limits, a linear relationship will be created.

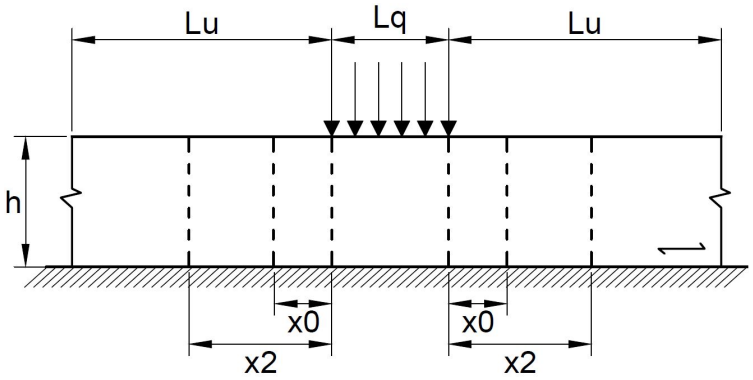

Figure 4.13: Boundary lengths for amount of total energy

Design of the calculation model:

The new calculation model based on energy considerations will have the following design:

$$\sigma_{c,90} \leq k_1 \cdot k_2 \cdot f_{c,90} \tag{4.19}$$

where

$$\sigma_{c,90} = \frac{F_{c,90}}{A} = \frac{F_{c,90}}{L_q \cdot b} \tag{4.20}$$

$f_{c,90}$	compressive strength
k_1	strength factor
k_2	height factor
$F_{c,90}$	applied compressive load perpendicular to the grain
A	loading area
L_q	loading length
b	cross-sectional width

The load applied to the system, will only be taken by the area of the actual loading surface, not an effective area as defined in the current regulations in Eurocode 5. Since the additional bearing capacity, caused by the load being distributed to nearby timber, is taken directly into account during the calculation of the total energy, there is no need to define an effective loading length.

k_1 is the factor that accounts for the extra capacity generated from having different amounts of untouched timber on the side of the loading area, and is defined in the following way:

$$k_{1,j} = \frac{E_j}{E_0} \tag{4.21}$$

E_j is the amount of energy that is needed to reach the given plastic deformation of the height, for a sill with untouched timber length equal to j. The energy for the different cases is scaled against the reference energy, E_0, which leads to the definition of the strength factor k_1, given in Equation 4.21.

As a result of the limits defined previously in this chapter for the different amount of untouched timed, the value of the strength factor k_1, will have a valid value in the following domains:

$$k_1 = \begin{cases} k^l & L_u \leq x_0 \\ k^l + \frac{k^u - k^l}{x_2 - x_0}(L_u - x_0) & x_0 < L_u < x_2 \\ k^u & L_u \geq x_2 \end{cases}$$

k^l is a lower limit for the strength factor, and is applicable for a sill with an amount of untouched timber less than x_0. k^u is the upper limit, and is applicable for lengths larger than x_2. Between these to limits, a linear relationship is generated

Since the CEN-model by definition allows a different limit for the plastic deformation depending on the cross-section's height, this should be included in the capacity calculations. To include this in a model, it will be defined a reference value, that the other heights are scaled against. Compression tests performed on a specimen with the reference height, h_{ref}, will result in a given $f_{c,90,ref}$. By changing the height in the tests and allowing new limits to the deformations (0.01h), it will be generated new values $f_{c,90,j}$ for the different cases.

Based on these assumptions, a factor k_2 can be defined in the following way:

$$k_{2,j} = \frac{f_{c,90,j}}{f_{c,90,ref}} \tag{4.22}$$

Domain	**h [mm]**	k_2
1	≤ 30	?
2	30-60	?
Ref	90	1.0
3	90-120	?
4	120-150	?
5	≥ 150	?

Table 4.2: Height factor within the different domains

The domains in Table 4.2, are based on the tests conducted in this master thesis, where the maximum height was limited to 150 mm.

Summary:

- Based on energy considerations
- Uses the CEN-model to find the compressive strength
- Uses generated functions that describe the real material behaviour
- Takes the height of the cross-section into account
- The model is applicable for capacity control on continuously supported timber sills

4.2 Serviceability Limit State (SLS)

4.2.1 Earlier starting point

In the current Eurocode 5 regulations, there are no specific requirements or models to calculate in a Serviceability Limit State. The way the model is designed, Ultimate and Serviceability Limits are mixed into the same calculation formula, and separated by changing or adding different parameters. This leads to a definition of the two cases that can be messy and sometimes a bit unclear.

4.2.2 Model for calculating in serviceability state

This study aims to create a model that provides the possibility of calculating in Serviceability Limit State, so designers can determine the limits of the allowed deformations based on their own needs and preferences. To be able to do this, a calculation method that gives a relationship between an applied load and the associated deformations must be derived.

The Serviceability Limit State and the requirements to the allowed deformations, should be limited to avoid failure mechanisms that are essential for the bearing capacity. Therefore it should not be allowed deformations in serviceability that violates the acceptable limits found in Ultimate Limit State

To define serviceability limits, restrictions will be made to the maximum allowed total deformations, Δ_{max}, underneath the loading area. These limits will consist of a combination of a permanent, Δ_{per}, and non-permanent, Δ_{rev}, part.

With the current regulations, the maximum allowed plastic deformation is restricted to 0.01 times the height (CEN-model). Allowing this deformation also allows for non-permanent deformations (Figure 4.14). Combined, these two contributions form the foundation of the maximum serviceability limit, which will automatically satisfy the requirements set forth as accepted deformation in Ultimate Limit State.

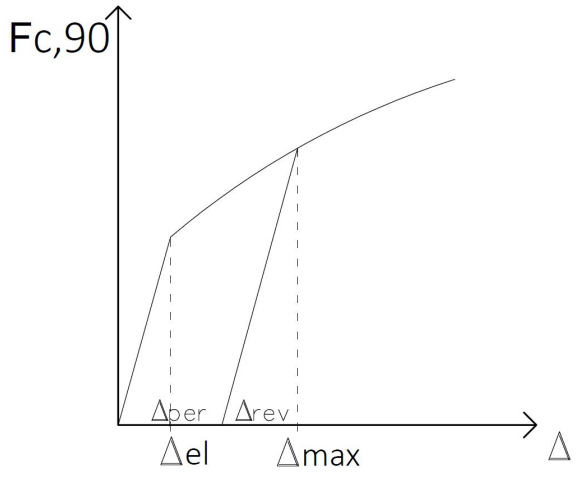

Figure 4.14: Total allowed deformation in Serviceability Limit State

To describe how the timber deforms under a load perpendicular to the grain, the starting point will be to look at the load-deformation curves generated from compression tests. This will give a direct description of the material behaviour, and provide a correlation between the two parameters. This study attempts to find a function for this correlation, which give the designer an easy and precise way to calculate deformations.

A function that describes the correlation between load and deformation can be found through a curve fitting with the help of Least Square Method (LSM). The function that is being used must have properties that can represent the load-deformation curve in an accurate way. It must also be able to describe both linear and non-linear behaviour.

The load-deformation curve shows a relationship at the beginning of the load cycles that can be described with a linear function, but after a certain point the relationship becomes non-linear. This is a result of the wood properties that under small loads behaves elastically, but which enters a ductile region when the load reaches a certain level. When the material exceeds the yield limit, the fibre structure changes and the forces in the cross-section will be redistributed. In the ductile region, the material will undergo a hardening process, making the system able to carry more load without getting failure mechanisms, but with rapidly increasing permanent deformations.

Simplified Calculation Method:
A simplified way to describe the relationship between load and deformation, is to treat the material behaviour as generally ductile. With this method it is assumed irreversible deformations from the beginning of the load cycle, ignoring the initial elastic properties.

A way to generate a ductile relationship, is to use the Power Law or Voce Law, which are known functions in Material Mechanics, often used to describe such material behaviours.

Power Law	Voce Law
$F = K \cdot \Delta^n$	$F = C_1(1 - e^{-C_2\Delta})$

In the functions, F is the applied load required to obtain a plastic deformation Δ. K, n, C_1 and C_2 are all constants describing the material behaviour, and are found by curve fitting with Least Square Method.

Both of these functions describe the load-deformation curves in a representative way, and by inverting the formula, an expression for the total deformation of the system can be found. The expression will be dependent on the applied compressive load, and will give the designer the ability to determine acceptable deformations. The desired total deformation can not exceed the serviceability limits, because this will violate with the definition of the bearing capacity of the system.

Power Law	Voce Law
$\Delta = (\frac{F}{K})^{\frac{1}{n}}$	$\Delta = -\frac{1}{C_2} ln(1 - \frac{F}{C_1})$

From the definition of the limit state and total allowed deformations found by the CEN-model, the capacity is dependent on the height of the cross-section. As a result of this definition, different deformation limits are allowed for different heights. To account for this effect, the height factor k_2, defined in Section 4.1.3, will be included in the serviceability calculations.

In this thesis, Voce Law will be used to describe the non-linear material behaviour of the wood, on behalf of the Power Law.

Based on these assumptions, the following requirement in the Serviceability Limit State should be satisfied:

$$\Delta < \Delta_{max} \cdot k_2 \tag{4.23}$$

As previously described, the load-deformation curves are largely dependent on the amount of untouched timber on the side of the loading area. To take this into account in the serviceability calculations, two separate limit states will be defined, both for the reference case and for systems with amount of untouched timber larger than the upper limit x_2. For the intermediate case, the requirements will be equal to the reference case.

Lower case ($L_u \leq x_2$):

$$\Delta_0 = -\frac{1}{C_{2,0}} ln(1 - \frac{F}{C_{1,0}}) < \Delta_{0,max} \cdot k_2 \tag{4.24}$$

Upper case ($L_u > x_2$):

$$\Delta_2 = -\frac{1}{C_{2,2}} ln(1 - \frac{F}{C_{1,2}}) < \Delta_{2,max} \cdot k_2 \tag{4.25}$$

More Accurate Calculation Method:

A more accurate model to describe the material behaviour, that takes both the linear and non-linear behaviour into account, is to divide the load-deformation curve into two domains. This will give a linear function at the beginning of the loading cycle, and a non-linear function after a certain limit.

The limits dividing the different domains for the linear and non-linear functions will be found by looking at the material behaviour from the compression tests, and taken from the load-deformation curves.

Based on the given assumptions, a model for the serviceability state can be expressed as following:

Elastic domain ($0 \leq \Delta \leq \Delta_{el}$):

$$\Delta^{el} = \frac{F}{B}$$

B is a constant describing the material behaviour in the elastic domain, which is found by curve fitting, and F is the applied compression load.

Plastic domain ($\Delta_{el} < \Delta \leq \Delta_{max}$)**:**

By using the defined Voce function, the following expression can be used to describe the non-linear domain:

$$\Delta^{pl} = -\frac{1}{C_2} ln(1 - \frac{F}{C_1})$$

In this case, separate serviceability limits, Δ_{max}, must be defined, because of the differences in strength between systems with and without untouched timber. The height factor, k_2, is also included, and the calculation methods for the intermediate state between the reference case and the upper limit will be put equal to the reference case. This will give the following design for serviceability state for the different domains:

$$\Delta^{el} < \Delta_{el} \cdot k_2 \tag{4.26}$$

$$\Delta^{pl} < \Delta_{max} \cdot k_2 \tag{4.27}$$

Lower case ($L_u \leq x_2$):

Elastic domain:

$$\Delta_0^{el} = \frac{F_{c,90}}{B_0} < \Delta_{0,el} \cdot k_2 \tag{4.28}$$

Plastic domain:

$$\Delta_0^{pl} = -\frac{1}{C_{2,0}} ln(1 - \frac{F}{C_{1,0}}) < \Delta_{0,max} \cdot k_2 \tag{4.29}$$

Upper case ($L_u > x_2$):

Elastic domain:

$$\Delta_2^{el} = \frac{F_{c,90}}{B_2} < \Delta_{2,el} \cdot k_2 \tag{4.30}$$

Plastic domain:

$$\Delta_2^{pl} = -\frac{1}{C_{2,2}} ln(1 - \frac{F}{C_{1,2}}) < \Delta_{2,max} \cdot k_2 \tag{4.31}$$

Summary:

- Based on a predefined function to describe the material behaviour (Voce Law)
- Used the material behaviour directly
- Based on allowed deformation underneath the loading area
- Two different serviceability limits:

  One applicable for amount of untouched timber less or equal to x_2

  The other for amount larger than x_2
- Two different calculation methods:

  Simplified Method: Ductile material behaviour in the whole deformation domain

  More Accurate Method: Accounts for both an elastic and plastic material behaviour

4.2.3 Different types of wood

The constants describing the load-deformation curves, found by the Least Square Method, will vary with the type of wood. This is due to the changes in strength properties. Compression tests should therefore be conducted to find the properties and material constants that describes the load-deformations curves for every type of wood. The deformation limits will most likely change between the different types, and these limits should also be determined and tabulated together with the constants. Tables 4.3 and 4.4, show some of the standard types found on the market for combined glue-laminated timber.

Lower case ($L_u \leq x_2$):

$L_u < x_2$	GL24c	GL26c	GL28c	GL30c	GL32c	GL34c
B						
C_1						
C_2						
Δ_{max}						

Table 4.3: Parameters and deformation limits for the *Lower case*

Upper case ($L_u > x_2$):

$L_u > x_2$	GL24c	GL26c	GL28c	GL30c	GL32c	GL34c
B						
C_1						
C_2						
Δ_{max}						

Table 4.4: Parameters and deformation limits for the *Upper case*

Chapter 5

Test description

To determine and verify the various parameters in the new calculation models derived in this thesis, different tests will be conducted in the laboratory at the Department of Structural Engineering. Compression tests will be performed with loads perpendicular to the grain on systems with different sill lengths and cross-sectional heights. This will generate data that will be used to describe the material behaviour of the wood, and provide a basis for the parameters implemented in the models developed for both Serviceability Limit State (SLS) and Ultimate Limit State (ULS).

5.1 Test set-up and software

The aim of these tests is to gain an increased understanding of the complex deformation patterns in timber sills loaded perpendicular to the grain. There are several mechanical phenomena that mobilizes during such loadings, and advanced measuring equipment is required to be able to capture and distinguish between the various effects.

5.1.1 ARAMIS

ARAMIS is a software that is used to run and process data from tests based on image analysis. The program provides an opportunity to describe deformation patterns in different directions, and gives the ability to generate graphical representations of the results. ARAMIS uses high resolution images taken of specimens during testing to describe the pattern based on correlations between images taken at different stages of a load cycle.

Before the compression test is initiated, the surface of the specimens are covered with a white color in the areas where data is to be retrieved. On top of the white surface, a random pattern of black dots is sprayed on, which will serve as reference points for the deformation measurements (Figure 5.1). During the loading cycle of the specimen, the black dots will change position from their reference point, and by looking at the relative change, a deformation pattern in the different directions can be defined. The relative changes are measured by continuously taking pictures of the specimens during the deformation process. Each picture represents a time step with a given load and an associated deformation, and by comparing the different time steps, a deformation pattern and stress/strain field in the specimens can be found.

The cameras will take a predetermined amount of images in a specified time interval, and each of these intervals are recorded as *stages*. The first stage is set equal to 0, and from this starting point, changes in the strains, stresses, or deformations can be calculated. The duration of the tests will vary within the different load configurations (See Section 5.1.2). This variation will affect the number of photos taken during the tests, as well as change the time intervals. This is done only to be able to take pictures throughout the whole deformation process for the different configurations, and does not impact anything else. For the reference block a total number of 120 images is chosen, with a time interval equal to 5 seconds between each picture. This will give an overall picture period of 10 minutes per specimen. For tests with different amounts of untouched timber, the total number of images is increased to 150, with a rate of one picture every 7 seconds. This results in a image period of 15 minutes per specimen.

When the different images taken during the load cycle are implemented in the analysis section in ARAMIS, it may, in some cases, give areas on the analysis surface of the specimen, that the program is not able to generate data from. ARAMIS has a built-in function in the software that makes it possible to run a 3D-interpolation between the side-lying points, where data has been collected. By doing this, a complete data set can be found for the entire surface.

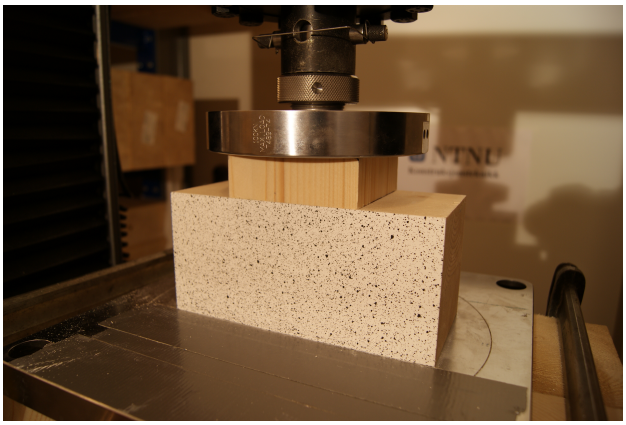

Figure 5.1: Test system

5.1.2 Test system

The test system will consist of a continuously supported timber sill loaded perpendicular to the grain. To get a realistic loading system as possible, the load will be transferred through a block of wood between the machine and sill, representing the timber stud coming down in the connection (Figure 5.1). The block will be loaded in the longitudinal direction of the wood, and changed to after a given number of tests. Since the load coincides with the longitudinal direction of the grain for the block, it will not produce disturbances in the measurements of the total deformations of the sill, because of a significant higher stiffness in this direction. On the top surface of the specimen the loading area is drawn, making it easy to place the loading block in the correct position before initiating the compression tests. The duration of the compression test is chosen so that the estimated fracture load will occur within 300 seconds (5 min). This is a value recommended in NS-EN 408:2010+A1:2012 [16].

To be able to get as comparable result between the different tests as possible, the specimens was carefully checked for irregularities such as knots and cracks, and the orientation of the annual rings strictly underneath the load is kept constant.

The machine producing the compression force, is an INSTRON, with a maximum load equal to 100 kN. This machine is able to measure both the applied load and the associated deformations.

The compression machine will be given settings which provides a certain deformation of the height per minute. For both the reference block and the specimens with untouched timber, this speed will be set equal to 2 millimetres per minute (mm/min). For the reference blocks, the tests will end when the specimens have reached a total deformation under the loading area equal to 20 mm. This is more than enough to find the parameters needed in the various models derived in this thesis. With the current regulations, only a deformation in the range of 0-5 mm is needed to define the different parameters. The reason for running the tests to a deformation as high as 20 mm, is to see how the material behaves and which mechanical phenomena that occur at this magnitude of deformation. With a loading speed equal to 2 mm/min, and a maximum deformation set to 20 mm, it will result in a total test period equal to 10 min for each specimen. This is the same time length as the image period implemented in ARAMIS. For the specimens with untouched timber, it will be allowed a total deformation under the loading area equal to 30 mm, because of a greater capacity, which will result in failure modes at larger deformations. This will give a total test period equal to 15 mm for each specimen (the same length as the image period implemented in ARAMIS).

Since the camera system that is photographing the specimens during the tests is attached to a foot with certain height, the test set-up had to be modified, to be able to get the two aligned. This was done by putting massive timber blocks underneath the specimens, with thick metal plates in between (Figure 5.2). The direction of the fibres in the timber blocks was chosen so the loading direction was parallel with the longitudinal direction (the strongest axis). This was done to prevent disturbances in the deformation measurements of the test specimens. The blocks were cut flat on the top, making the loading area uniform over the entire surface.

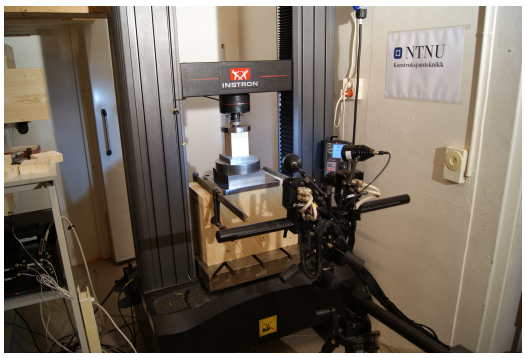

Figure 5.2: Test system with massive timber blocks and metal plates

Figure 5.3: Cameras and light sources used for optical analysis

To be able to capture accurate results from the image analysis, the surfaces of the specimens are illuminated by different light sources. Two light sources directly mounted on the camera system and one additional spotlight was used (Figure 5.3). This will provide a clear contrast between the bright painted surface and the black dots (Figure 5.1). It is important for the test results, that the specimens are neither overexposed nor too dark. To avoid reflections from the metal plate located underneath the specimens, the plates were covered by a gray coloured tape.

5.1.3 Specimens

An overview of the geometries for the different test specimens are located in appendix A. The two different test systems are shown in Figure 5.4 and 5.5.

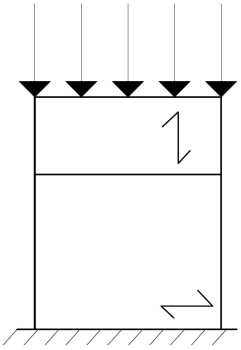

Figure 5.4: Test system 1

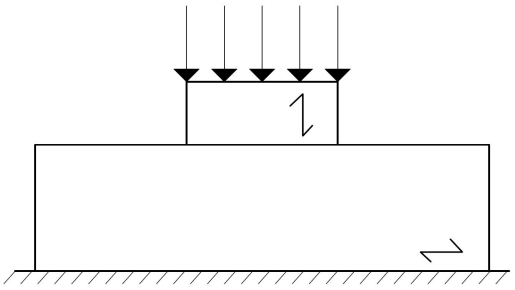

Figure 5.5: Test system 2

Chapter 6

Test results

6.1 Parameters

It is desired from the various compression tests conducted in this paper to describe and find the different parameters included in the new calculation models derived in Chapter 4.

The following parameters will be determined from the compression tests:

k_2	Factor regulating the capacity for different cross-section heights (Model 2)
k_1	Factor accounting for the variation of total energy required to reach the fracture criterion for different amount of untouched timber (Model 2)
h_s	The effective tension height for the *Hammock effect* (Model 1)
$\varepsilon_{H,j}$	Strain concentrations on the side of the loading area for different amount of untouched timber (Model 1)

6.2 Test 1: Reference block

During this test set-up, all the specimens had a constant cross-sectional geometry equal to 90x89 mm (LxB), with the entire top surface loaded in compression. Tests were conducted with variations in the heights of the cross-sections, ranging from 30-150 mm. For each height, 4-5 tests were performed. The reason for conducting this specific test, is to determine the factor k_2, which scales the total bearing capacity for different cross-sectional heights.

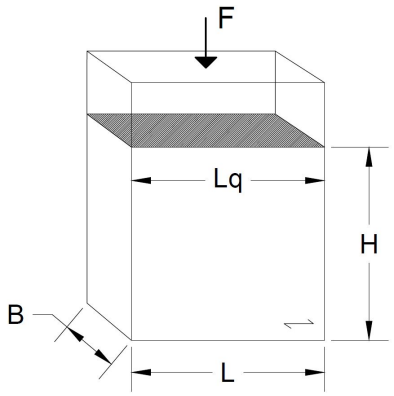

Figure 6.1: Test system 1: Reference block

6.2.1 Specimen R30

For cross-sections with small heights, the initial material behaviour is quite stiff compared to higher sections. This is a result of the small magnitude of air and void in the wood structure that needs to be pressed together. Figure 6.2 shows how the capacity is rapidly increasing when the deformation reaches a certain size. As the specimen is pressed together, a more compact cell structure is generated, resulting in a very stiff system (Figure 6.3). When the height of the cross-section is quite small, it will not reach a point where critical failure mechanisms occurs, and the specimens can in theory be loaded with an infinitely large compression force.

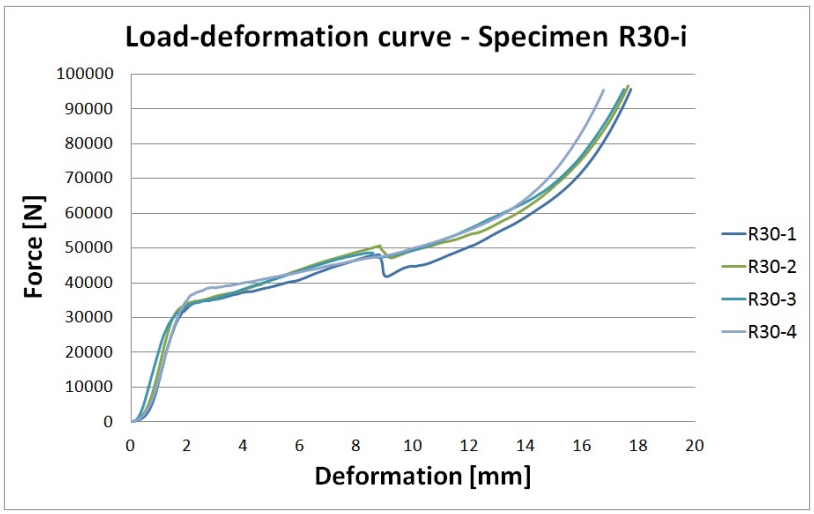

Figure 6.2: Load-deformation curves - Specimen R30-i

The test result shows a similar material behaviour for all the four different specimens. They all have a linear elastic domain during the first 2 mm of deformation, reaches a yielding point at 35 kN, which then leads the material into a ductile domain and a plastic behaviour. When the total deformation reaches 9 mm, all specimens experience a failure mechanism, which results in a drop in bearing capacity. This mechanism is shown in Figure 6.4, and is a result of the cell structure being ripped apart in the transition between annual rings. Farther into the loading domain, a rapid increase of capacity is generated, as a result of the cell structure getting more and more compact, and no more failure mechanisms will occur after this point.

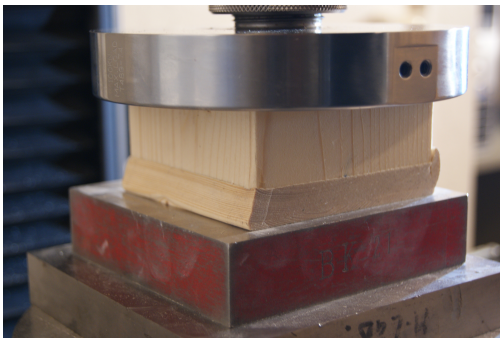

Figure 6.3: Compact cell structure generated for specimen R30

Figure 6.4: Failure mechanisms for specimen R30-i

The results from the compression tests, shows an almost identical load-deformation curve for all specimens, and it is therefore reasonable to believe that a good and accurate material behaviour has been found for this type of cross-section.

All tests conducted for the different cross-section heights, were stopped when a total deformation of 20 mm was reached, except for this one. Because of limitations to the maximum load of the test machine (100 kN), the tests had to be stopped after a deformation of only 18 mm.

6.2.2 Specimen R60

The tests performed on subjects with sectional height equal to 60 mm, resulted in an equal material behaviour and load-deformation curves for all the different specimens. This indicates good and uniform samples with few faults or irregularities. The initial stiffness is lower for this test, compared to the specimens with a height of 30 mm, because of the increase of air and voids in the timber cells that needs to be compressed.

When the specimens reaches a total deformation of 9-10 mm, the cells are starting to separate in the transition between the annual rings (Figure 6.6), which results in a drop of the bearing capacity.

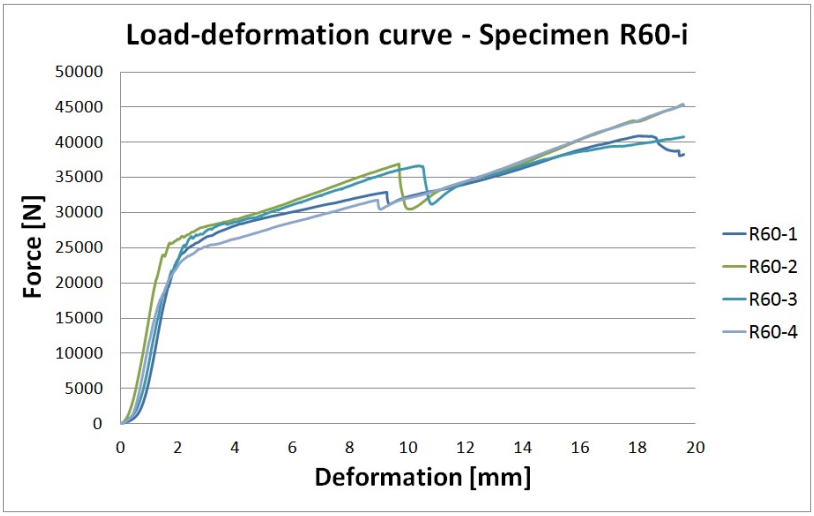

Figure 6.5: Load-deformation curves - Specimen R60-i

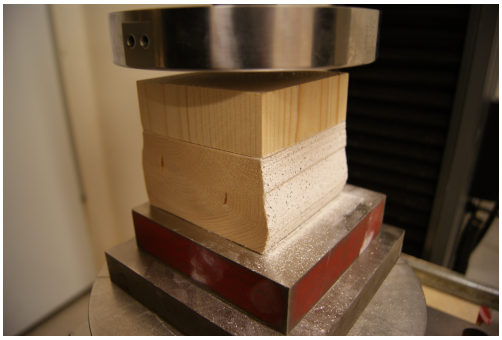

Figure 6.6: Failure mechanism for R60-i

6.2.3 Specimen R90, R120 og R150

When the test specimen reaches a certain height, the initial stiffness starts to approach each other. This gives a linear region for the higher cross-sections, which are overlapping. By increasing the load further into the plastic domain, it results in different failure mechanisms for the higher cross-sections, leading to a spread of the total capacities and the material behaviours. These failure mechanisms will occur in different places in the load-deformation cycle, resulting in capacity drops that do not coincide with the various compression tests, like it did for the lower cross-sections.

The failure mechanisms resulting in the capacity drops are the same as for the lower heights, where the transition along the annual rings are ripped apart (Figure 6.8). Before the mechanism is generated, the section is bulging out both at the front and back, creating a tension force that is pulling the fibres apart. Another failure mechanism that occurred in most of the tests, resulting in large capacity drops, was fracture transverse to the radial direction of the grain (Figure 6.9). This is also a consequence of the generated tension force coming from the bulging of the section. A commonality of all the failure mechanisms was the propagated fracture acting in the same direction of the compression force, and along the height of the cross-section.

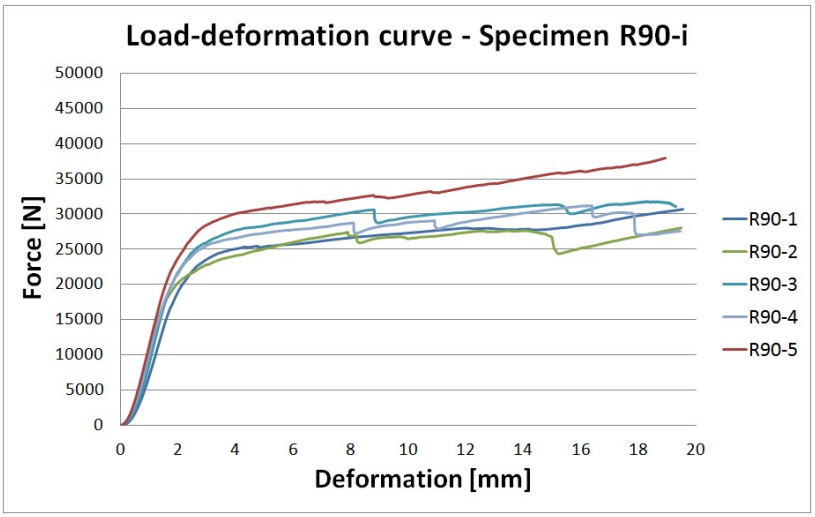

Figure 6.7: Load-deformation curves - Specimen R90-i

For the compression test on specimen R120-3, a clear drop in capacity was found at a deformation of 9 millimetres. This was a result of a large part of the front being ripped off from the rest of the specimen (Figure 6.8). This resulted in the remaining cross-section having a significantly smaller area to carry the load. As can be seen in Figure 6.10, the capacity rapidly decreased after this fracture mechanism occurred.

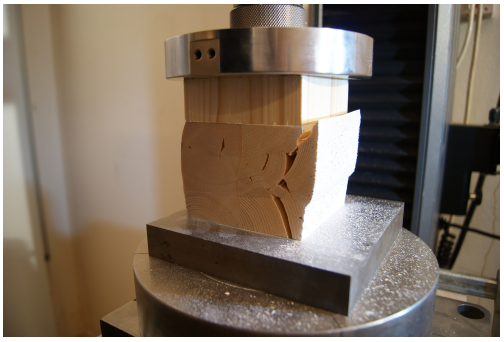

Figure 6.8: Failure mechanism along the annual rings

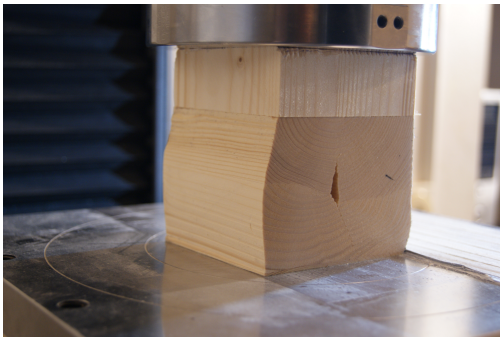

Figure 6.9: Failure mechanism transverse of the radial direction

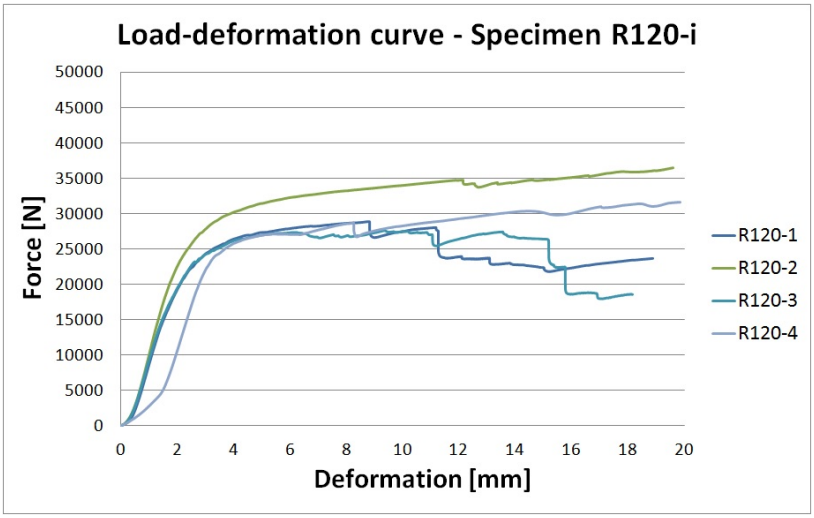

Figure 6.10: Load deformation curves - Specimen R120-i

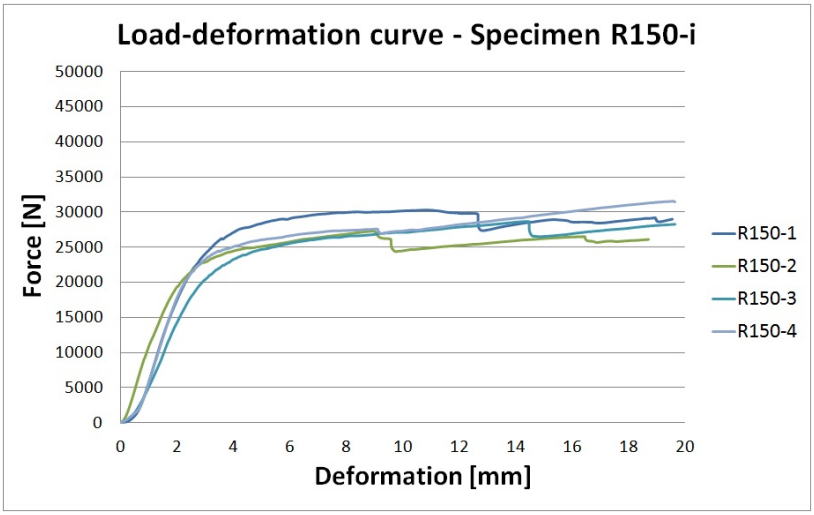

Figure 6.11: Load-deformation curves - Specimen R150-i

6.3 Test 2: Sill

During these tests, the cross-sectional height and loading length were held constant, with values equal to H = 200 mm and L_u = 90 mm. Compression tests were conducted with different amounts of untouched timber on the side of the loading area, with lengths varying from 30 to 200 mm. The background for these tests is the desire to determine the parameters k_2, ε_{Hi} and h_s, included in the calculation models derived in Chapter 4.

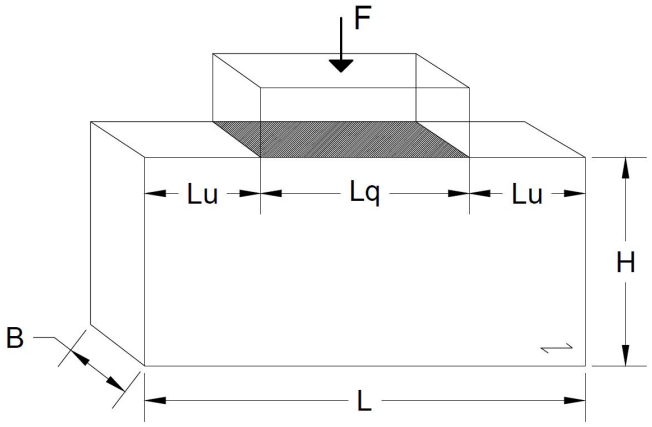

Figure 6.12: Test system 2: Sill

6.3.1 Specimen Lu30

The geometry of the specimens in this test is very similar to the reference blocks R90, as a result of a small amount of untouched timber. Yet there is already a clear difference in the bearing capacity, because of the load being distributed over a larger surface. The initial stiffness has increased, and it requires significantly greater loads to get the same deformations as found for the reference case.

The compression test conducted on the first specimen, Lu30-1, was stopped after a total deformation of 20 mm, the same magnitude as the reference block. According to the results from the load-deformation curve, no distinct failure mechanisms had occurred during this deformation, and it was therefore decided to increase this value to 30 mm. This was done to be able to capture the behaviour and failure mechanisms for these type of sections.

All test specimens showed a very similar material behaviour in both the linear and non-linear domain. After a deformation in the area of 7 mm, wood on the edge of specimen started to rise up along the annual rings, which can be seen in Figure 6.13, as a drop in the load-deformation curve. This resulted in a clear visual fracture mode, but only a small drop in the capacity of the cross-section was registered (Figure 6.14).

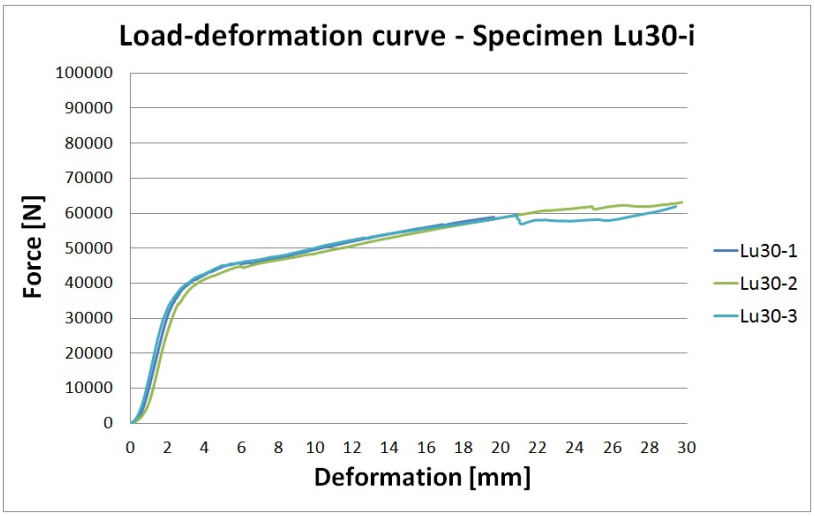

Figure 6.13: Load-deformation curves - Specimen Lu30-i

The differences between the fracture mechanisms for the reference block and the specimens with untouched timber equal to 30 mm, was essentially the direction of the fracture propagation. For the reference block, the propagation of the fracture was mainly in the direction of the applied load, while in the transverse direction for R30 (Figure 6.14). The fractures were also generated further down in the cross-section for the cases with no untouched timber.

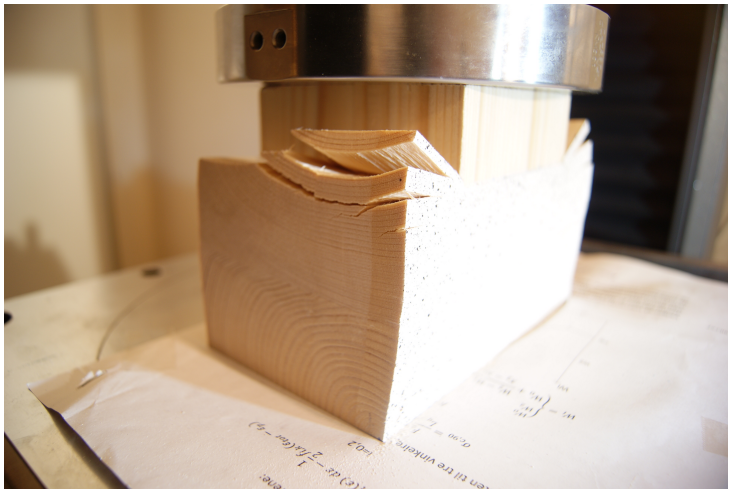

Figure 6.14: Wood lifted up at the edges of the specimen

6.3.2 Specimen Lu50

For the specimens with untouched timber equal to 50 mm on each side of the loading area, a slightly bigger spread in capacity between the different tests was found. The linear domain behaves the same for all tests, but a larger spread appears when entering the ductile domain. In addition to the uplift of the wood at the ends, some cracks extending from the middle of the loading area to the edges appeared. The time of occurrence of these cracks, varied between the different tests, which resulted in variations in the load-deformation curves. This led to different bearing capacities and fracture points for the specimens. By loading further into the plastic domain, these effects became more prominent, and the amount of wood lifted up at the edges increased (Figure 6.16).

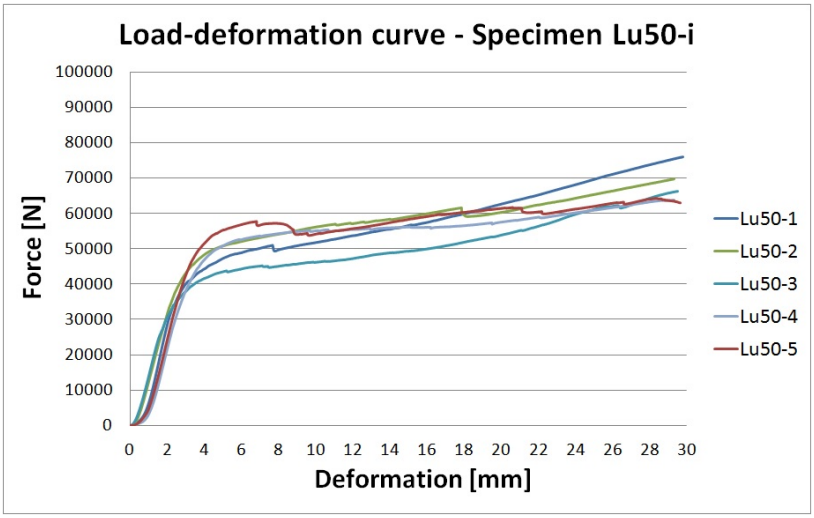

Figure 6.15: Load-deformation curves - Specimen Lu50-i

For test specimen Lu50-5, a large drop in capacity was found at a deformation equal to 9 mm. This was a result of a crack propagation along the height of the specimen, which occurred in the same way as the failure mechanism described for the reference block.

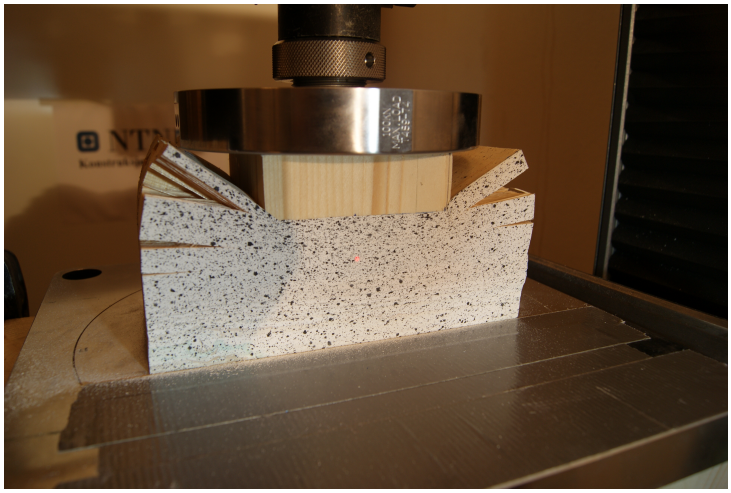

Figure 6.16: Large amount of wood lifted up at the edges of the specimen

6.3.3 Specimen Lu70 and Lu100

The results for these two lengths of untouched timber showed a small change in capacity for deformations up to 30 mm. For all the specimens during these tests, cracks were generated extending from the middle of the loading area to the edges, which lead the drop in capacity. These cracks occurred somewhat later for Lu100 then Lu70. The load-deformation curves are still increasing after a deformation of 30 mm for specimen Lu100, which means that a fatal failure mechanism has not yet occurred. The curves for Lu70 are starting to stabilize, meaning that the total bearing capacity is most likely found, and an further increase in load will probably result in a fracture mode.

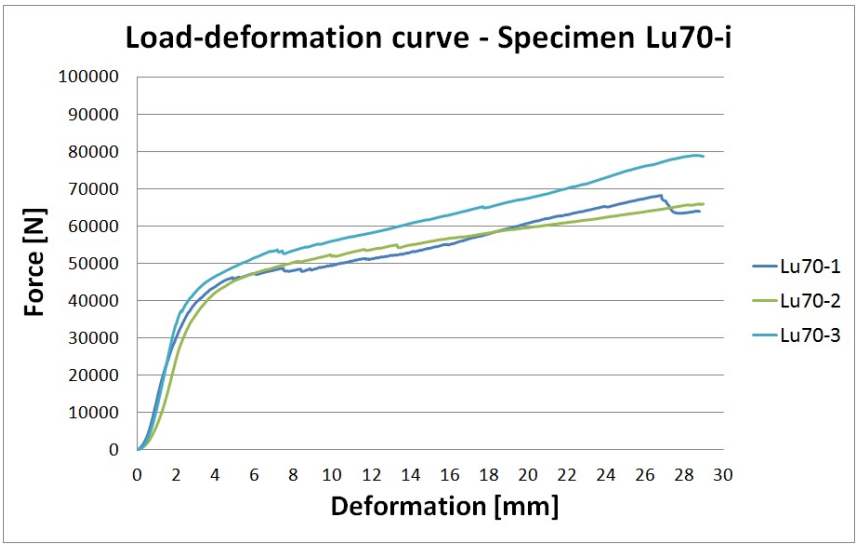

Figure 6.17: Load-deformation curves - Specimen Lu70-i

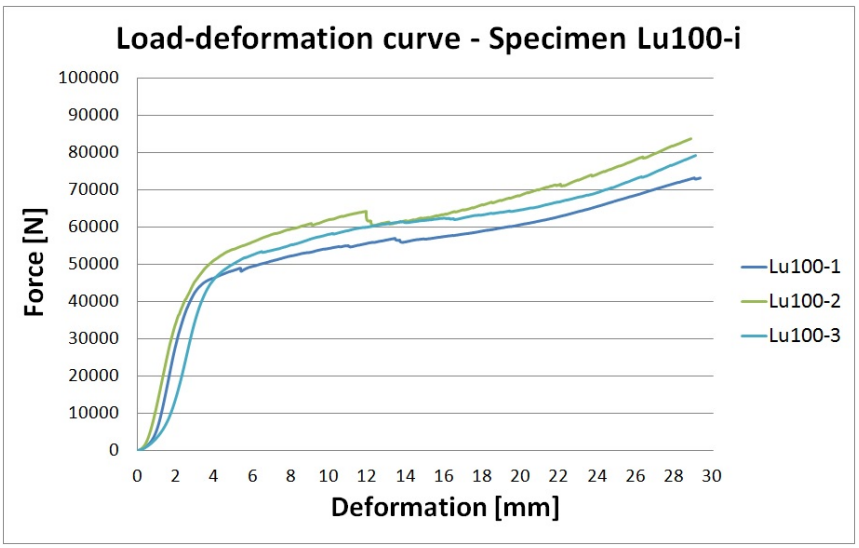

Figure 6.18: Load-deformation curves - Specimen Lu100-i

6.3.4 Specimen Lu150 and Lu200

For the two longest specimens, the test set-up was not large enough to provide continuous support under the entire sill. The support plate had a length of 300 mm, which resulted in some wood not being supported at the edges. This was the case for lengths of 45 mm and 85 mm for Lu150 and Lu200, respectfully. The lack of edge support for some timber lengths was not deemed to significantly influence the results.

For higher amount of untouched timber, a strictly increase of the capacity is found during the entire loading domain. The fracture mechanisms are quite similar to those with smaller lengths, but occur later in the deformation process. The amount of wood that is lifted up on the edges was also significantly larger, and did not occur until a total deformation of 20 mm was reached.

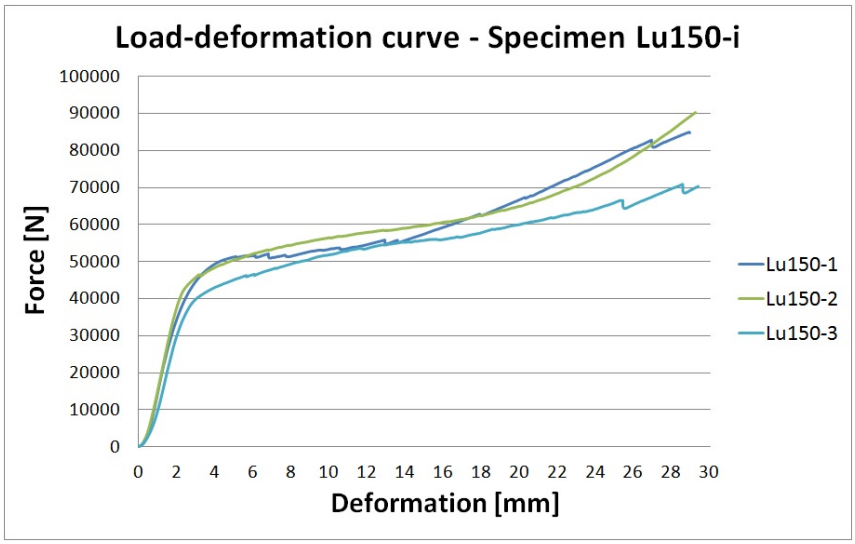

Figure 6.19: Load-deformation curves - Specimen Lu150-i

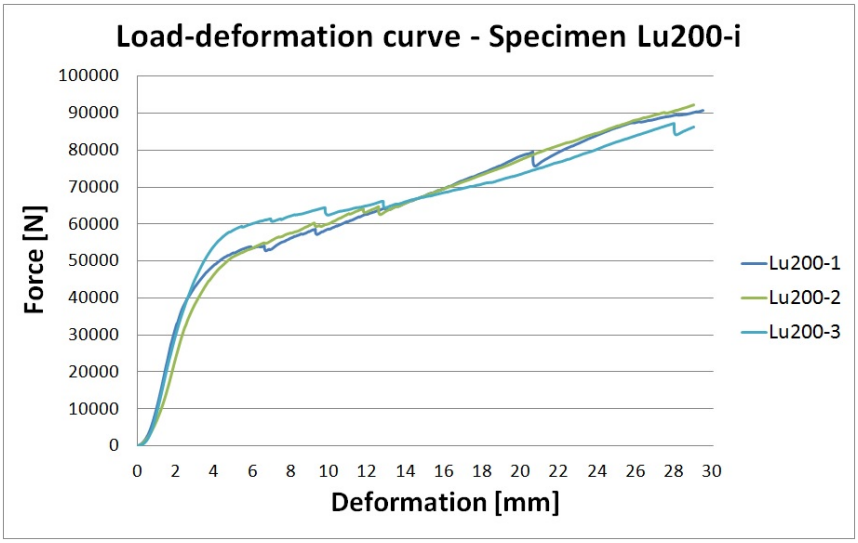

Figure 6.20: Load-deformation curves - Specimen Lu200-i

Some of the specimens, such as Lu150-2 did not suffer from cracks or raised edges, which resulted in a deformation pattern only directly underneath the loading area (Figure 6.22). In this case, the loading block between the specimen and machine was pushed into the sill, and side-lying fibres were cut off, resulting in only a local failure mode. This resulted in a much smoother load-deformation curve without the sudden drops in capacity, generated from the various failure mechanisms. Though the deformation pattern is different for the specimen Lu150-2, the load-deformation curve and the total capacity is the same as for the other tests. Based on the deformation pattern, where the block is only pressed into the sill without any form of global fracture mechanisms and cracks, there is a reason to believe that a critical length has been reached, and that a further extension will not give a significant impact on the bearing capacity.

As a result of the limitations of the compression machine used in this thesis, it was not possible to do tests on sills with untouched lengths longer than 200 mm on both side of the loading area. Some of the specimens still had some global fracture modes such as the lifting of the wood at the edges, and more tests should be conducted with increased lengths, to verify the upper limit.

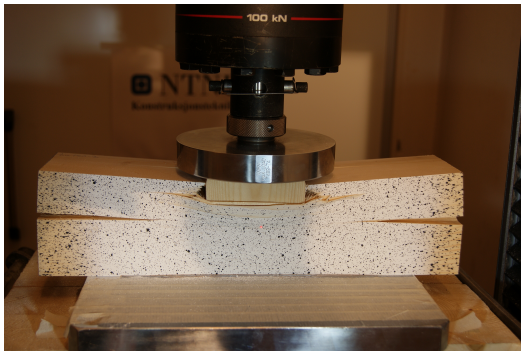

Figure 6.21: Global fracture mechanism

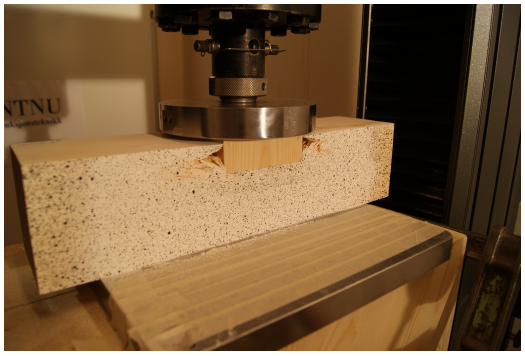

Figure 6.22: Local fracture mechanism

6.4 Mean values

From the tests with different cross-sectional heights and lengths, a mean value is calculated for each case. This gives the best approximation of the overall material behaviour of the specimen, and is used when the parameters in the new capacity models are determined. The load-deformation curves between the different specimens starts to differ from each other in a greater magnitude when entering the ductile domain and deformations larger than 10 mm. A mean value calculated beyond this deformation will not describe the material behaviour in an accurate way. Using information and data values from this domain to calculate parameters will result in poor results, and therefore will not be done in this thesis. The new parameters will be found in the domain bounded by the first 10 mm, where the average value describes the material behaviour in a satisfactory manner, and where no failure mechanisms have yet occurred.

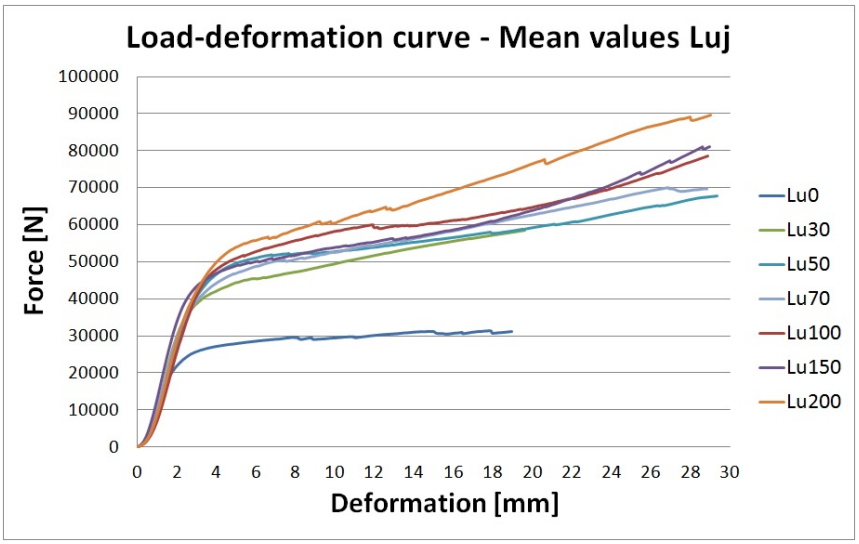

Figure 6.23: Load-deformation curves (Mean values) - Specimen *Luj*

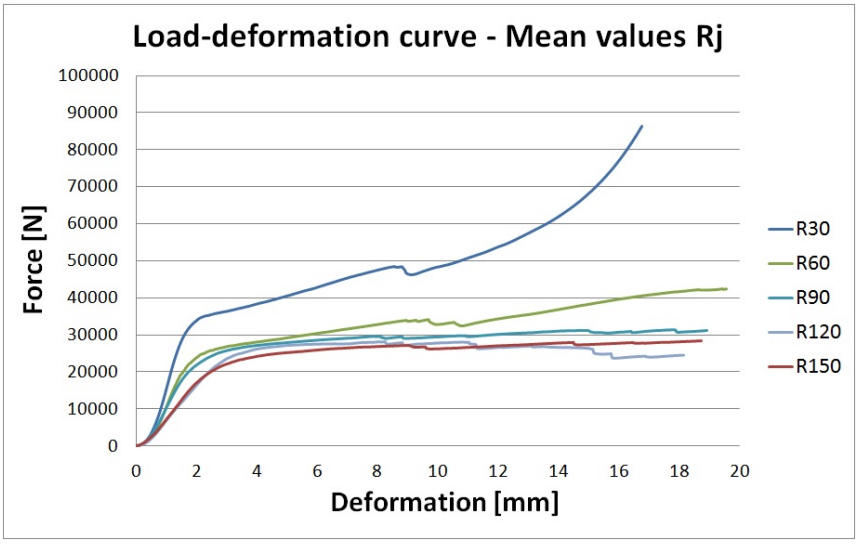

Figure 6.24: Load-deformation curves (Mean values) - Specimen *Rj*

Specimens that differed considerably in strength and material behaviour from the rest, such as R120-2 and R150-1, were neglected in the calculation of the mean values. The reason for the large capacities of these to specimens, was knots located directly underneath the loading area.

6.5 The effect of untouched timber

The influence that the amount of untouched timber has on the capacity described in Section 3.3, agrees well with the results from the compression tests conducted in this thesis. Figure 6.25 shows the results from compression tests conducted by Suerson in 1939 [10], while Figure 6.26 shows the result generated in this thesis. For the case without untouched timber (reference block), a significantly smaller capacity is found compared to the other cases. When the amount of untouched timber increases, it will result in a greater stiffness of the system, which gives a steeper load-deformation curve. Similar to the results found in this thesis, the initial stiffness does not change significantly for the cases with increased amount of untouched timber, which gives load-deformation curves with equal behaviour in the linear domain. As the plastic deformation of the specimens increases, the curves will start to spread, and the effect of having larger amounts of untouched timber for the total bearing capacity is shown.

To transfer the forces and deformations into stresses and strains, the force is divided by the loading area ($B \cdot L_q = 89mm \cdot 90mm$), and the deformation on the height of the specimens (H=90 mm).

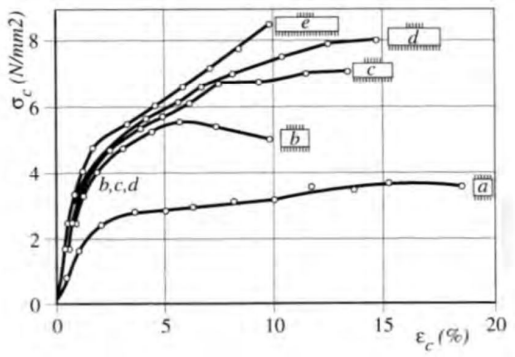

Figure 6.25: The effect of untouched timber found by Suerson [10]

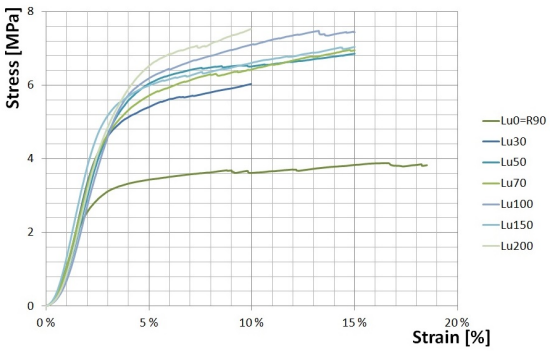

Figure 6.26: The effect of untouched timber found in this thesis

6.6 Load distribution

Based on theory and calculation models derived by Madsen and van der Put, the generated stresses from the applied load is distributed down in the cross-section with a certain angle. This scattering angle is found by looking at the amount of wood that is affected by the stresses, in both the longitudinal and transverse direction of the load. From numerical analyses conducted by Madsen in 1983, it was concluded that the spread was limited to 1.5 times the cross-sectional height. This was also later verified theoretically by Van Der Put, through his model based on equilibrium considerations.

In 2011, a series of compression tests were performed on wooden sills at the Pieter van Musschenbroeck Faculty in the Netherlands, by Leijten, Jorissen and de Leijer [4]. The background for the tests, was the desire to analyse the load distribution underneath the loading area, and to verify the theory presented by Madsen and van Der Put. Both numerical analyses and optical measurements were conducted.

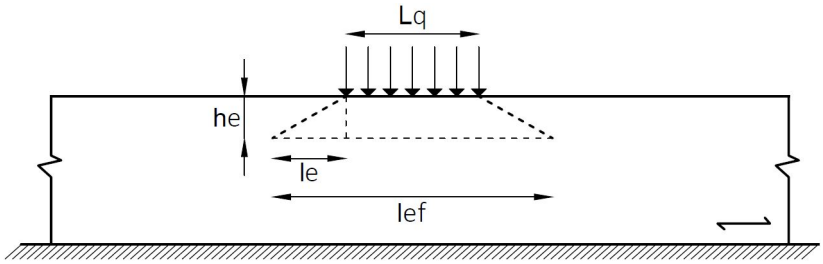

Figure 6.27: Load distribution

The scattering angle is taken from the load distribution, and determined by looking at the amount of wood in the height (h_e) and length (L_e) that is affected by the applied load. By quantifying these two parameters, the scattering angle can be found by simple trigonometry considerations.

$$\tan\Theta = \frac{l_e}{h_e} \tag{6.1}$$

From the tests it was concluded that the scattering angle had a value equal to 1.5, which is the same value derived and found by Madsen and van Der Put. The numerical analysis also verified these results.

Because of the large amount of data collected on the stress field in a timber sill generated in this thesis, the scattering angle will be analysed and verified. By utilizing the results and data found from the optical measurements in ARAMIS, it is possible to define the values of the affected height (h_e) and length (l_e) of the specimens.

To find the height of the affected area, *sections* underneath the loading surface will be defined (Figure 6.28). A deeper explanation of the various defined *sections* will be given in Chapter 7.

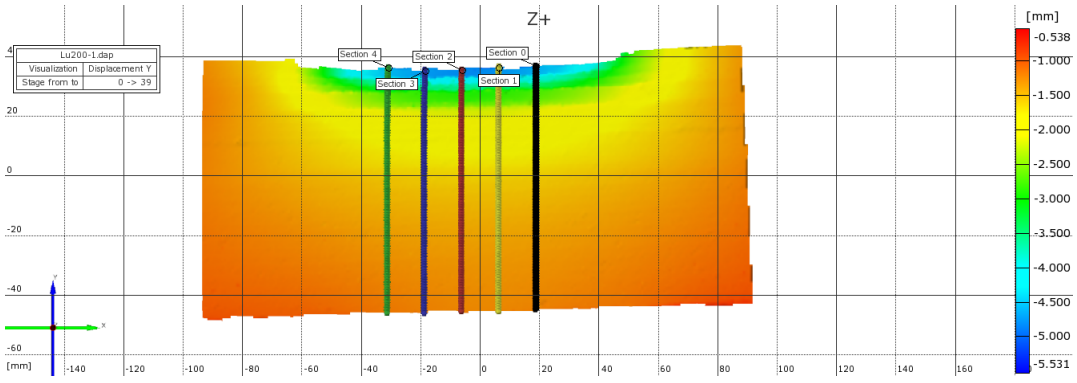

Figure 6.28: Section to find the height (h_e) of the load distribution

By looking at the deformations in the y-direction along the defined sections, it can be concluded that the effective height that is experiencing the applied load is limited to the upper 30 mm of the cross-section (Figure 6.29). This matches the results of the tests conducted by Leijten, Jorissen og de Leijer [4]. They found that the effective height is changing with the height of the cross-section, with an upper limit equal to 140 mm for sections with heights larger than 350 mm. The smallest cross-section they used in their tests, had a height equal to 120 mm, which gave an effective height $h_e = 50$ mm. In this thesis, tests were performed on cross-sections with heights equal to 90 mm, which resulted in a value of the effective height that was a little smaller.

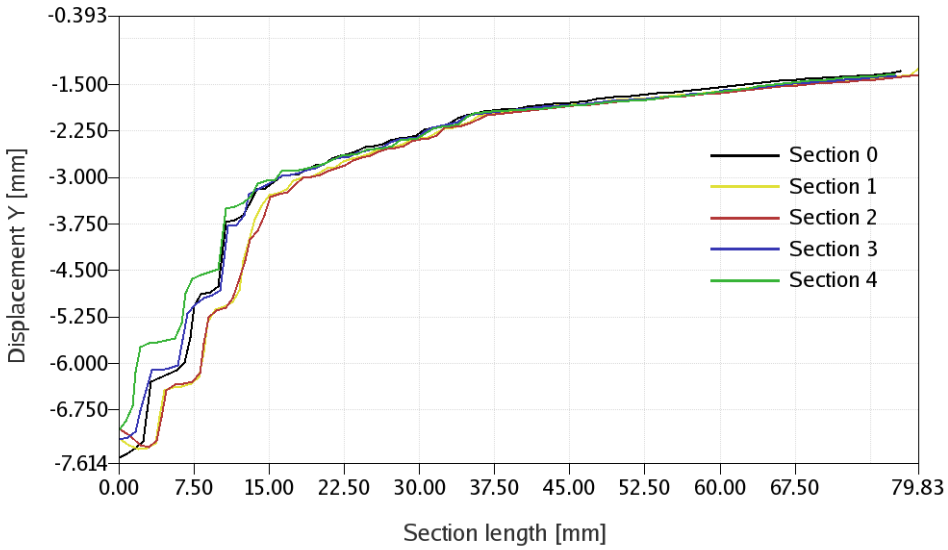

Figure 6.29: Deformations in the y-direction underneath the loading area along the height of the cross-section

To find the distribution of the stresses along the direction of the grain, l_e, horizontal sections were made (Figure 6.30). This resulted in the deformations in the y-direction along the defined sections given in Figure 6.31.

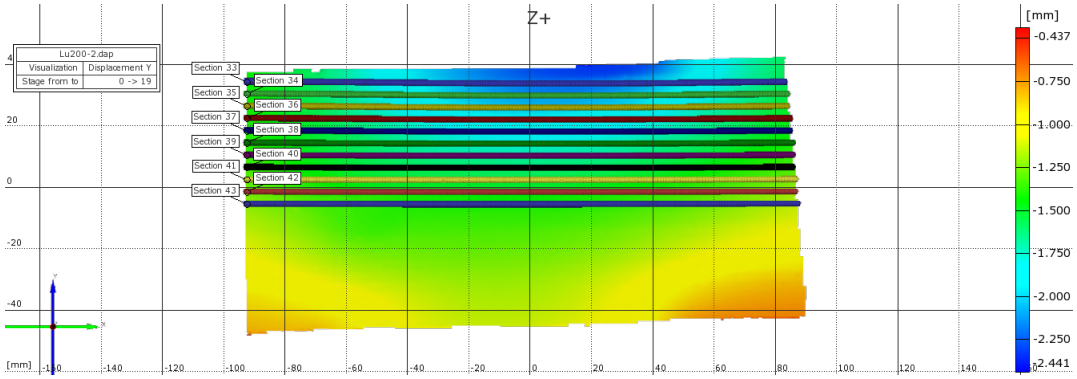

Figure 6.30: Sections to find the length (l_e) of the load distribution

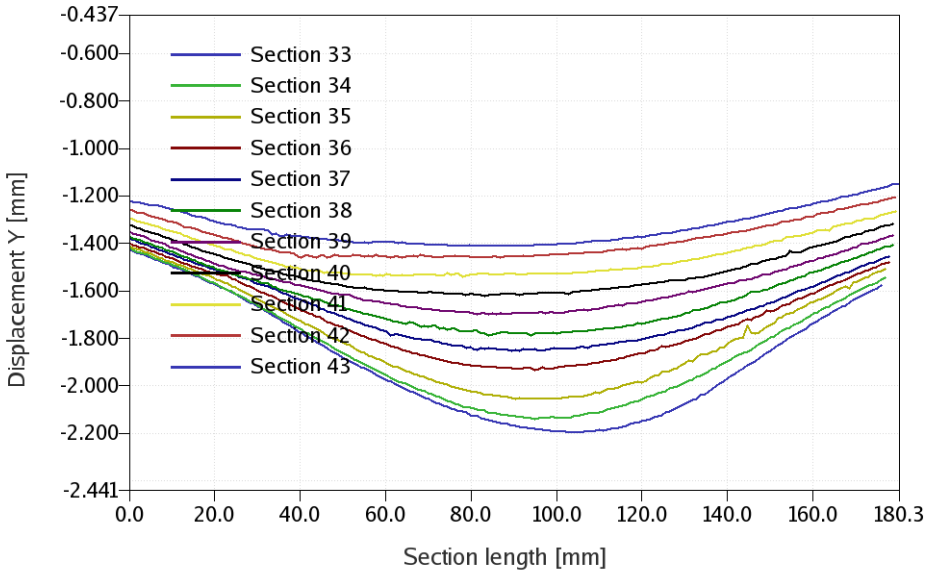

Figure 6.31: Deformations in the y-direction underneath and on the side of the loading area

Because of a predefined size of the analysis area, which had to be defined in advance of the compression tests, the entire length of the specimens was not analysed. As shown in Figure 6.31, the deformation area is limited to a length of 180 mm along the direction of the grain. This will give a maximum of 45 mm on the side of the loading area with recorded deformation data. It is still possible from Figure 6.31 to say something about the distribution of the load. By looking at Figure 6.31, the deformation will most likely stabilize just outside the generated domain. From these assumptions, the length of the affected area is found to be in the range of 40-50 mm.

By inserting the values of the effective lengths into Equation 6.1, the following scattering angle is found:

$$\tan\Theta = \frac{45}{30} = 1.5 \tag{6.2}$$

This is equivalent to the results found by Leijten, Jorissen og Leijer during their experiments, and contributes to the verification of the theory and parameters used in the capacity models derived by Madsen and van Der Put.

Chapter 7

Determination of parameters

From data collected from the various compression test conducted in this thesis, the different parameters derived in the new calculation models will be determined. The values will be found by using the mean values calculated in the previous chapter, which gives the most accurate description of the material behaviour.

With the current regulations in Eurocode 5, only a plastic deformation of 1% of the height is allowed. By looking at the load-deformation curves generated from the different tests in this thesis, this limit seems a little conservative. No distinct failure mechanisms will occur before quadrupling this limit, and it is therefore a reason to believe that the cross-section has larger bearing capacity than the current regulations allows for .

With this in mind, the parameters in the new calculation models will be determined from two different cases. One relying on the current regulations with 1% allowed plastic deformation, and one with custom limits defined from own assumptions based on the test results generated in this thesis.

7.1 Current regulations

Some of the parameters in the new calculation models can be derived directly from the data found by the compression machine (INSTRON), while others require more thorough methods by means of optical analysis (ARAMIS).

7.1.1 Parameters determined by the compression machine (INSTRON)

Height factor k_2:
To determine the height factor, k_2, the results from the tests conducted on the reference blocks, described in Section 6.2, will be analysed. Based on the mean values of the load-deformation curves for the different cross-sectional heights, a capacity with the current regulations will be calculated for each case.

The method for finding the compressive strength of a specimen loaded perpendicular to the grain, is described in Section 3.1, and is done by using the CEN-model. This method relies on a material behaviour that is linearly elastic in the starting domain, and after reaching a certain load, passes over to a plastic non-linear behaviour. From the various tests conducted on the different cross-sectional heights, the results show a small area in the initial part of the loading domain, that is acting non-linear. In order to use the current computational model to find the capacity, this area will be neglected, so that a linear material behaviour is generated from the start. The size of the non-linear area that will be subtracted from the total deformation will vary for the different heights. The value of the subtracted part is found by drawing a line between the two points defined by the CEN-model, $0.1F_{c,90,max,est}$ and $0.4F_{c,90,max,est}$, and making it intersect as close as possible to the origin where the load and deformation equals zero.

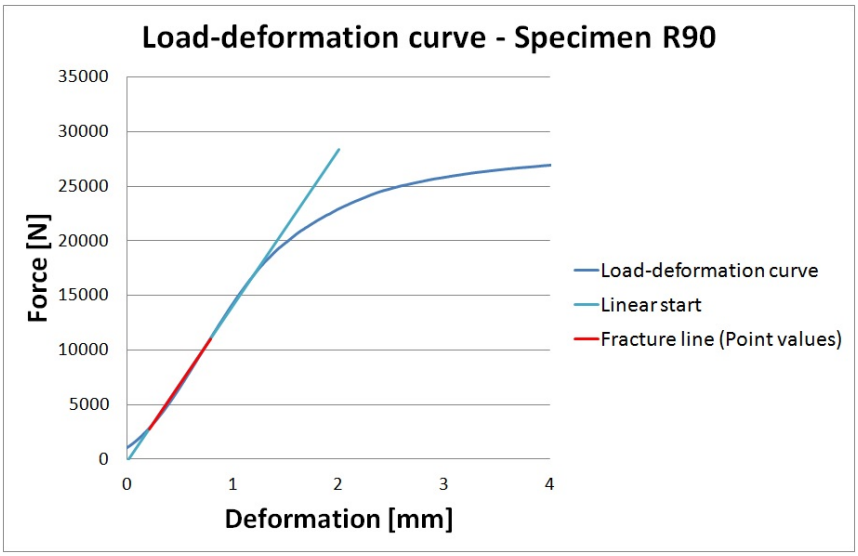

Figure 7.1: Fracture line through the origin generated for specimen R90

Figure 7.1, shows the generated fracture line drawn for the load-deformation curve for specimen R90, and by subtracting a deformation part equal to 0.3 mm, it results in a material behaviour that is linearly elastic from the beginning of the loading domain. This procedure is conducted for all the other load-deformation curves, with their representative subtracted values.

When the material behaviour is linear from the initial loading phase, a compressive strength for the different cross-sectional heights can be calculated by using the CEN-model. Since the method of calculating the strength is equal for all the different cases, only one complete example for one cross-sectional height will be showed.

Example

Example of compressive strength calculation - Specimen R90:
The first step is to define an estimated fracture load $F_{c,90,max,est}$, then compute the values $0.1F_{c,90,max,est}$ and $0.4F_{c,90,max,est}$. In this example it was chosen $F_{,c,90,max,est} = 25500N$, which gave the values $0.1F_{c,90,max,est} = 2550N$ and $0.4F_{c,90,max,est} = 10200N$. For these two load values, the related deformations can be found from the load-deformation curve. From the data points used to draw the curve, there is no exact value equal to 2550 N and 10200 N, so a linear regression will be performed.

The force $0.1F_{c,90,max,est} = 2550N$ has the following deformation values

Force [N]	**Deformation [mm]**
2544.91877	0.18268
2577.25151	0.18599

By using linear regression, it gives a value of the deformation equal to

$$0.18268 + \frac{0.18599 - 0.8268}{2577.25151 - 2544.91877} \cdot (2577.25151 - 2550) = 0.185476mm$$

The force $0.4F_{c,90,max,est} = 10200N$ has the following deformation values

Force [N]	**Deformation [mm]**
10181.0671	0.73264
10232.9648	0.73599

By using linear regression, the second value of the deformation equals

$$0.732645 + \frac{0.73599 - 0.73264}{10232.9648 - 10181.0671} \cdot (10232.9648 - 10200) = 0.73477mm$$

Based on the values of the force and the coherent deformation, it is possible to define points on the load-deformation curve. Through these two points a straight line will be drawn. This line is then shifted to the right along the deformation axis, with a value equal to a defined allowed plastic deformation. With the current regulations, this value equals 0.1 times the height of the cross-section, which for this case results in an offset of $0.1h = 0.1 \cdot 90mm = 0.9mm$. At the point where this line intersects with the load-deformation curve, the value of the compression capacity can be read out.

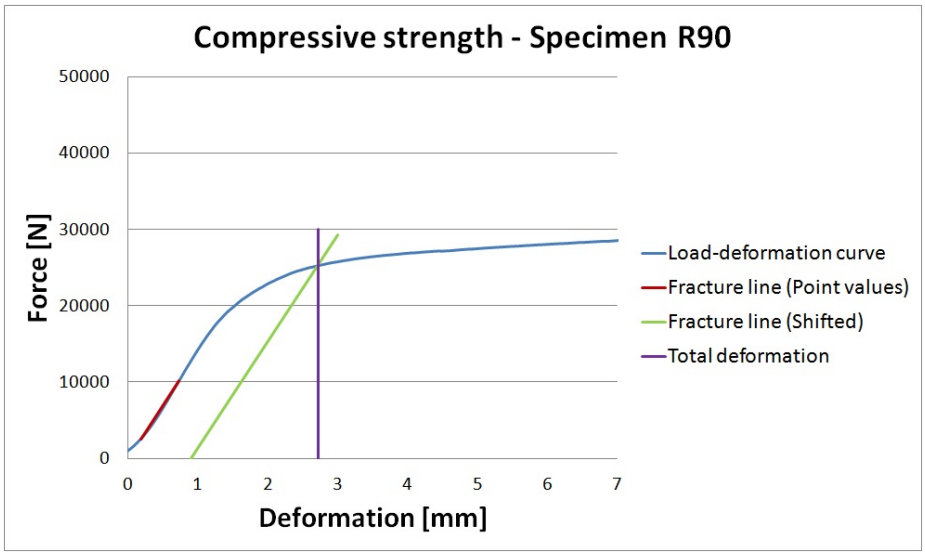

Figure 7.2: Method for finding the compressive strength (CEN-model)- Specimen R90

If the value of the found strength is within 5% of the estimated starting value, it can be used to define the compressive strength of the system. In this case the line intersects the curve in a point $F_{c,90,max} = 25347.1021N$, which gives a deviation equal to:

$$\frac{F_{c,90,est} - F_{c,90,max}}{F_{c,90,est}} = \frac{25500 - 25347.1021}{25500} = 0.6\%$$

The value is within the defined tolerance of 5%.

The calculation method to find the strength of the remaining cross-section heights is done in the same way as described in the example. The cases are only separated by amount of plastic deformation allowed of the height, i.e. how much the calculated fracture line is shifted along the deformation axis.

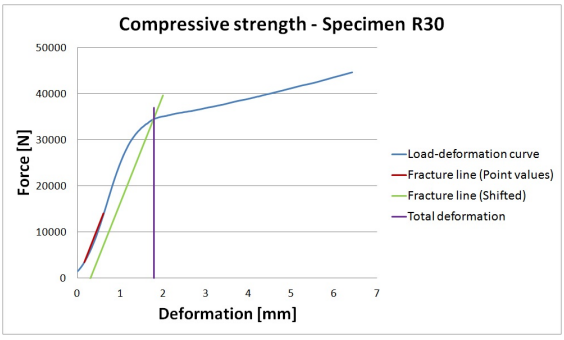

Figure 7.3: Compressive strength - Specimen R30

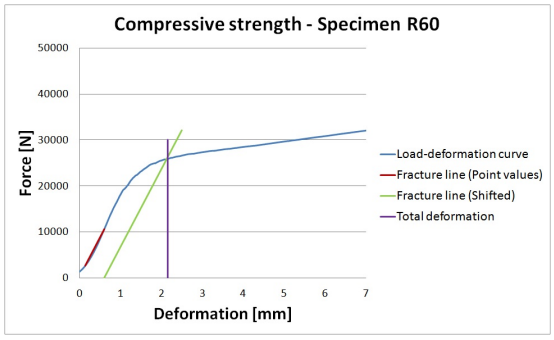

Figure 7.4: Compressive strength - Specimen R60

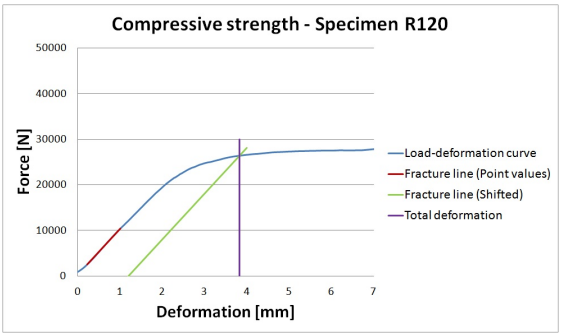

Figure 7.5: Compressive strength - Specimen R120

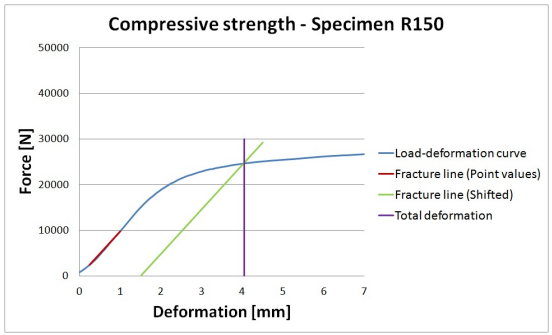

Figure 7.6: Compressive strength - Specimen R150

Using the calculation method described in the example it results in values of the compressive strength for the different cross-sections equal to:

h [mm]	$F_{c,90}[N]$	$f_{c,90}[N/mm^2]$
30	35000	4.37
60	26500	3.31
90 (ref)	25500	3.18
120	26000	3.25
150	24500	3.06

Table 7.1: Compressive strength for the different cross-section heights

Where

$$f_{c,90} = \frac{F_{c,90}}{b \cdot l_q} \tag{7.1}$$

$b = 89mm$ and $l_q = 90mm$

The height factor, k_2, is calculated by scaling the different strengths against a reference strength found from the cross-section with height 90 mm.

$$k_2 = \frac{f_{c,90,j}}{f_{c,90,ref}} \tag{7.2}$$

Since the strengths increases with decreasing cross-section heights, the capacities found for the height equal to 30 mm, will be valid for a domain less than 30 mm, the one found for 60 mm valid for 30-60 mm etc. This will lead to conservative values of the strength in the different height domains, making sure that the capacity is not being overestimated.

The values of the height factors are given in Table 7.2, with their valid height domain:

Domain	**Height [mm]**	k_2
1	≤ 30	1.37
2	30-60	1.04
Ref	90	1.00
3	90-120	1.02
4	120-150	0.96
5	≥ 150	1.00

Table 7.2: Height factor in the different domains

Based on the results presented in Table 7.2, a distinct difference in strength can be found between small and larger heights. This is a result of the compact structure that the smaller cross-sections gets, which leads to a stiff system with small deformations. When the height of the sections increases, more void needs to be compressed, which lowers the stiffness of the system, and the factors converge towards the same value. This is similar the results found by Blass and Görlacher, where they concluded that the height did not have any effect on the compressive strength of the system. The capacities of the larger cross-sections converge towards the same value, as a result of the initial stiffness being nearly identical. Current regulations for the deformation with a plastic limitation of 0.1h, leads to a small movement into the ductile domain, where variations in the material behaviour are larger.

For smaller cross-sections, the height factor will take a value that is larger than 1.0, and provide a significant contribution to the bearing strength. For heights in this domain, it will be quite conservative to use a value equal to 1.0, so the height factor should therefore be included in the capacity calculations.

A cross-section with a height of less than 30 mm is not often used in the construction industry. The height factor will for the most cases be equal to 1.0, and provide no additional contribution to the total capacity. However, it is beneficial to know that an increased carrying capacity can be used when dealing with smaller cross-sections.

Strength factor k_1:
The strength factor, k_1, is found by looking at the total energy required to achieve a certain deformation underneath the loading area. The amount of energy will vary with the lengths of untouched timber, and will be determined by looking at the mean values of the different load-deformation curves derived in Section 6.4.

In addition to this, it is desirable to have a material behaviour that is linear elastic from the beginning of the load domain, which leads to the small initial non-linear region being neglected. This behaviour is consistent for all the tests with various amount of untouched timber, conducted in this thesis. Since the strength factor, k_2, is a scalar, found by weighing the different

values against a reference case, the neglecting of the initial region will not affect the final values (since it is conducted for each case, including the reference case).

To be able to calculate the total energy that is required to get a plastic deformation of 0.01 times the height, functions representing the load-deformation curves for the different specimens will be created. These functions will be generated by the use of Least Square Method (LSM), which is a method that minimises the difference between real data points and constructed data points generated by a defined function.

Least Square Method (LSM)
Is a method that calculates different parameters included in a defined function $f(x_i, \beta)$, that in the best possible way matches a set of real data points. In the defined function, β is a constant, while x_i are the real measured values found from tests. The goal is to find a value of the parameter β, that in the best way represents all the real measured values x_i. This is done by minimising the difference, S, between the real values, and the values generated from the defined function $f(x_i, \beta)$.

Mathematically, this is written as following:

$$S = \sum_{i=1}^{n} r_i^2 \tag{7.3}$$

Where

$$r_i = x_i - f(x_i, \beta) \tag{7.4}$$

To get a good fit between the defined function and the load-deformation curves, it is important to select a function that is able to describe the material behaviour, and that follows the curves in a satisfactory way. The chosen function, is a function that is often used in the field of Material Mechanics: Voce Law. This function has the ability to both describe a linear and a non-linear material behaviour, which makes it suitable for wood loaded in compression.

$$F = C_1 \cdot (1 - e^{-C_2 \cdot \Delta}) \tag{7.5}$$

In the function, F is the applied compressive load perpendicular to the grain, while Δ is the coherent deformation underneath the loading area. C_1 and C_2 are factors that are found by curve fitting with Least Square Method.

By using the mean values of the load-deformations curves for case $L_u j$, functions with associated constants C_1 and C_2, will be generated for each case.

With the Least Square Method, the following curves describing the real load-deformation curves are found:

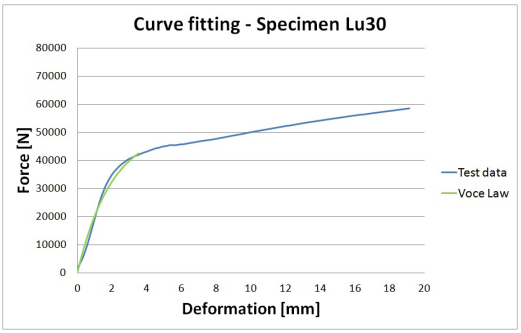

Figure 7.7: Generated function describing the material behaviour - Specimen Lu30

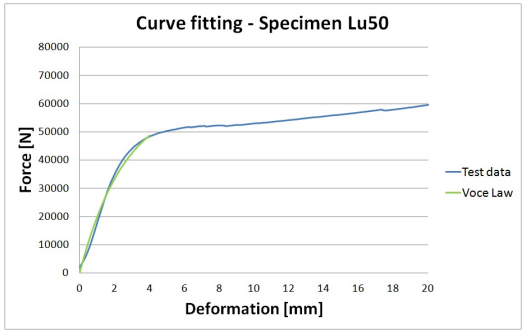

Figure 7.8: Generated function describing the material behaviour - Specimen Lu50

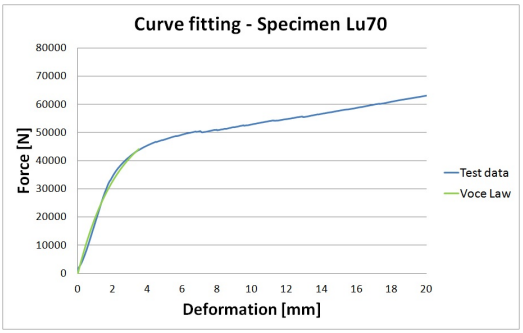

Figure 7.9: Generated function describing the material behaviour - Specimen Lu70

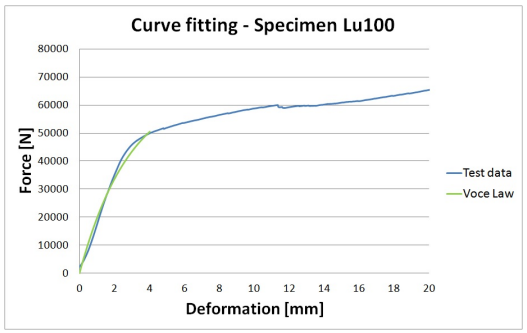

Figure 7.10: Generated function describing the material behaviour - Specimen Lu100

Figure 7.11: Generated function describing the material behaviour - Specimen Lu150

Figure 7.12: Generated function describing the material behaviour - Specimen Lu200

The figures generated above, shows how the chosen function (Voce Law) is able to describe the material behaviour of the wood in a satisfactory way (the functions align almost perfectly with the load-deformation curves). The lengths of the generated functions, is determined by how much is needed to cover the desired analysis area, and will vary between the different cases.

When the different load-deformation curves are expressed with functions, it is possible to calculate the total energy by integrating the area underneath the graph. Based on the definition of the fracture limits given by the CEN-model, the area will be bounded by the generated function and the allowed total deformation Δ_{max}. Since the load-deformation curves are dependent on the amount of untouched timber, it will generate deformation limits that are unique for each specimen. These limits will get the notation $\Delta_{max,j}$.

Figure 7.13 shows how the deformation limits are defined for the reference block R90. By drawing a straight line from the compression capacity calculated by the CEN-model down to the deformation axis (x-axis), it will result in a deformation limit $\Delta_{max} = 2.72$ mm. This is conducted for all the load-deformation curves, which gives the restricted areas that represents the total energy needed to reach the fracture limit, shown in Figure 7.14-7.19 for each specimen (green area). The different deformation limits, $\Delta_{max,j}$, are summarized in Table 7.3.

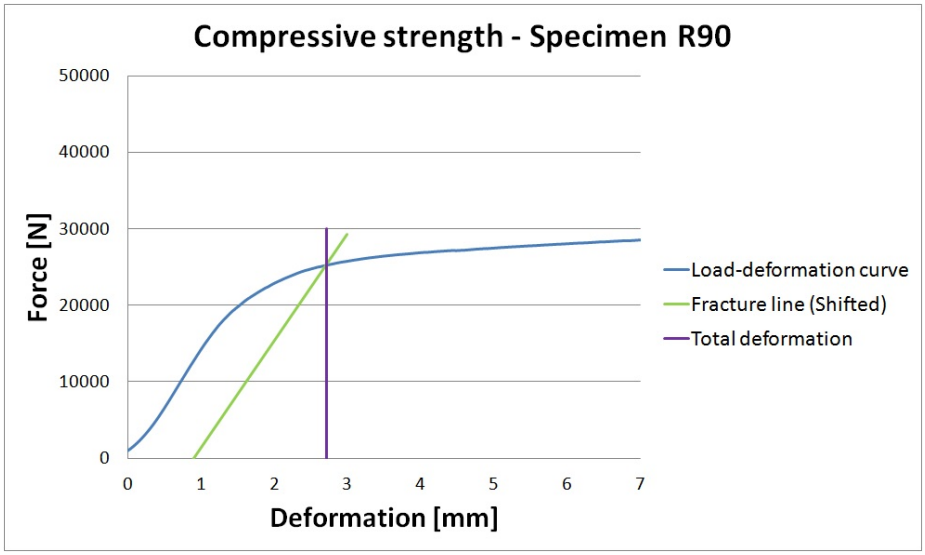

Figure 7.13: Deformation limit - Specimen R90

Luj	$\Delta_{max,j}$ [mm]
0	2.72
30	3.05
50	3.55
70	3.00
100	3.69
150	3.08
200	3.53

Table 7.3: Deformation limits - Specimen Luj

The total energy required to get the allowed plastic deformation, is calculated for the different cases by using Equation 7.6.

$$E_j = \int_0^{\Delta_{max,j}} \mathrm{f_j}(\Delta)\mathrm{d}\Delta \tag{7.6}$$

where

$$f_j(\Delta) = C_1 \cdot (1 - e^{-C_2 \cdot \Delta}) \tag{7.7}$$

$f_i(\Delta)$ generated function for specimen Luj, found by curve fitting
$\Delta_{max,j}$ deformation limit for specimen Luj

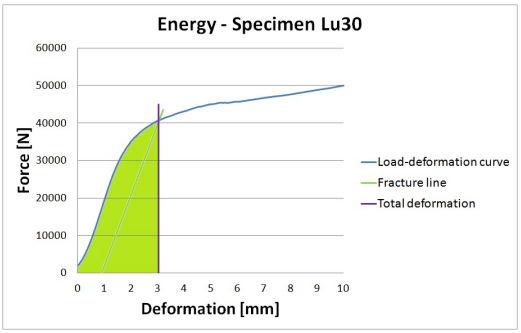

Figure 7.14: Total energy - Specimen Lu30

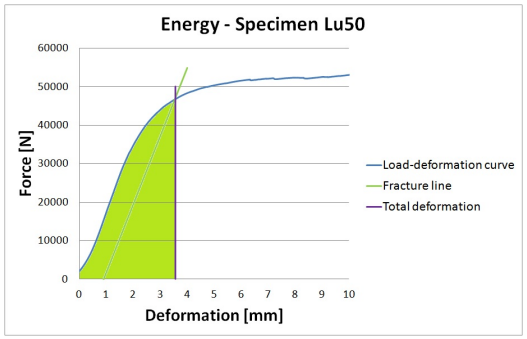

Figure 7.15: Total energy - Specimen Lu50

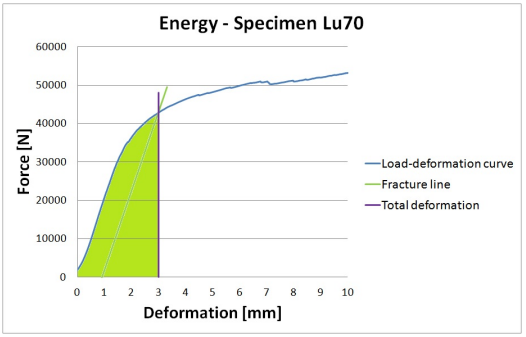

Figure 7.16: Total energy - Specimen Lu70

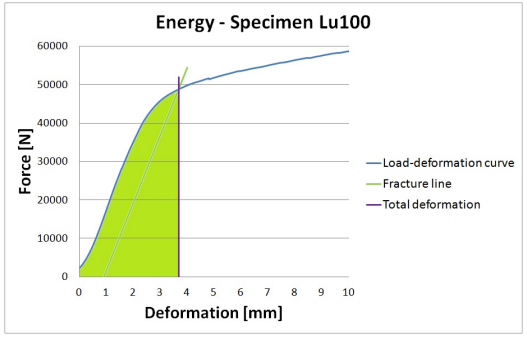

Figure 7.17: Total energy -Specimen Lu100

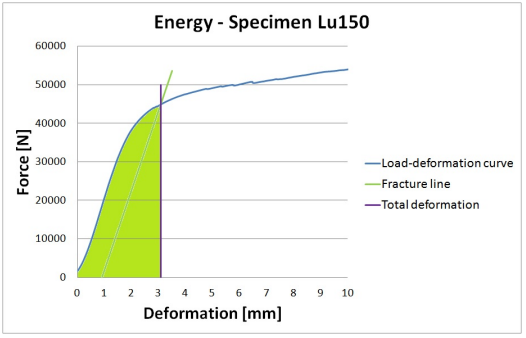

Figure 7.18: Total energy -Specimen Lu150

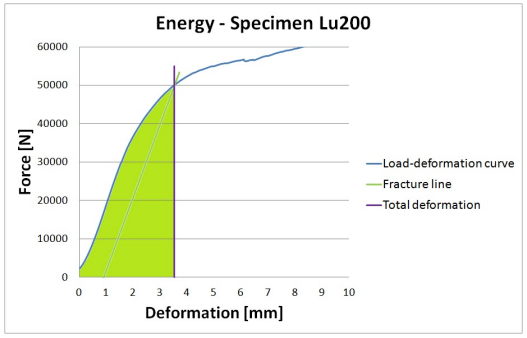

Figure 7.19: Total energy -Specimen Lu200

The procedure for calculating the energy is the same for all cases; a full calculation will therefore only be showed for one of the specimens.

Example

Calculating the total energy - Specimen Lu150:
The function found by curve fitting for the specimen with the amount of untouched timber equal to 150 mm, is the following:

$$f(\Delta) = 52791 \cdot (1 - e^{-0.58\Delta})$$

The maximum allowed deformation, which limits the energy area, is taken from Table 7.3, and equals $\Delta_{max} = 3.08$ mm.

The following values are inserted into Equation 7.6, which gives a total energy equal to:

$$E_j = \int_0^{3.08} 52791 \cdot (1 - \mathrm{e}^{-0.58 \cdot \Delta}) \mathrm{d}\Delta = 86830.0J$$

The same procedure for calculating the total energy is carried out for all the different specimens, with parameters equal to:

Luj	C_1	C_2
30	51180	0.51
50	61818	0.39
70	56477	0.44
100	67047	0.35
150	52791	0.58
200	73882	0.32

Table 7.4: Parameters describing the material behaviour found by LSM

Inserted into Equation 7.6 and 7.7, the total energy is found for all the different specimens:

Luj	E_j [J]
30	43096.3
50	100644.0
70	75362.8
100	106070.0
150	86830.3
200	104534.0

Table 7.5: Total energy - Specimen Luj

The factor scaling the total capacity to fit the different configurations with various amount of untouched timber, k_1, defined in Section 4.1.3, is found by dividing the total energy for the different cases, with the reference case R90 (Lu0).

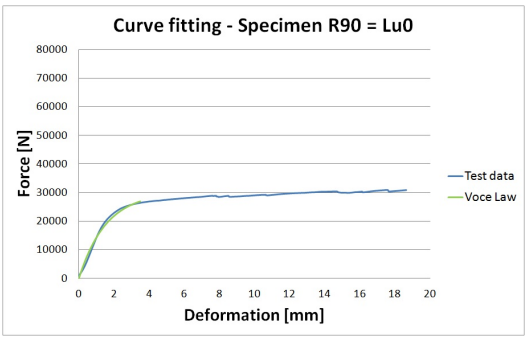

Figure 7.20: Generated function describing the material behaviour - Specimen R90

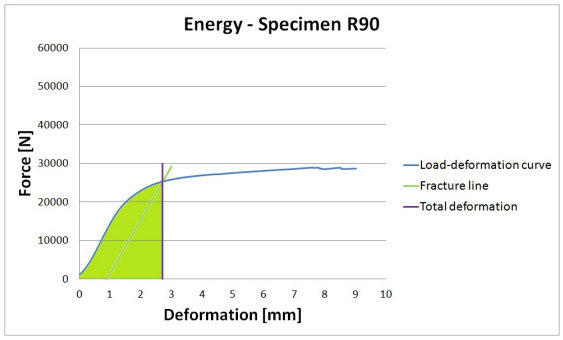

Figure 7.21: Total energy - Specimen R90 (Lu0)

R90 = Luj	C_1	C_2
0	30105	0.64

Table 7.6: Parameters describing the material behaviour found by LSM

By inserting the values from Table 7.6 into Equation 7.6 and 7.7, it gives a total energy $E_0 = 43096.3$ J. By scaling the other calculated values with this reference value, it results in a strength factor k_1 for the different cases equal to:

$$k_{1,j} = \frac{E_j}{E_0} \tag{7.8}$$

Luj	k_1
0	1.00
30	1.79
50	2.34
70	1.75
100	2.46
150	2.01
200	2.43

Table 7.7: Strength factors - Specimen Luj

By looking at the results in Table 7.7, the strength factor increases significantly from the reference case to the case with untouched timber. This is consistent with the theory described earlier in the thesis, where the capacity increases as a result of additional effects being mobilized by having untouched timber on the side of the loading area. The load will be spread out and distributed over an effective surface, and carried by a larger area than the loading area. As the amount of untouched wood increases, the fibres on the side of the loading area will be tilted, and additional carrying effects such as the *Hammock effect* will also contribute to the total bearing capacity.

The expected result of the strength factor, k_1, is a steady increase value with increasing amount of untouched timber. This behaviour occurs because of a higher resistance against the fracture mechanisms, where wood is being lifted up at the edge, and the effects where the applied load is distributed over a larger area. Table 7.7 shows tendencies of this increase, but not in a strictly consistent way.

The reason for this is most probably the amount of tests conducted for the different specimens. With mean values calculated for each length with 3-5 test samples, it gives a data foundation that is poor, which provides an inaccurate representation of the material behaviour. Since the total energy is calculated directly from the load-deformation curves, some of the resulting values for the strength factor will be inaccurate. To get more consistent values, the amount of test samples need to be increased for each cross-section. Because of the size of this thesis and the limited time available, the number of tests for each configuration ranges from 3-5 samples. The values derived in this paper are only meant to give an overview of the magnitude of the different factors, and more tests need to be conducted to get accurate results. The few tests used for determining the parameters, revealed quite similar material behaviour for many of the specimens, which indicates that the factors might be in the right domain for some of the cases.

When the amount of untouched timber reaches lengths in the range of 150-200 mm, the fracture mechanisms are limited to an area underneath the loading surface, and mechanisms where wood is lifted up at the edges are absent. This indicates that the limit length, where an increase in the amount of untouched timber would not give an extra contribution to the total capacity, is near. It is therefore reasonable to believe that the strength factor k_1, will converge against a value that is a little higher than the one found for Lu200, since some global failure mechanisms still occurred at this point.

7.1.2 Parameters determined by optical analysis (ARAMIS)

Effective tension height h_s:

The effective tension height is a parameter that is included in calculation Model 1, derived in Chapter 4. It has previously been shown [9] how concentrations of strains are generated on the side of the loading area when a timber sill is loaded perpendicular to the grain. This is a result of the *Hammock effect*, and it will create an area in the upper part of the cross-section, which experiences tension forces, that will contribute to the carrying of the load. This force will be uniform over the width of the section, and to be able to find the effective tension area A_s, the affected height from the top of the cross-section needs to be defined.

Since the strain concentration depends on the deformation underneath the loading area, limits need to be defined for the allowed deformation. As previously described in Section 4.1.2, the compression strength will be determined based on a combination of the ASTM- and CEN-model.

To find the value of the allowed total deformation, the results from the test conducted on the reference block R90 will be used (the reference height). Using the CEN-model with the current regulations to decide the compressive strength, resulted in a value of the total deformation equal to 2.72 mm (Figure 7.22)

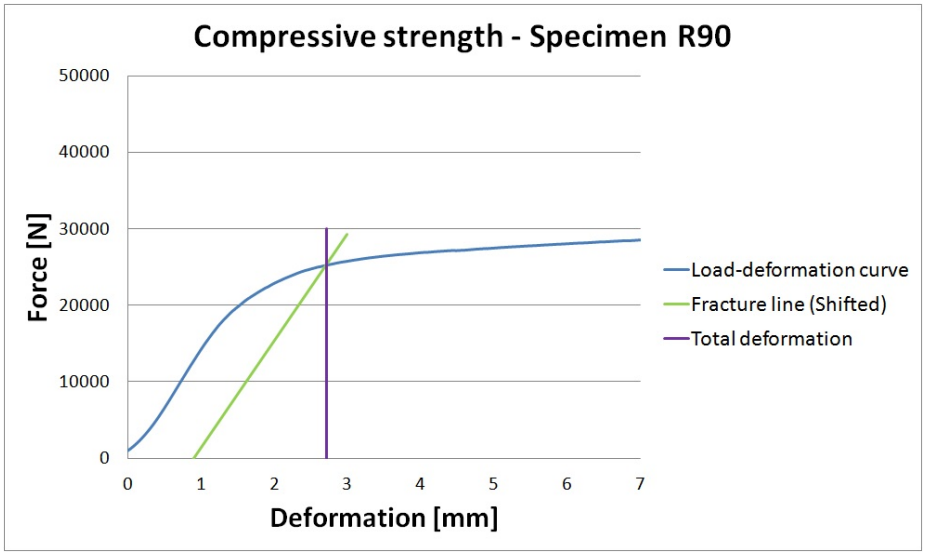

Figure 7.22: Allowed total deformation underneath the loading area - Specimen R90

To determine the effective tension height, it will be looked into the data generated from the image analysis in ARAMIS. To obtain as accurate results as possible, all the specimens will be analysed using this method. This will generate large amounts of data describing the deformation pattern in sills loaded perpendicular to the grain, and ensure that all the mechanical phenomena in the wood are captured. Before starting to analyse the material behaviour generated from the optical measurements, a restricted area of the specimen from which data will be collected needs to be defined (Figure 7.23).

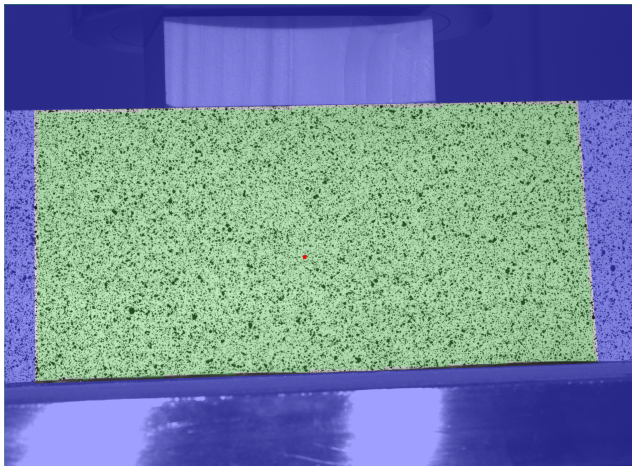

Figure 7.23: Defined analysis area

An easy way to extract data in a desired area in ARAMIS, is to define different *sections* (Figure 7.24 and 7.25). A *section* consists of a line with multiple points, and from these points it is possible to capture data for both strains, stresses and deformations in various directions (Figure 7.26 and 7.27). As the specimen deforms, the points on the *sections* changes positions from its original location, and by looking at the relative change, strains, deformations and stresses can be calculated. It is possible to define sections in both horizontal and vertical directions, chosen by the user depending on the type of data it is desired to extract from the analysis. Number and distance between the defined *sections*, is also defined by the user, and is selected so that the entire analysis area is covered. For most of the analyses conducted in this thesis, a total number of nine sections were made, with center distance equal to 2.3 mm. Because of symmetry, it is only necessary to look at one half of the specimen for some of the tests, as shown in Figure 7.24.

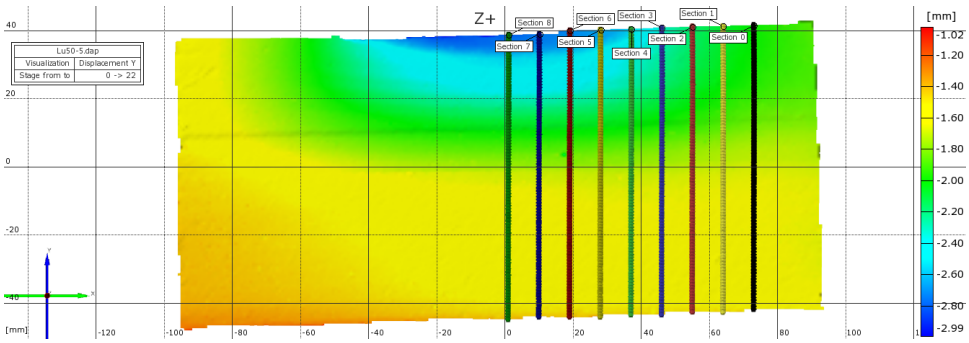

Figure 7.24: Vertical *sections*

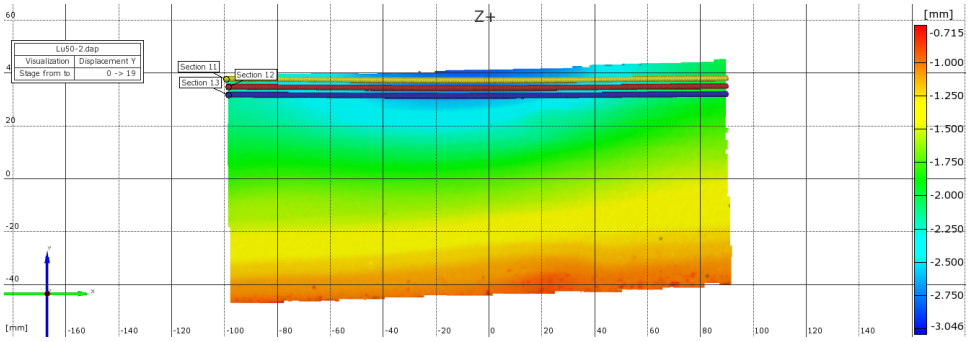

Figure 7.25: Horizontal *sections*

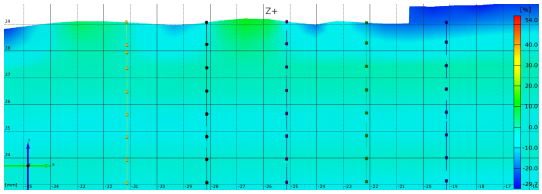

Figure 7.26: Points on vertical *section-lines*

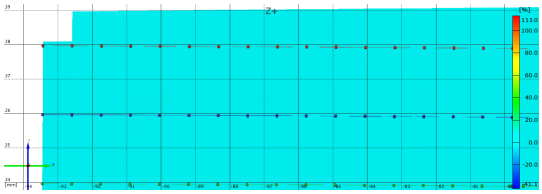

Figure 7.27: Points on horizontal *section-lines*

Before the compression tests were conducted, time intervals for the images taken during the deformation process were defined in ARAMIS. Each interval was saved as a *stage*, where the unloaded specimen had a *stage* number equal to 0. To read out the correct values of the strain concentrations and the effective tension height, the *stage* with the permitted total deformation had to be analysed. The first step in finding the different parameters, was to search for the *stage* that contained a deformation of 2.72 mm underneath the loading area (which is the defined fracture limit). This was done by creating vertical *sections* underneath the load area (Figure 7.28).

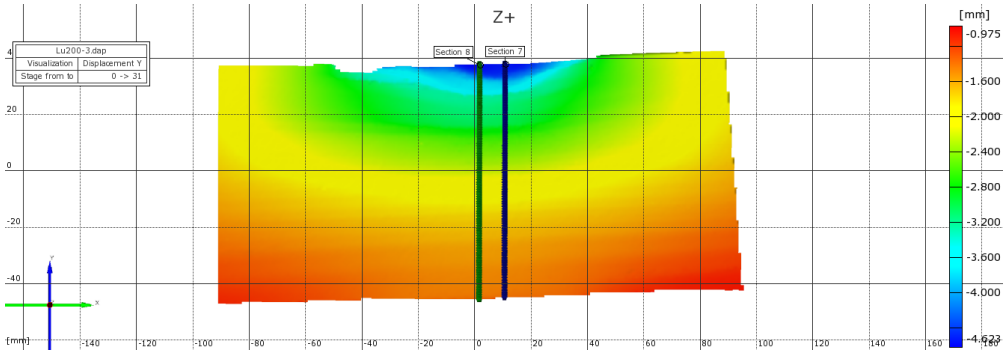

Figure 7.28: Vertical *section* created underneath the loading area

For each *stage*, graphs were generated showing the amount of deformation underneath the loading area (in the y-direction), for every point on the defined section lines. By examining when the top points of the sections (the points directly underneath the load) reaches the deformation limit, the correct *stage* can be defined.

At which *stage* number the deformation limit was reached varied for the different specimens, and is summarized in Appendix B.

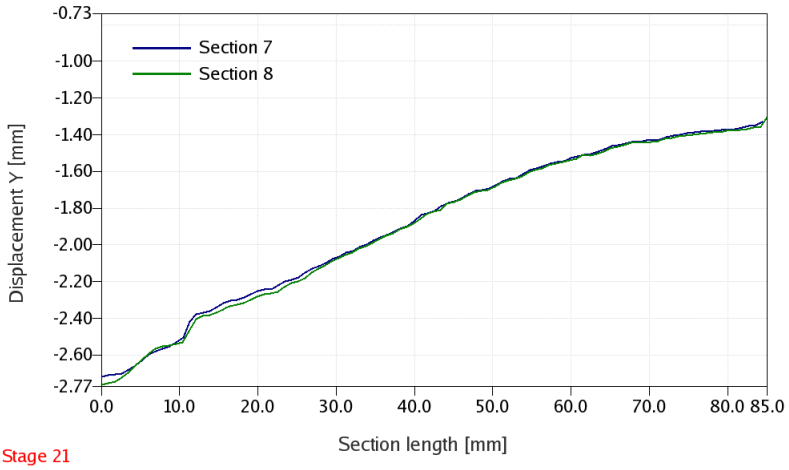

Figure 7.29: Deformation underneath the loading area (y-direction)

The horizontal axis (x-axis) in Figure 7.29, is describing the length of the defined *sections*, where the top of the cross-section equals length 0. It is chosen to define *sections* extending over the entire height of the cross-section (0-90 mm), which is not necessary since the desired data is generated only from the top points of the *sections*. Seen from Figure 7.29, the value of the total deformation directly underneath the loading equals the defined limit. For this case, which is taken from the analysis of specimen Lu30, the correct *stage number* equals 21.

Another way to find the correct *stage number*, is to create horizontal *sections* just underneath the top of the specimen (Figure 7.30). This will provide a different representation of the deformation in the y-direction, but the results will be the same. From Figure 7.31, the deformation in the middle of the *section* equals the defined limit at a *stage* equal to 21, which is the same number as previously found. In this case, the x-axis also represents the length of the created *sections*, but in the horizontal direction.

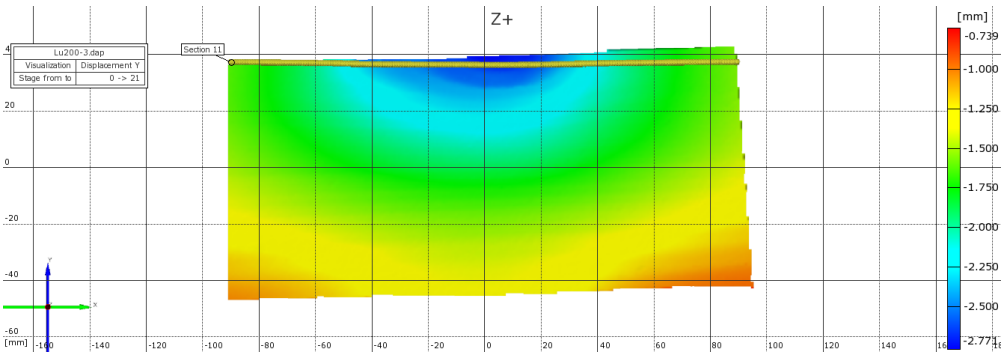

Figure 7.30: Horizontal *sections* created in the top area of the specimen

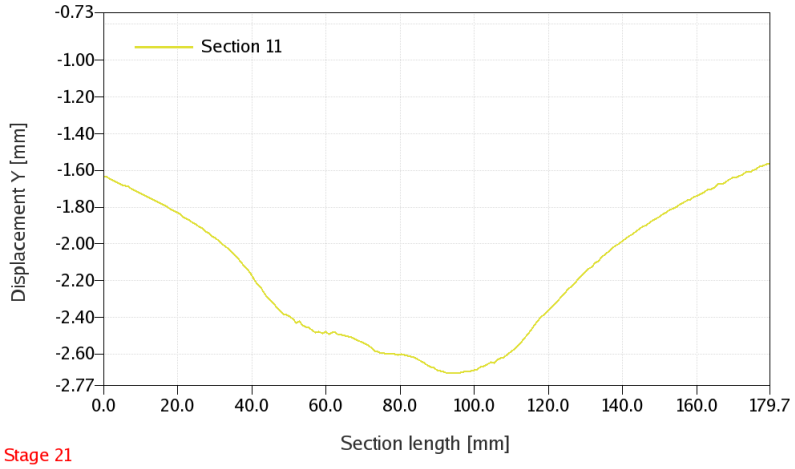

Figure 7.31: Deformation in the y-direction on the top area of the specimen

When the correct *stage* is determined for the specimens, the strain field generated in these specific *stages* can be analysed. Based on the strains generated in the y-direction in the different *stages*, a value of the effective tension height can be defined. This value is found by creating *sections* covering the surface on the side of the loading area for each specimen. By looking at the behaviour of the strains from the top of the cross-section, it is possible to define an effective height that is affected by the generated tension force on the side of the loading area. This method is conducted on all the different specimens. Figure 7.32 and 7.33 shows the results taken from two analyses, namely Lu200 and Lu50. The graphs indicate that an area restricted to the upper 15-20 mm of the cross-section is affected by the tension force. This results was consistent for most of the specimens.

To be on the conservative side, the effective tension height, h_s will be given a value equal to 15 mm.

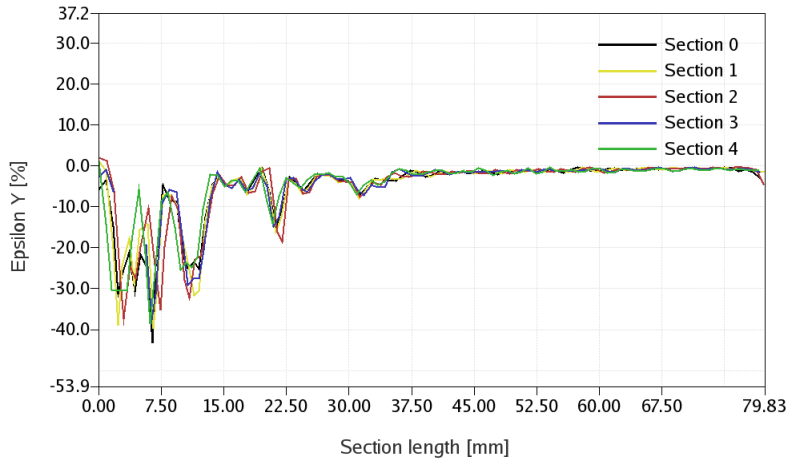

Figure 7.32: Strains in the y-direction on the side of the loading area - Specimen Lu200

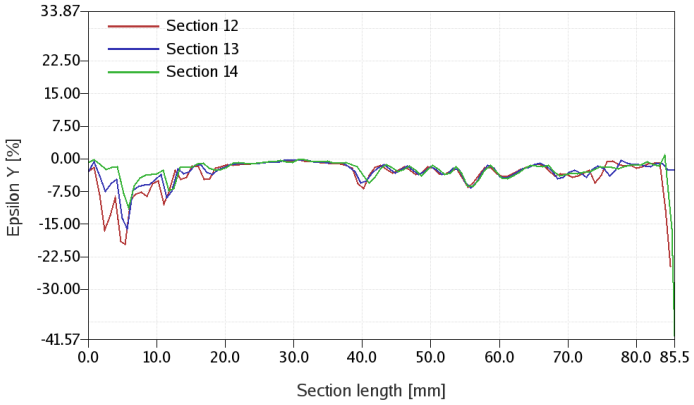

Figure 7.33: Strains in the y-direction on the side of the loading area - Specimen Lu50

For the specimens with an amount of untouched timber that is less than 50 mm, no strain concentrations were found on the side of the loading. Figure 7.35, which is taken from the analysis of specimen Lu30, showed no significant effects from the generated tension force. As a result of this behaviour, it is possible to determine the quantities of untouched timber that needs to be available in order to generate strain concentration, and to be able to account for additional capacity coming from the *Hammock effect*. This will be derived in the next section, where the values of the concentrations and the critical strain domains will be determined.

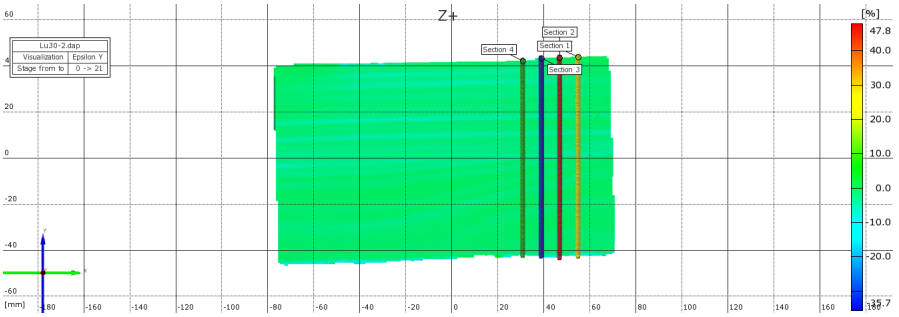

Figure 7.34: Vertical *section* created on the side of the loading area

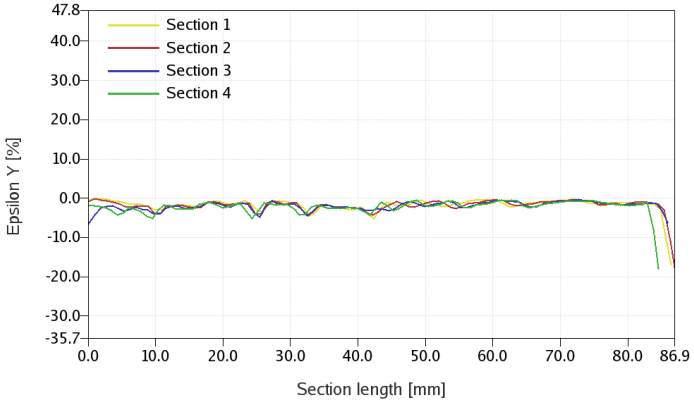

Figure 7.35: Strains in the y-direction on the side of the loading area - Specimen Lu30

Strain concentrations $\varepsilon_{H,j}$:
From previous research [9], it has been shown how strain concentrations are generated on the side of the loading when a sufficient amount of untouched timber is available. The new model based on strains (Model 1) defined in Chapter 4, is dependent on the values of these concentrations for the calculation of the total capacity. To find the values, all the specimens with untouched timber will be analysed in ARAMIS, providing a large amount of data to quantify an accurate parameter.

The procedure in finding the different parameters, is the same as used to define the effective tension height, where *sections* in the desired area of analysis is created.

To determine the values of the strain concentrations for different amounts of untouched timber, $\varepsilon_{H,j}$, which is used to calculate the additional carrying from the *Hammock effect*, the values must be quantified in the specific *stage* where the limit of the allowed deformation is reached. The permitted total deformation, was derived in the section about the effective height, and the value was determined to equal 2.72 mm (Figure 7.22).

By analysing the strains in the y-direction on the side of the loading area in the given *stage*, it is possible to determine a value for the generated concentrations for each specimen.

A simple way to describe how the strains in y-direction varies over the length of the specimens, is to create a horizontal *section* extending over the entire top surface. This will provide plots with given strain values both underneath and on the side of the loading area. Figure 7.36 shows how a *section* is created for specimen Lu200.

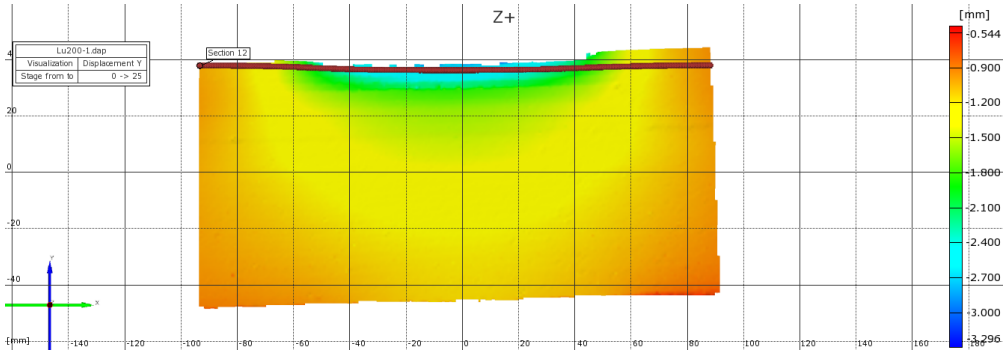

Figure 7.36: Horizontal *section* for specimen Lu200

By creating a plot consisting of the strains in the y-direction along the *sections*, it is possible to see if concentrations on the side of the loading area are generated or not. Figure 7.37 shows the strains in the y-direction on the created *section* given in Figure 7.36.

Figure 7.37: Strains in y-directions along the top surface of the specimen - Specimen Lu200

From the results represented in Figure 7.37, distinct concentrations on the side of the loading area are found. The magnitude of the concentration is in the range of 8%, a value that was consistent for the specimens with untouched timber larger then 150 mm. This corresponds to the results found by Aldvis Hardeng [8], where a value of 6% was found for an amount of untouched timber equal to 157.5 mm

Distinct strain concentrations were also found for specimen Lu50, which has an amount of untouched timber equal to 50 mm on both sides of the loading area. The magnitude of these concentration were smaller, and in the range of 3%.

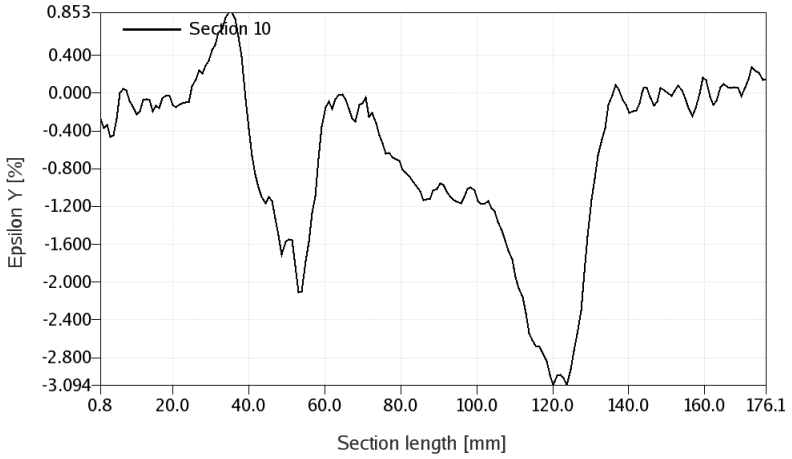

Figure 7.38: Strains in the y-direction along the top surface of the specimen - Specimen Lu50

For the specimens with untouched timber equal to 30 mm, the tests showed a strain field with no distinct concentrations on the side of the loading area. This also corresponds with previous results found from tests conducted by Alvdvis Hardeng [8], that shows how these effects is absent when the amount of untouched timber approaches the reference block. Hardeng found that 67.5 mm was not enough to generate strain concentrations. This length is a little higher than the one found by the image analysis in this thesis, where concentrations are generated for lengths down to $z_0 = 50$ mm.

From the results found in the sections above, it is possible to define domains with certain values for the strain concentrations that are valid for different amounts of untouched timber. It will also be given conservative values for the strain concentrations in the different domains, to ensure that the capacity is not being overestimated. This leads to a value of the concentration for *partial effect* that is valid for lengths of untouched timber between 50-150 mm. The lengths needed to account for *full effect*, will be amounts larger than $z_2 = 150$ mm. The different values and critical lengths are summarized in Table 7.8

Case	L_u [mm]	$\varepsilon_{H,j}$ [%]	Effect
1	$L_u \leq 50$	0	No
2	$50 < L_u < 150$	3.0	Partial
3	$L_u \geq 150$	8.0	Full

Table 7.8: Strain concentration for different amounts of untouched timber

7.2 Custom regulations

The various compression tests conducted in this thesis shows that a fracture capacity limited to 1% plastic deformation could be seen as quite conservative. No distinct failure mechanisms or visual cracks occurred before the total deformation reached a value in the range of 8-9 mm underneath the loading area. Based on these results, a new failure limit will be defined equal to 3% (0.03h) plastic deformation of the cross-section height (3 times larger than the current regulations).

By allowing larger deformations, the parameters used to calculate the total capacity must be checked. Because of this, new parameters must be found, generated from a plastic deformation equal to 3%. The methods used to determine the values are equal to those showed for the current regulation with 1%.

7.2.1 Parameters determined by the compression machine (INSTRON)

Height factor k_2:
By allowing a plastic deformation equal to 3%, the following capacities were found by the CEN-model:

h [mm]	$F_{c,90}[N]$	$f_{c,90}[N/mm^2]$
30	36000	4.49
60	28000	3.50
90 (ref)	27500	3.43
120	27500	3.43
150	27000	3.37

Table 7.9: Compression capacity for different cross-section heights

Where

$$f_{c,90} = \frac{F_{c,90}}{b \cdot l_q} \tag{7.9}$$

$b = 89$ mm and $L_q = 90$ mm.

By looking at the different capacities summarized in Table 7.10, the values do not increase proportionally with the increase in allowed deformation. This is a result of load-deformation curves that stabilize quickly after reaching the yielding point.

The compressive strength found with the current and custom regulations are summarized and compared in Table 7.10.

h [mm]	$F_{c,90}[N]$ **(3%)**	$F_{c,90}[N]$ **(1%)**	Increase [%]
30	36000	35000	3 %
60	28000	26500	5 %
90 (ref)	27500	25500	7 %
120	27500	26000	5 %
150	27000	24500	9 %

Table 7.10: Comparison of the compression capacity for different fracture limits

The results show a slightly higher load with the custom regulations, which will lead to larger allowed compressive strength in the capacity calculations. The same domains created with the current regulations will be defined for this case as well.

To find the height factor, k_2, the different capacities found with the new fracture limit is scaled against the reference capacity found for the cross-section with height equal to 90 mm

Domain	**Height [mm]**	k_2
1	≤ 30	1.31
2	30-60	1.02
Ref	90	1.00
3	90-120	1.00
4	120-150	0.98
5	≥ 150	1.00

Table 7.11: Height factor for the different domains

From the results given in Table 7.11, it shows how the capacity is independent of the chosen cross-section height (in all cases except for the smallest height), and this does not change with a less conservatively defined fracture limit. The values for the height factors are mainly the same as the ones previously found with the current regulations, where the factor is significant for cross-sections with small heights, but stabilizes quickly towards a value equal to 1.0 when the height increases. By allowing a deformation equal to 3% of the height, it will not provide different values for the height factors, since this is a factor scaled against a reference case with the same increase in capacity, but it will give a larger value of the compressive strength $f_{c,90}$.

Based on the result found from both the current and custom fracture limits, the height factor k_2, will receive a value equal to 1.0 for cross-sectional heights larger than 30 mm, and 1.3 underneath this limit. These values are valid independently of the chosen fracture limit.

Strength factor k_1:

This factor is determined in the same way as previously shown, but by allowing a plastic deformation equal to 3% of the height, this will provide new boundaries for the area underneath the load-deformation curve. By using the CEN-model with the new fracture limit, it will give the following values for the maximum allowed deformation, $\Delta_{max,j}$, for the different specimens:

Luj	$\Delta_{max,j}$ [mm]
0	4.46
30	5.02
50	5.58
70	5.15
100	5.70
150	5.05
200	5.60

Table 7.12: Deformation limits - Specimen Luj

Figure 7.39 shows how the maximum deformation is found for specimen R90 with the new limits. By allowing a plastic deformation of the height equal to 3%, it leads to a deformation value $0.03 \cdot h = 0.03 \cdot 90mm = 2.7mm$. By conducting this procedure for all the specimens with different amounts of untouched timber, it gives the restricted areas underneath the load-deformation curves shown in Figure 7.40-7.45.

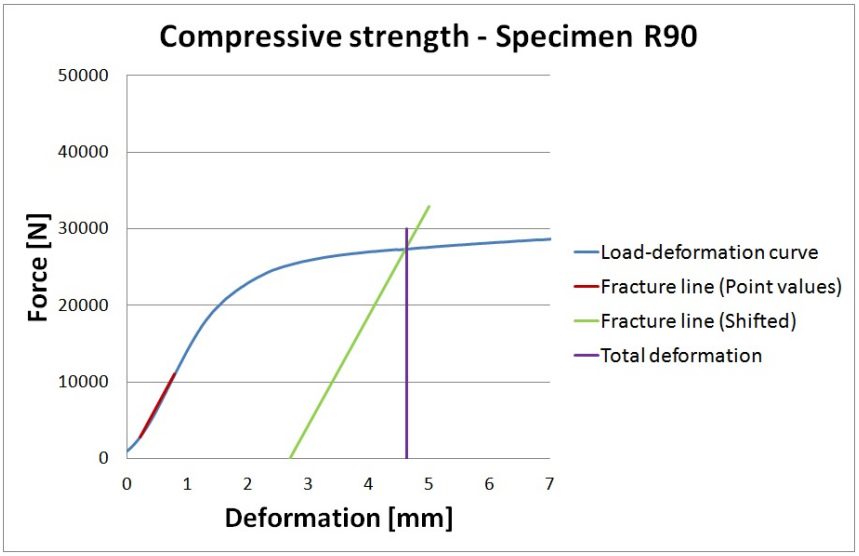

Figure 7.39: Allowed total deformation under the loading area - Specimen R90

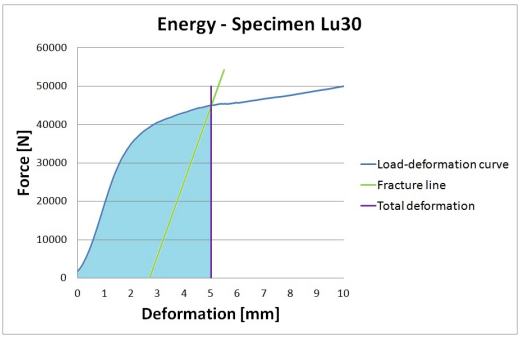

Figure 7.40: Total energy - Specimen Lu30

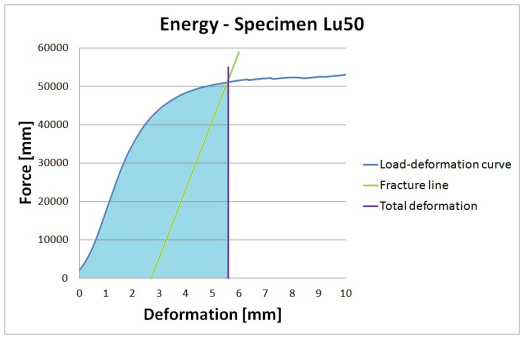

Figure 7.41: Total energy - Specimen Lu50

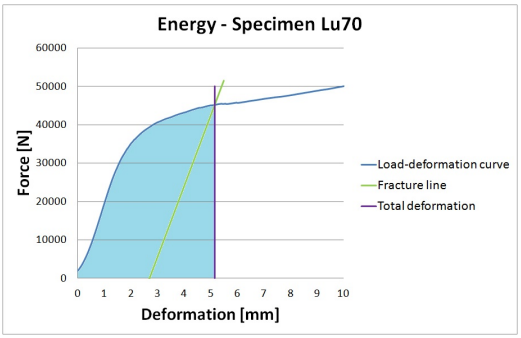

Figure 7.42: Total energy - Specimen Lu70

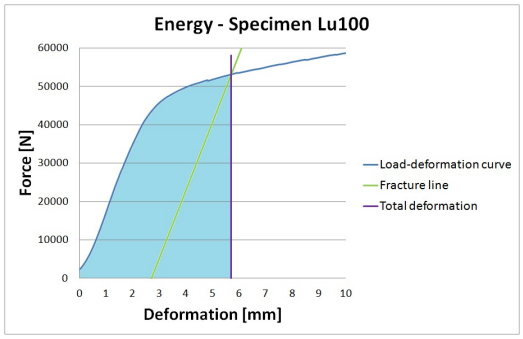

Figure 7.43: Total energy -Specimen Lu100

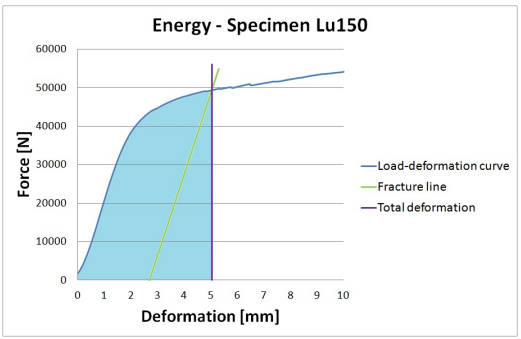

Figure 7.44: Total energy -Specimen Lu150

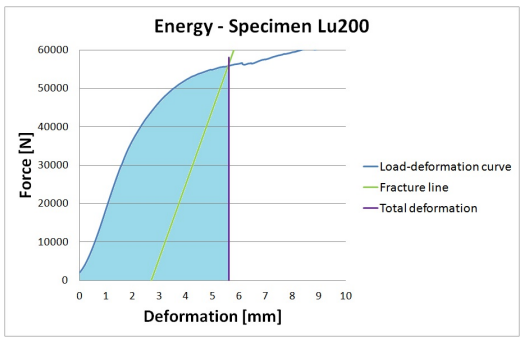

Figure 7.45: Total energy -Specimen Lu200

The parameters used in Voce Law to describe the different load-deformation curves, are summarized in Table 7.13 (even though it is the same load-deformation curves that are used during the calculation of the areas with the custom limit, the parameters in the Voce Law changes, because of a larger analysis domain). The new values are determined in the same way by curve fitting with Least Square Method.

Luj	C_1	C_2
30	50123	0.52
50	60744	0.39
70	54330	0.46
100	65973	0.34
150	53865	0.55
200	70661	0.33

Table 7.13: Parameters describing the material behaviour found by LSM

By inserting the parameters and limits given in Table 7.12 and 7.13 into Equation 7.10 and 7.11, the values of the total energy for the different specimens with a custom limit of 3% plastic deformation are found.

$$E_j = \int_0^{\Delta_{max,j}} \mathrm{f_j}(\Delta)\mathrm{d}\Delta \tag{7.10}$$

where

$$f_j(\Delta) = C_1 \cdot (1 - e^{-C_2 \cdot \Delta}) \tag{7.11}$$

Luj	E_j [J]
30	162312.0
50	200871.0
70	172743.0
100	209948.0
150	180173.0
200	215313.0

Table 7.14: Total energy - Specimen Luj

To determine the strength factor, k_1, the total energy calculated in Table 7.14 for the different specimens, are scaled against the value found for the reference case R90. With the new limit, the total energy of the reference block received a value $E_0 = 92758.5$ J. This value is calculated from the area generated in Figure 7.46, with the parameters given in Table 7.15

R90 = Luj	C_1	C_2
0	28414	0.72

Table 7.15: Parameters to describe the material behaviour found by LSM

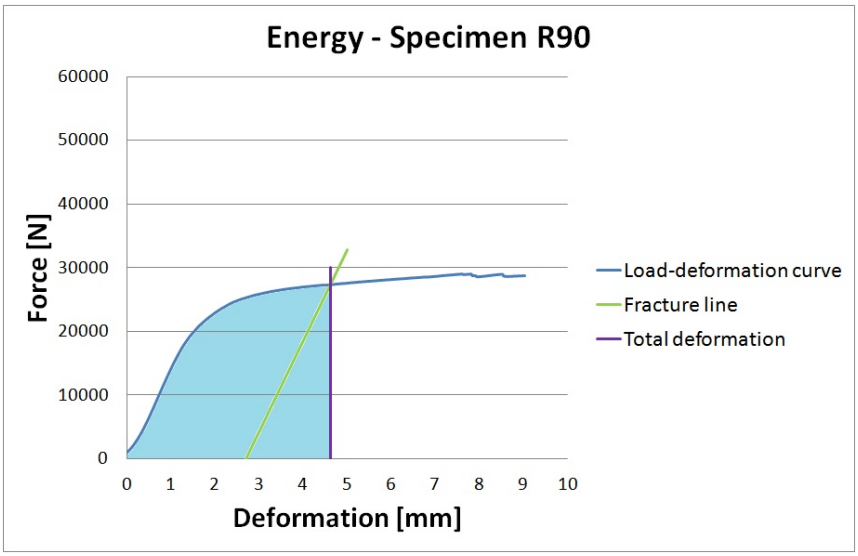

Figure 7.46: Total energy - Specimen R90

The strength factor, k_1, that includes the additional capacity generated from various amounts of untouched timber, is found for the different cases by dividing the total energy with the reference energy E_0. This results in the values given in Table 7.16.

$$k_{1,j} = \frac{E_j}{E_0} \tag{7.12}$$

Luj	k_1
0	1.00
30	1.75
50	2.17
70	1.86
100	2.26
150	1.94
200	2.32

Table 7.16: Strength factor - Specimen Luj

A clear increase in capacity can be found for the cases with untouched timber versus the reference case. By only adding 30 mm of wood on the side of the loading area, the bearing capacity increases by 75%. The values show a tendency to increase with increased untouched timber. Because of the small amount of tests conducted for the different specimens, there will be some uncertainties in the measurements, which creates values that are not completely consistent with this theory. By increasing the amount of tests, the strength factor will most likely give more consistent values.

The values of the strength factor k_1, found from the two different fracture limits, remains quite stable. This is a good property, because it allows the values to be used if different fracture limits are used. The values found by the custom deformation limit, use a larger area of the load-deformation curves, including a larger amount of the linear and non-linear area. This makes it more suitable for capturing an accurate relationship between the different system configurations. The parameters found by the current regulations become more uncertain, because of a more inaccurate material behaviour in the start of the loading domain. In this domain the specimens behave almost identically (the same initial stiffness), because of the lack of secure data coming from few measurements.

The values of the strength factor found with the two different fracture limits are summarized and compared in Table 7.17.

	Current limit	Custom limit	
Luj	k_1 (1%)	k_1 (3%)	Difference
0	1.00	1.00	0.0 %
30	1.79	1.75	2.0 %
50	2.34	2.17	7.3 %
70	1.75	1.86	6.5 %
100	2.46	2.26	8.0 %
150	2.01	1.94	3.6 %
200	2.43	2.32	4.3 %

Table 7.17: Comparison of the strength factor for different fracture limits

By increasing the amount of untouched timber beyond Lu200, the value of the strength factor, k_1, will most likely stabilize and converge towards a value in the range of 2.5. For the largest specimens Lu200, it was only generated local fracture mechanisms underneath the loading area for some of the tests, which implies that increasing the amount of untouched timber, will not result in an increased contribution to the total capacity. Based on these assumptions, it is possible to define limits for the strength factor, which applies to both a lower and upper case.

The lower limit for the strength factor k_1, will receive a value equal to 1.0, which represents the reference case without untouched timber on the side of the load. The upper limit will be equal to 2.5, based on the assumption made in the previous section, where the value found for Lu200 will be increased a certain amount to account for the additional capacity of an increased sill length. The two limits will be valid for cases where the amount of untouched timber is smaller than 30 mm and larger than 250 mm, respectfully. This gives the values of the two parameters x_0 and x_2, derived in Section 4.1.3. No tests have been conducted with untouched timber lengths smaller than 30 mm, and to be on the conservative side of the capacity, the strength factor will be set equal to the reference case.

For intermediate values in between the two limits, a linear representation will be used. The starting point (k^l) will be the strength factor found for specimen Lu30, which is equal to a value in the range of 1.75. The upper value (k^u), will be 2.5, which is the highest value of the strength factor found by increasing the value derived for Lu200 by a small amount. By changing the length of untouched timber (L_u), values of the additional strength factor k_1 are found, depending on which domain the lengths are valid in. Equation 7.13, is independent of the inserted units, which gives values that do not change whether the desired unit is in meters or millimetres.

$$k_1 = k^l + \frac{k^u - k^l}{x_2 - x_0}(L_u - x_0) \tag{7.13}$$

$$k_1 = \begin{cases} 1.0 & L_u \leq x_0 \\ 1.75 + \frac{0.75}{x_2 - x_0}(L_u - x_0) & x_0 < L_u < x_2 \\ 2.5 & L_u \geq x_2 \end{cases}$$

Figure 7.47, shows the result of modelling the strength factor as a linear function with the given boundaries. By conducting more compression tests, the curves generated from the different values of the strength factor for both fracture limits will most probably stabilize and align with the linear function. The functions show a steady increase, but fluctuating as a result of the inaccurate values generated from the small number of tests conducted.

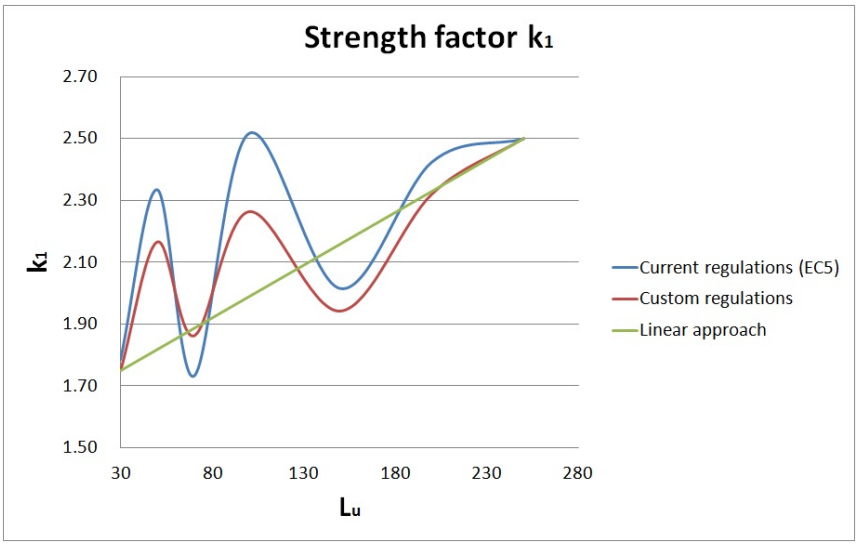

Figure 7.47: Strength factor k_1 for $x_0 < L_u < x_2$

7.2.2 Parameters determined by optical analysis (ARAMIS)

Effective tension height h_s:

As the result of a less conservative fracture limit, larger deformations of the sill will be allowed than with the current regulations. The effective tension height will be determined in the same way as previously shown, but with a larger allowed deformation underneath the loading area. By using the CEN-model with a fracture limit equal to 3% plastic deformation, it will result in a total allowed deformation equal to 4.62 mm (Figure 7.48).

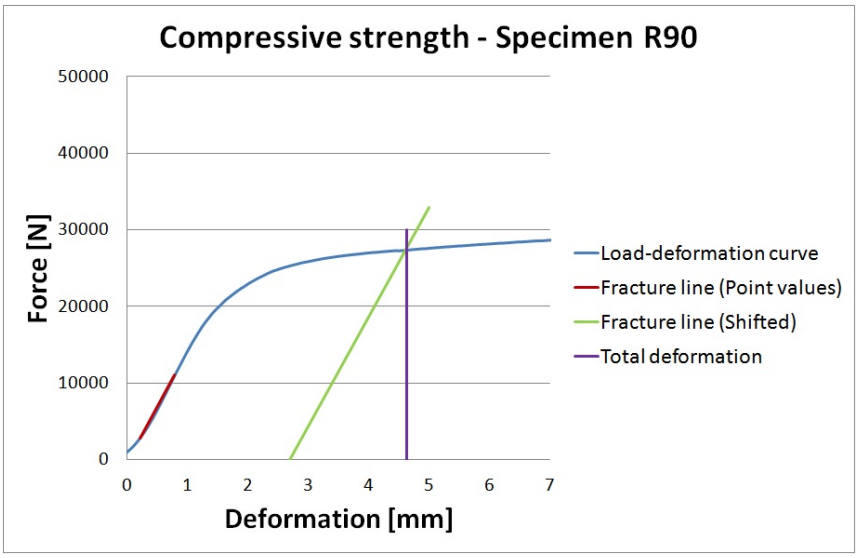

Figure 7.48: Allowed total deformation - Specimen R90

To find a value of the effective tension height, h_s, which represents the height that is effected by the generated tension force on the side of the loading area, the correct *stages* need to be defined. The correct *stages* for the different specimens will be the ones that have a total deformation equal to 4.62 mm underneath the loading area. By using the same method as described earlier, where *sections* are created, the different *stages* can be found.

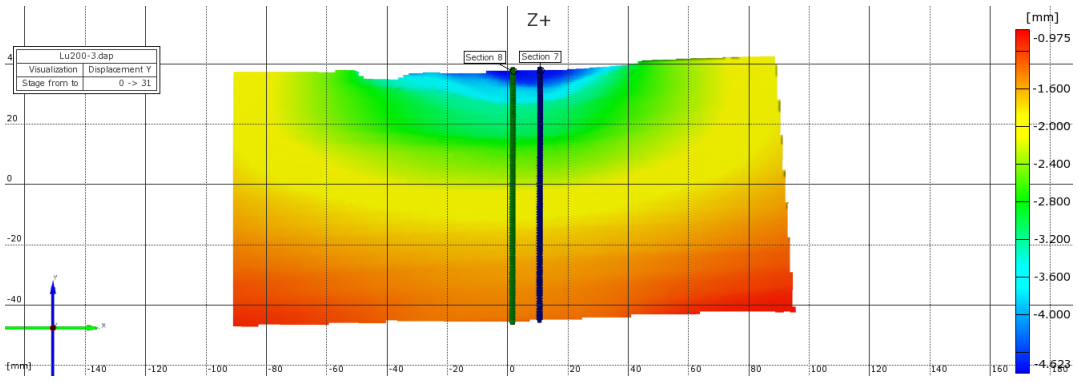

Figure 7.49: Vertical *sections* to determine the correct *stage*

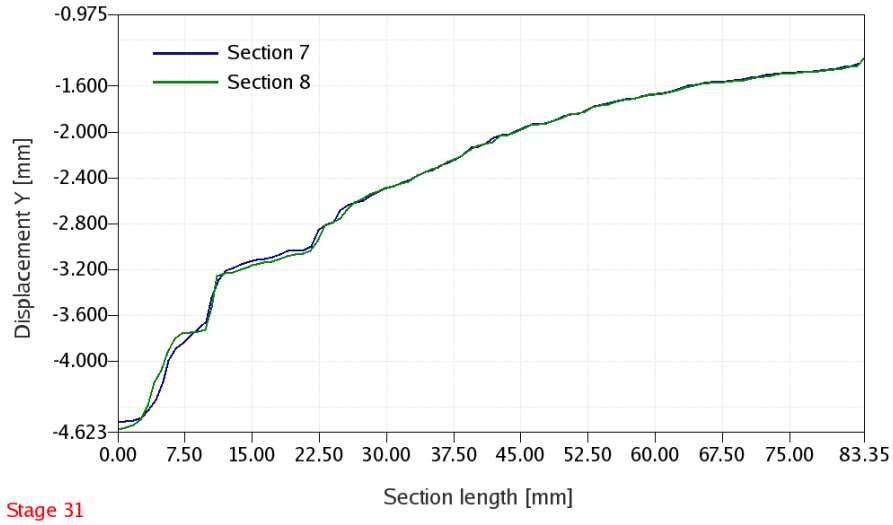

Figure 7.50: *Stage* with the correct total deformation

Figure 7.49 and 7.50, are taken from the deformation analyses conducted on specimen Lu200, and by comparing the *stage number* with the one previously found with the current limits, this value has increased from 21 to 31. This is a result of the custom fracture limit being reached later in the deformation process.

When the *stages* have been defined for the different specimens, *sections* will be created on the side of the loading area, in order to determine the strains in the y-direction downwards in the cross-sections.

By looking at the results from the analysis, the part of the cross-section height that is experiencing significant strains in the y-direction is found to be in the top 20 mm for both cases. This value is a little higher than the one found with the current fracture limits. This is a result of a greater amount of wood being mobilized to carry the generated tension force, because of a larger deformation in the loading area. Based on these results, the effective tension height, h_s, will receive a value equal to 20 mm with the custom fracture limit.

Strain concentrations $\varepsilon_{H,j}$:

The strain concentrations are also dependent on the amount of deformation underneath the loading area. The custom limits allows a total deformation that is $\frac{4.62mm-2.72mm}{4.62mm} \approx 40\%$ larger than the current regulations, and the effects of this on the concentrations should be analysed.

By using the same *stages* previously found in the determination of the effective tension height with the custom limits, it is possible to determine the values of the strain concentrations and the associated critical domains. This is done in the same way as described is Section 7.1.

Horizontal *sections* are created along the upper part of the analysis area, which provides the opportunity to determine the strain variations in the y-direction along the top of the specimen. This method is carried out for all of the specimens. By analysing the variations, it becomes apparent that the strain concentrations do not seem to change significantly with the custom limit. Based on these results, the values defined with the current regulations will also be applicable for the custom limits.

7.3 Serviceability parameters

Based on the previously derived formula for calculating in serviceability state, different parameters and limits need to de defined. The calculation model is based directly on the material behaviour in compression, by using the coherence between applied load and associated deformations.

Simplified calculation method:

To describe the coherence between the applied load and deformations, functions that represent the material behaviour will be generated. Voce Law has shown qualities that allows it to accurately describes the behaviour of wood loaded in compression.

Since the material behaviour is quite different for specimens with and without untouched timber on the side of the loading area, two separate formulas for the two cases will be created. The first will be valid for sills with untouched timber less than 250 mm, which is the critical limit where an increase of sill length no longer provides the system an increase in carrying capacity. The second formula will apply for sills above this limit. The first case will be based on the material behaviour of the reference block, which will provide conservative values. The second case will be based on the specimens with untouched timber equal to 200 mm (Lu200). The behaviour found for the second case, will also be on the conservative side, since the upper limit is valid for lengths larger than 250 mm, which has a higher strength.

For the two cases, the functions describing the material behaviour, are found by curve fitting with LSM, which gives the following results (Figure 7.51 and 7.52):

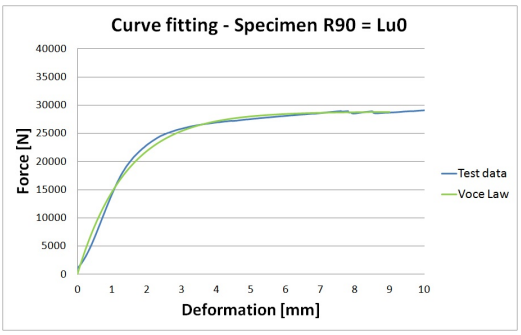

Figure 7.51: Function describing the material behaviour - Specimen R90

Figure 7.52: Function describing the material behaviour - Specimen R200

By using the functions generated to describe the coherence between load and deformation for the two cases, an expression for the total deformation dependent on the applied load can be found. This leads to the following serviceability models for the two cases:

Lower case ($L_u \leq 250mm$):

$$\Delta_0 = -\frac{1}{C_{2,0}} ln(1 - \frac{F_{c,90}}{C_{1,0}}) < \Delta_{0,max} \tag{7.14}$$

Upper case ($L_u > 250mm$):

$$\Delta_2 = -\frac{1}{C_{2,2}} ln(1 - \frac{F_{c,90}}{C_{1,2}}) < \Delta_{2,max} \tag{7.15}$$

It needs to be defined limits, Δ_{max}, for the maximum allowed deformations underneath the loading area. These serviceability limits should be in equilibrium with the fracture limits defined in ultimate state, so that the allowed deformations do not violate the bearing capacity of the system. These deformation limits are found by looking at the capacity calculations with the CEN-model. The CEN-model calculates the compression capacity by allowing a given plastic deformation of the height. By allowing a certain plastic deformation, it also allows large amounts of elastic reversible deformations in the system. A serviceability limit for the total allowed deformation, will be derived by looking at a combination of these two contributions. This will provide limits that do not violate the Ultimate Limit State regulations.

The limits defining the allowed total deformations, Δ_{max}, are strictly dependent on the chosen fraction criterion. By using the current regulations with 1% plastic deformation of the height, it will lead to the values given in Figure 7.53 and 7.54, and by allowing a custom deformation of 3%, it results in the values given in Figure 7.55 and 7.56.

Figure 7.53: Allowed total deformation in Serviceability Limit State (1%) - Case $L_u <$ 250 mm

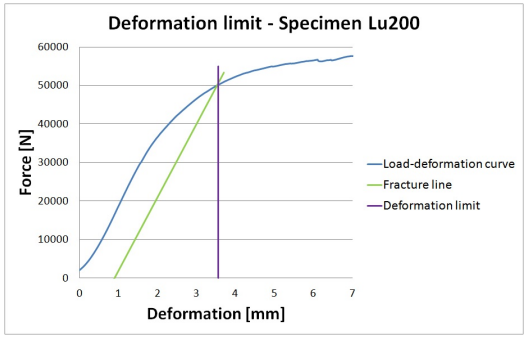

Figure 7.54: Allowed total deformation in Serviceability Limit State (1%) - Case $L_u >$ 250 mm

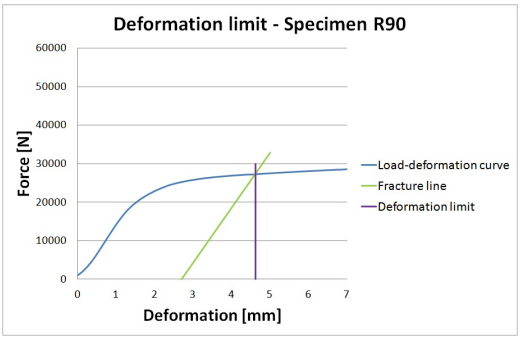

Figure 7.55: Allowed total deformation in Serviceability Limit State (3%) - Case $L_u <$ 250 mm

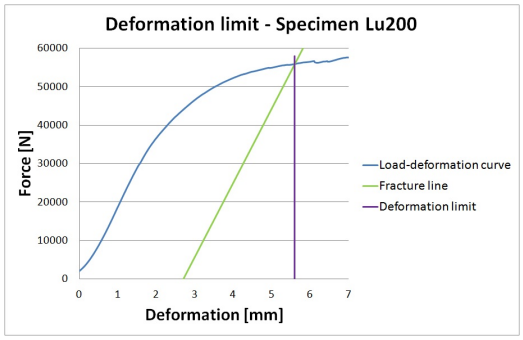

Figure 7.56: Allowed total deformation in Serviceability Limit State (3%) - Case $L_u >$ 250 mm

	Current (1%)	Custom (3%)
$\Delta_{0,max}$ [mm]	2.72	3.55
$\Delta_{2,max}$ [mm]	4.62	5.60

Table 7.18: Allowed total deformations in SLS

According to the results of the compression tests, no fracture mechanisms are occurring prior to a total deformation in the range of 8-9 mm. When this deformation value is reached, timber starts to rise on both edges of the specimen, resulting in visual fracture mechanisms. Figure 7.57, shows how a specimen looks after a deformation underneath the loading area in the range of 10 mm. When deformation limits are defined in serviceability states, they are chosen to prevent visible and unfortunate deformations in the construction material, which may lead to difficulties in the usage of the system or related parts. The material will not fail when reaching these limits, but cracks and malfunctions can be generated. The limits found by using the current regulations, are far below the range where these mechanisms occurs, which leads to quite conservative results. By using the custom deformation limits, a larger total deformation is allowed, and the values are getting closer to the critical limit of 8-9 mm.

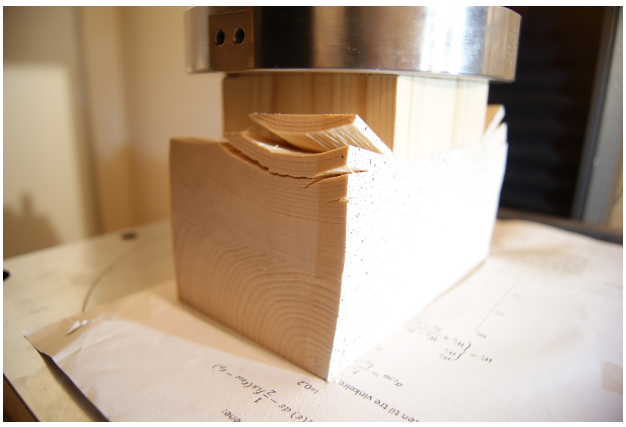

Figure 7.57: Failure mechanisms after 10 mm deformation underneath the loading area

The parameters in the serviceability state model given in Equation 7.16, are taken directly from the material behaviour of the specimens tested in this thesis, which consists of a certain wood type (Norwegian CE L40C≈GL32c). Since the compression properties varies between the different types, separate material parameters, adapted to each case, must be generated. This needs must be done for both all constructional timber types and glue-laminated types. All the parameters are collected in a table, which provides the designer the opportunity to choose the desired type of timber with the associated strength values. In this thesis, only the values for timber type GL32c are derived, and these can be found in Table 7.19 and 7.20.

When calculating in serviceability state, the desired values are chosen from either Table 7.19 or 7.20, depending on the amount of untouched timber. These values are inserted into Equation 7.16. From this equation, the designer can determine the total deformation of the sill, by inserting a value of the desired compression load, $F_{c,90}$.

The equation (Equation 7.16) used in the Serviceability Limit State calculations, has certain restrictions. The value of the applied load perpendicular to the grain $F_{c,90}$, can not be larger than the value of C_1 for the different wood types. This will give undefined deformation values, as a result of the term inside the logarithmic part of the equation (ln(x)) becoming negative.

$$\Delta = -\frac{1}{C_2} ln(1 - \frac{F_{c,90}}{C_1}) < \Delta_{max} \tag{7.16}$$

Lower case ($L_u \leq 250mm$):

$L_u < 250mm$	GL24c	GL26c	GL28c	GL30c	GL32c	GL34c
C_1					28813	
C_2					0.71	
Δ_{max} [mm] (Current)					2.72	
Δ_{max} [mm] (Custom)					3.55	

Table 7.19: Parameters used in the Serviceability Limit State calculation for $L_u \leq 250$ mm

Upper case ($L_u > 250mm$):

$L_u > 250mm$	GL24c	GL26c	GL28c	GL30c	GL32c	GL34c
C_1					72330	
C_2					0.32	
Δ_{max} [mm] (Current)					4.62	
Δ_{max} [mm] (Custom)					5.60	

Table 7.20: Parameters used in the Serviceability Limit State calculation for $L_u > 250$ mm

Comments:
In Chapter 4, in the section about the derivation of the new Serviceability Limit State model, it was proposed to use two different calculation models, one called *Simplified Calculation Model* and the other *More Accurate Calculation Model*. The second model was derived to be able to capture the elastic behaviour of the material when conducting the serviceability calculations. By looking at the derived functions describing the material behaviour in Figure 7.51 and 7.52, by using Voce Law, they are able to represent the entire deformation domain. Based on these results, it was concluded that a separate model for the two cases was unnecessary. The calculation model and parameters found during the derivation of the *Simplified Method* will be adequate for both cases, and the *More Accurate Calculation Model* will not be used.

The height factor, k_2, was also introduced in Chapter 4, as one of the parameter in the Serviceability Limit State calculations. It was supposed to account for the change in capacity for the different section heights. This was introduced because it was believed that the strength would change significantly between the various heights, providing an effect that needed to be accounted for when defining the deformation limits. As found during the analysis of the results, the height did not affect the total capacity, and the height factor was therefore omitted from the calculation model.

The parameters derived in Table 7.19 and 7.20, used to describe the material behaviour, are taken directly from the load-deformation curves. It has been shown how the height of the cross-section does not affect the material behaviour in any significant way, but no tests have been conducted with variations in the loading length (L_q). This may be a factor that changes the behaviour and coherence between the load and deformations. As the result of limitations in time given in this thesis, this will not be tested and verified. The formula used for the Serviceability State Limit calculations will therefore only be dependent of the amount of untouched timer and the type of wood, and variations in width, height and loading length will not affect the final results.

Chapter 8

Test of calculation models

To verify the validity of the new models derived in this thesis, they will be tested through various examples, and compared with the current calculation model. Examples will be constructed that covers some of the different load situations encountered in today's building methods. The models will mainly be tested against variation in load length as well as the amount of untouched timber on the side of the loading area, which are the parameters that contribute the most in changing the capacity.

8.1 Ultimate Limit State (ULS)

Three examples with different loading lengths will be created. Within the examples, the calculation models are also tested against variations in untouched timber lengths. Parameters such as height and width, will not have an impact on the results within the different calculation models, and are therefore kept constant. At the end of each example, it will be presented a summary, where the carrying capacity for each calculation model is compared. The three different examples will be calculated with both the current and the custom made regulations for the fracture limit.

The value of the compressive strength used in the examples, will be the one derived in this thesis, and not the value given in the documentation paper of the timber (Appendix C). The characteristic compressive strength is defined as the values calculated for the reference case R90, which equals $f_{c,90,k} = 3.18$ MPa with the current regulations, and $f_{c,90,k} = 3.43$ MPa with the custom. By comparing the calculated value found with the current regulations in this paper with the one given in the documentation in Appendix C (which is equal to 2.7 MPa), it gives a 15% higher compressive strength.

The chosen value of the strength, $f_{c,90}$, will not affect the final result, since this parameter will be the same in both the new and current calculation model, and the results consists of a comparison of the two. The chosen strength parameter will change the values of the final capacities, but not the difference in capacity between the calculation models, which is the desired finding. All the examples will consist of a sill loaded perpendicular to the grain with a load in the mid-span, with equal amounts of untouched timber on both sides of the loading area. The

length, l_1 (Figure 8.1), is supposed to be between two different loads on the sill, taken from the current regulations. This length will be given a value equal to the distance from the applied load and edge of the sill, a, which is the same as the length defining the amount of untouched timber L_u.

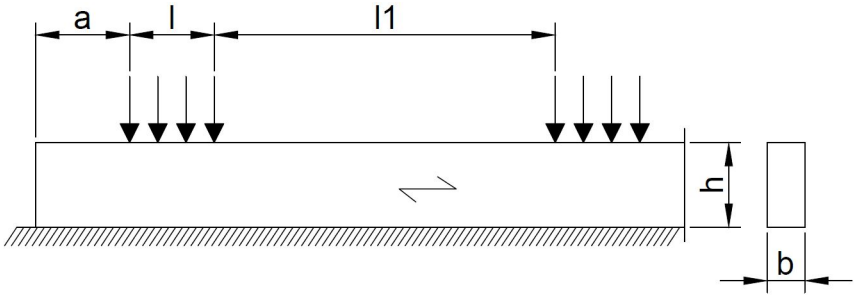

Figure 8.1: Sill loaded perpendicular to the grain (EC5-1-1 length definitions)

8.1.1 Current regulations (1% plastic deformation)

Example 1:
In this example the loading length, l (L_q), is kept constant equal to 90 mm, while the amount of untouched timber, a (L_u), varies. The different lengths are taken from Figure 8.1.

Case	h [mm]	b [mm]	l=L_q [mm]	a=L_u [mm]	l_1 [mm]
1	90	89	90	0	0
2	90	89	90	20	20
3	90	89	90	35	35
4	90	89	90	50	50
5	90	89	90	90	90
6	90	89	90	120	120
7	90	89	90	150	150
8	90	89	90	200	200
9	90	89	90	500	500
10	90	89	90	1000	1000

Table 8.1: Geometry and loading configurations - Case 1-10 (Example 1)

The method for calculating the compression capacity is the same for all cases 1-10, and therefore only one complete calculation for one of the cases (Case 5) will be shown. The only thing that separates the calculations, are the parameters taken from table 8.1. The example will first be calculated with the current regulations given in Eurocode 5 part 1-1, and subsequently with the two new capacity models derived in this thesis.

Example

Compression capacity perpendicular to the grain with Eurocode 5 part 1-1:
(The text given in *italic* is taken directly from EC5-1-1 [13])

The following expression should be satisfied:

$$\sigma_{c,90,d} \leq k_{c,90} \cdot f_{c,90,d} \tag{8.1}$$

where

$$\sigma_{c,90,d} = \frac{F_{c,90,d}}{A_{ef}} \tag{8.2}$$

The effective contact surface perpendicular to the grain, A_{ef}, is determined by looking at an effective loading length in the direction of the grain, where the actual loading length, l, is increased on each side with a value up to 30 mm, but not more than a_1, l or $l_1/2$ (Figure 8.1).

The requirement $l_1/2$ will not be taken into account, since this length is less than a, for smaller lengths of untouched timber. The load will be distributed in the same length at both sides of the loading area, and is therefore regulated by the distances to the edges. This leads to the following expression:

$$A_{ef} = b \cdot [l + \sum_{i=1}^{2} \Delta l_i] \tag{8.3}$$

$$\Delta l_i = min\{30mm; a_i; l\} \tag{8.4}$$

The values in Table 8.1, which belongs to Case 5, are inserted into Equation 8.4, and results in a increased length at both sides of the loading area equal to:

$$\Delta l_i = min\{30; 90; 90\} = 30mm$$

This leads to the effective loading area:

$$A_{ef} = 89 \cdot [90 + 2 \cdot 30] = 13350mm^2$$

The value of $k_{c,90}$ shall be put equal to 1.0, unless the conditions in the following section are applicable. In those circumstances, the highest value of $k_{c,90}$ can be used, but the value should never exceed $k_{c,90} = 1.75$

For construction parts that rests on a continuous support, and where $l_1 \geq 2h$ (Figure 8.1), the following values of $k_{c,90}$ is assumed:
$k_{c,90} = 1.5$ *for glue-laminated timber*

In Case 5, there is not enough untouched timber on the side of the loading area to satisfy the requirement $l_1 \geq 2h$ ($90mm \leq 2 \cdot 90 = 180mm$), and the factor $k_{c,90}$ should therefore be equal to 1.0.

The design compressive strength $f_{c,90,d}$, is found from the following formula:

$$f_{c,90,d} = k_{mod}\frac{f_{c,90,k}}{\gamma_M} \tag{8.5}$$

Where γ_M is a partial factor for the material properties, and k_{mod}, a strength factor that takes the effects of load duration and moisture content into account. The two parameters have the following values:
$\gamma_M = 1.15$ (EC5-1-1: NA.2.4.1)
$k_{mod} = 0.8$ (EC5-1-1: Table 3.1)

$$f_{c,90,d} = 0.8 \cdot \frac{3.28}{1.15} = 2.21MPa$$

By inserting the derived values into Equation 8.1 and 8.2, the maximum load,$F_{c,90}$, that can be applied on the timber sill is calculated:

$$F_{c,90,d} \leq k_{c,90} \cdot f_{c,90,d} \cdot A_{ef} = 1.0 \cdot 2.21 \cdot 13350 = 29532N = 29.5kN$$

By conducting the same calculation procedure as shown for Case 5, for all the cases 1-10, it leads to the following values of the different parameters that is inserted into the capacity formula:

Case	$\Delta l_i[mm]$	$A_{ef}[mm^2]$	$k_{c,90}$
1	0	8010	1.0
2	20	11570	1.0
3	30	13350	1.0
4	30	13350	1.0
5	30	13350	1.0
6	30	13350	1.0
7	30	13350	1.0
8	30	13350	1.5
9	30	13350	1.5
10	30	13350	1.5

Table 8.2: Parameters to calculate the compression capacity for Case 1-10

The strength factor $k_{c,90}$, does not take a value larger than 1.0, after Case 7. This is a result of the condition $l_1 \geq 2h$, not being satisfied for the shorter sill lengths, since the amount of untouched timber is too small. For a cross-sectional height equal to 90 mm, it requires $l_1 > 180$ mm, which is only satisfied for Case 8-10. When this condition is satisfied, the regulations in EC5-1-1, gives the possibility to increase $k_{c,90}$ to a value equal to 1.5.

The effective loading area, A_{ef}, will vary for the shortest sills, but as the length increases, it will converge towards a constant value. This because of the additional loading lengths, Δl_i, being limited to a maximum value equal to 30 mm on both sides (Equation 8.4).

By inserting the values found in Table 8.2, into Equation 8.1 and 8.2, the design load, $F_{c,90}$, can be calculated for the different cases.

Tilfelle	$F_{c,90}[N]$	$F_{c,90}[kN]$
1	17720	17.7
2	25595	25.6
3	29533	29.5
4	29533	29.5
5	29533	29.5
6	29533	29.5
7	29533	29.5
8	44299	44.3
9	44299	44.3
10	44299	44.3

Table 8.3: Design load perpendicular to the grain for Case 1-10

Table 8.3, shows how the design load converges toward an upper value equal to 44.3 kN, for the example with loading length equal to 90 mm. The capacity will not increase with longer sills, since the effective area has reached its limit, and the strength factor is constant equal to 1.5 when the condition $l_1 \geq 2h$ is satisfied.

Example

Compression capacity perpendicular to the grain with new calculation models *(Model 2)*

The following expression should be satisfied:

$$\sigma_{c,90,d} \leq k_1 \cdot k_2 \cdot f_{c,90,d} \tag{8.6}$$

where

$$\sigma_{c,90,d} = \frac{F_{c,90,d}}{A} \tag{8.7}$$

For a system with height $h = 90$ mm, it will result in a value of the height factor k_2 equal to 1.0. As derived in Section 7.2.1.

The value of the factor that accounts for the variations in strength between systems with different amounts of untouched timber, k_1, is determined by the conditions given on the next page. The lengths x_0 and x_2 measure 30 mm and 250 mm, respectfully (see Section 7.2.1).

$$k_1 = \begin{cases} 1.0 & L_u \leq x_0 \\ 1.75 + \frac{0.75}{x_2 - x_0}(L_u - x_0) & x_0 < L_u < x_2 \\ 2.5 & L_u \geq x_2 \end{cases}$$

In Case 5, the amount of untouched timber, $a = L_u$, equals 90 mm on both sides of the loading area. This gives a value of the strength parameter k_1 equal to:

$$k_1 = 1.75 + \frac{0.75}{250 - 30}(90 - 30) = 1.95$$

A is the area where the applied load acts on the sill, and is equal to the width b, multiplied by the loading length l (l_q).

$$A = 90 \cdot 89 = 8010mm^2$$

The design compression strength, $f_{c,90,d}$, is found in the same way as defined in Eurocode 5 part 1-1:

$$f_{c,90,d} = k_{mod}\frac{f_{c,90,k}}{\gamma_M} = 0.8 \cdot \frac{3.28}{1.15} = 2.21MPa$$

By inserting the derived parameters into Equation 8.6 and 8.7, the maximum load $F_{c,90}$, can be calculated:

$$F_{c,90,d} \leq k_1 \cdot k_2 \cdot f_{c,90,d} \cdot A = 1.95 \cdot 1.0 \cdot 8010 = 34633.59N = 34.6kN$$

The procedure used to calculate the bearing capacity of the timber sill with the new model (Model 2), is done for all the cases 1-10, with the values given in Table 8.4

Case	$A[mm^2]$	$k_{c,90}$
1	8010	1.0
2	8010	1.0
3	8010	1.77
4	8010	1.82
5	8010	1.95
6	8010	2.06
7	8010	2.16
8	8010	2.33
9	8010	2.50
10	8010	2.50

Table 8.4: Parameters to calculate the compression capacity for Case 1-10

Since the design load is only being distributed over the actual loading area, A, this parameter will stay the same in all cases (Table 8.4). The strength factor, $k_{c,90}$, will vary with the amount of untouched timber, a (L_u), and take a different value for the different cases. For Case 1 and 2, the strength factor will be equal to 1.0, as a result of the distance to the edges being less than the lower limit $x_0 = 30$ mm. For the longer sills, such as Case 9 and 10, the upper limit $x_2 = 250$ mm will be reached, and the factor stabilizes towards the upper value of 2.5.

By inserting the different parameters found in Table 8.4 into Equation 8.6 and 8.7, it gives the following values of the maximum load perpendicular to the grain for Case 1-10:

Case	$F_{c,90}[N]$	$F_{c,90}[kN]$
1	17720	17.7
2	17720	17.7
3	31311	31.3
4	32217	32.2
5	34634	34.6
6	36446	36.4
7	38258	38.3
8	41278	41.3
9	44299	44.3
10	44299	44.3

Table 8.5: Design load perpendicular to the grain for Case 1-10

The capacity will get significantly larger with increasing sill length (Table 8.5). This is a result of the strength factor growing in value when the amount of untouched timber increases. As the sill reaches a certain length, the capacity will converge towards a value equal to 44.3 kN, since the upper limit of the additional strength factor is reached.

Example

Compression capacity perpendicular to the grain with new calculation model *(Model 1)*

The following expression should be satisfied:

$$\sigma_{c,90,d} \leq f_{c,90,d} + f_{H,90,d} \tag{8.8}$$

where

$$\sigma_{c,90,d} = \frac{F_{c,90,d}}{A_{ef}} \tag{8.9}$$

The expression for the *Hammock effect* is equal to:

$$f_{H,90,k} = \frac{k_u \cdot E_{s,\Theta} \cdot \varepsilon_{H,j} \cdot h_s}{C} \tag{8.10}$$

The effective loading area, A_{ef}, is calculated in the same way as the current method given in Eurocode 5 part 1-1, where the increase in bearing length on both side of the loading area equals:

$$\Delta l_i = min\{30; 90; 90\} = 30mm$$

This results in an effective loading area:

$$A_{ef} = 89 \cdot [90 + 2 \cdot 30] = 13350mm^2$$

The requirement that needs to be satisfied to be able to include the extra bearing capacity coming from the *Hammock effect*, $f_{H,90,d}$, is that the ratio between the loading length, l (L_q), and the allowed deformation underneath the loading area, Δh, is larger than 30 (Section 4.1.2). With the current regulations, the maximum allowed deformation equals 2.72 mm, which gives a ratio equal to:

$$\frac{l}{\Delta h} = \frac{90}{2.72} = 33.1 > 30$$

Since the ratio is larger than 30, the additional capacity coming from the *hammock effect* can be included in the calculation of the total capacity.

The load location factor, k_u, is taken from the two cases underneath:

$$l_u = \begin{cases} 1 & \text{untouched timber on one side} \\ 2 & \text{untouched timber on two sides} \end{cases}$$

Since the load is acting in the mid-point of the sill, it consists of a system with untouched timber on both sides of the loading area, which gives a load location factor $k_u = 2$.

The value of the strain concentration that is generated on the side of the loading area, $\varepsilon_{H,j}$, is determined by looking at the amount of untouched timber, and taken from Table 8.6.

Case	**a** (L_u) **[mm]**	$\varepsilon_{H,j}$ [%]	**Effect**
0	$a \leq 50$	0	No
1	$50 < a < 150$	3	Partly
2	$a \geq 150$	8	Full

Table 8.6: Strain concentrations for the different domains with untouched timber

Case 5, has an amount if untouched timber, a (L_u), equal to 90 mm, which leads to Case 1 in Table 8.6, and a strain concentration value equal to $\varepsilon_{H,1} = 3\%$.

The modulus of elasticity, $E_{s,\Theta}$, and the effective tension height, h_s, is derived and determined in Section 4.1.2 and 7.1.2, and equal to 800 N/mm^2 and 15 mm, respectfully.

The factor taking the loading length into account, C, is determined by using Equation 8.11 or directly from graph 8.2.

$$C = L_q \cdot \sqrt{\frac{1}{16} \cdot (\frac{L_q}{\Delta h})^2 + 1} \tag{8.11}$$

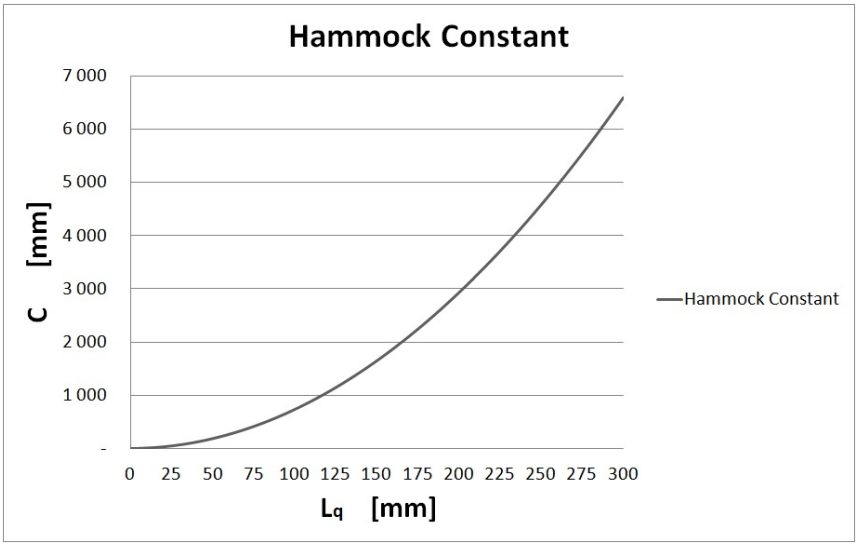

Figure 8.2: The Hammock Constant

For a loading length, l (L_q), equal to 90 mm, and a deformation limit Δh=2.72 mm, it leads to the following value of the *Hammock constant*:

$$C = 90 \cdot \sqrt{\frac{1}{16} \cdot (\frac{90}{2.72})^2 + 1} = 750mm$$

By inserting the derived values into Equation 8.10, it leads to the following value of the characteristic additional capacity coming from the *Hammock effect*:

$$f_{H,90,k} = \frac{2 \cdot 800 \cdot 0.03 \cdot 15}{750} = 0.96MPa$$

The design values of the two capacities, $f_{c,90,k}$ and $f_{H,90,k}$, are found by including the factor that accounts for the load duration and moisture content: γ_M and k_{mod}, respectfully.

$$f_{c,90,d} = k_{mod} \cdot \frac{f_{c,90,k}}{\gamma_M} = 0.8 \cdot \frac{3.18}{1.15} = 2.21MPa$$

$$f_{H,90,d} = k_{mod} \cdot \frac{f_{H,90,k}}{\gamma_M} = 0.8 \cdot \frac{0.96}{1.15} = 0.67MPa$$

By using Equation 8.8 and 8.9, the maximum load, $F_{c,90}$, is calculated.

$$F_{c,90} < (f_{c,90,d} + f_{H,90,d}) \cdot A_{ef} = (2.21 + 0.67) \cdot 13350 = 38449N = 38.5kN$$

The calculation process shown for Case 5, is conducted for all the cases 1-10, which leads to the following values for the different parameters included in the capacity calculations:

Case	Δl_i [mm]	A_{ef} $[mm^2]$	C [mm]	$\varepsilon_{H,j}$ [%]
1	0	8010	750	0
2	20	11570	750	0
3	30	13350	750	0
4	30	13350	750	3
5	30	13350	750	3
6	30	13350	750	3
7	30	13350	750	8
8	30	13350	750	8
9	30	13350	750	8
10	30	13350	750	8

Table 8.7: Parameters to calculate the compression capacity for Case 1-10

The *Hammock constant*, C, used in the capacity calculations to account for the *Hammock effect*, gets a constant value equal to 750 mm, for all cases, since the loading length is constant (equal to 90 mm). The values of the strain concentrations are determined based on the amount of untouched timber, and will vary dependent on the case. For Case 1-3, the lower limit equal to 50 mm will not be satisfied, which leads to a value of the strain concentration equal to 0%. For Case 4-6, there will be enough untouched timber to get a *partly effect*, which results in a value equal to 3.0%. For the remaining cases, a *full effect* of the strain concentration can be used, as a result of the distance from the load to the edges being larger than the upper limit equal to 150 mm.

By inserting the calculated values found in Table 8.7 into the capacity Equation 8.8 and 8.9, and including the load duration and moisture content factors, it leads to the following design values of the total bearing capacities for the two parts:

Case	$f_{c,90,d}$ [N]	$f_{H,90,d}$ [kN]
1	2.21	0.0
2	2.21	0.0
3	2.21	0.0
4	2.21	0.67
5	2.21	0.67
6	2.21	0.67
7	2.21	1.78
8	2.21	1.78
9	2.21	1.78
10	2.21	1.78

Table 8.8: Design values of the compression capacity for Case 1-10

When the system has a small amount of untouched timber, the bearing capacity mainly depends on the pure compressive strength, $f_{c,90,d}$. The size of this value is the same for all the cases, since it is determined by the choice of timber quality. As the length of the sill increases, the additional capacity coming from the *Hammock effect* is mobilized, which gives a larger total bearing capacity. By using Equation 8.8 and 8.9, the value of the maximum compression load perpendicular to the grain can be calculated for the different cases.

Case	$F_{c,90,d}$ [N]	$F_{c,90,d}$ [kN]
1	17720	17.7
2	25595	25.6
3	29533	29.5
4	38449	38.4
5	38449	38.4
6	38449	38.4
7	53310	53.3
8	53310	53.3
9	53310	53.3
10	53310	53.3

Table 8.9: Design load perpendicular to the grain for 1-10

The design load will converge against a value equal to 53.3 kN, since the strain concentration will not increase for cases with untouched timber larger than 150 mm, and the effective loading area has also stabilized at a certain value.

Comparison of the calculation models:
From Example 1 with loading length equal to 90 mm, the results show some variation in the total capacity for the different calculation models. By comparing the results found using the current regulations in EC5-1-1, with the calculation model based on energy (Model 2), the new model allows a greater compressive load where the amount of untouched timber is restricted, with the exception of Case 2. Case 2 gets a smaller capacity, because of the conservative approach where all cross-sections with untouched timber less than 30 mm are calculated with a value of the strength factor equal to 1.0. Up to this limit, the section is assumed to have the same strength properties as the reference block with a fully loaded top surface. For the longer sills, where the capacity is no longer restricted by the amount of untouched timber, the maximum design load will converge towards the exact same value for the two models (44.3 kN). This shows how the generated strength factor, k_1, is able to account for the distribution of the applied load, and a calculation method where an effective area is used, is unnecessary. This effect was taken directly into account when calculating of the total energy of the various systems.

Comparing the results from the calculation model based on strains (Model 1) with the current regulation in EC5-1-1, shows the same capacities for the first three cases. This is the result of a capacity that only relies on the pure compressive strength for both methods when the amount of untouched timber is below a certain limit. As the additional effects starts to mobilize, the total capacity found with the new model based on strains, will be a little higher than the ones found using the regulations given in EC5-1-1. It will get an overall design load that is 23% higher, with the exception of Case 7. In this case, the value is 45% higher with the new calculation model. This is a result of the factor including the *Hammock effect* not taking a value larger then 1.0 with the current regulations, before the amount of untouched timber is larger then 180 mm. The limit that allows a *full effect* of the strain concentrations with the new regulations is 150 mm.

	EC5-1-1	**Model 2**	**Model 1**
Case	$F_{c,90}$ [kN]	$F_{c,90}$ [kN]	$F_{c,90}$ [kN]
1	17.7	17.7	17.7
2	25.6	17.7	25.6
3	29.5	31.3	29.5
4	29.5	32.2	38.4
5	29.5	34.6	38.4
6	29.5	36.4	38.4
7	29.5	38.3	53.3
8	44.3	41.3	53.3
9	44.3	44.3	53.3
10	44.3	44.3	53.3

Table 8.10: Design load perpendicular to the grain for the different capacity models

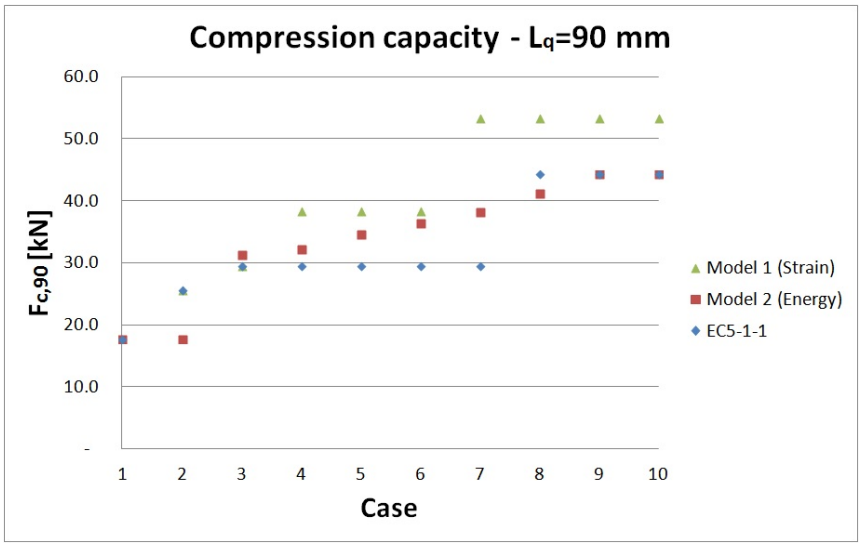

Figure 8.3: Design load perpendicular to the grain for the different calculation models

Example 2:

In this example the loading length, l (L_q), will be kept constant equal to 150 mm, while the amount of untouched timber, a (L_u) will vary. The different lengths can be found in Figure 8.1

Case	h [mm]	b [mm]	l=L_q [mm]	a=L_u [mm]	l_1 [mm]
1	90	89	150	0	0
2	90	89	150	20	20
3	90	89	150	35	35
4	90	89	150	50	50
5	90	89	150	90	90
6	90	89	150	120	120
7	90	89	150	150	150
8	90	89	150	200	200
9	90	89	150	500	500
10	90	89	150	1000	1000

Table 8.11: Geometry and loading configurations - Case 1-10 (Example 2)

The calculation procedures are the same as shown in Example 1, where only the values in the capacity formulas change. Only the final results will be presented in this example, and the parameters used in the calculation of the capacities can be found in Table 8.11. This example has a loading length equal to 150 mm, and to be able include the additional capacity coming from the *Hammock effect*, the condition for the ratio between the loading length and the total deformation needs to be satisfied.

$$\frac{l}{\Delta h} = \frac{150}{2.72} = 55.1 > 30$$

The condition is satisfied, and the *Hammock effect* can be included in the capacity calculations.

A loading length equal to 150 mm, gives the following value of the Hammock constant:

$$C = 150 \cdot \sqrt{\frac{1}{16} \cdot (\frac{150}{2.72})^2 + 1} = 2073mm$$

Comparison of the calculation models:
By using the current and the new capacity models to calculate the maximum compressive load for Case 1-10, it leads to the following results:

	EC5-1-1	**Model 2**	**Model 1**
Case	$F_{c,90}$ [kN]	$F_{c,90}$ [kN]	$F_{c,90}$ [kN]
1	29.5	29.5	29.5
2	37.4	29.5	37.4
3	41.3	52.2	41.3
4	41.3	53.7	45.9
5	41.3	57.7	45.9
6	41.3	60.7	45.9
7	41.3	63.8	53.4
8	62.0	68.8	53.4
9	62.0	73.8	53.4
10	62.0	73.8	53.4

Table 8.12: Design load perpendicular to the grain for the different capacity models

By comparing the results generated from the new calculation model based on energy (Model 2) with the model given in Eurocode 5 part 1.1, it gives a higher capacity for all cases except Case 1 and 2. Case 1 will get the same values since it relies only on the pure compressive strength, while Case 2 will get a smaller capacity as a result of the conservative approach of defining a limit length for the additional capacity equal to 30 mm of untouched timber. The design load will converge towards a value with the current regulation equal to 62 kN, while the new model based on energy (Model 2) will get a value equal to 73.8 kN. This will give an increases capacity equal to 20% for the longest sills.

The new model based on strains (Model 1), will lead to a bearing capacity that is closer to the values found with the current regulations in EC5-1-1. With an amount of untouched timber in the range of 50-150 mm, a small increase in capacity is generated. For the longest sill lengths, the design load will converge towards a value that is 14% smaller.

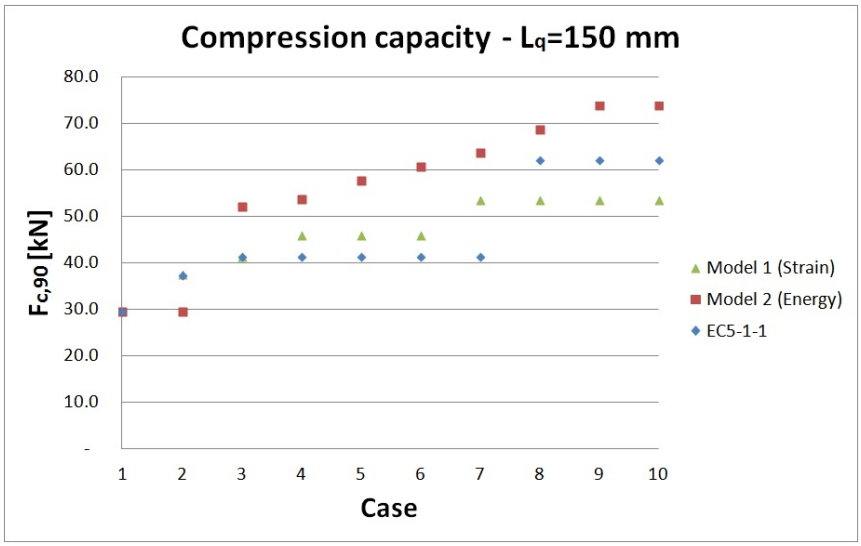

Figure 8.4: Design load perpendicular to the grain for the different calculation models

Example 3:

In this example the loading length, l (L_q), is kept constant equal to 50 mm, while the amount of untouched timber, a (L_u), will vary between the different cases. The different lengths can be found in Figure 8.1

Case	h [mm]	b [mm]	l=L_q [mm]	a=L_u [mm]	l_1 [mm]
1	90	89	50	0	0
2	90	89	50	20	20
3	90	89	50	35	35
4	90	89	50	50	50
5	90	89	50	90	90
6	90	89	50	120	120
7	90	89	50	150	150
8	90	89	50	200	200
9	90	89	50	500	500
10	90	89	50	1000	1000

Table 8.13: Geometry and loading configuration - Case 1-10 (Example 3)

Also in this example, only the final results of the capacities for the different cases will be presented. The lengths used to calculate the different parameters are taken from Table 8.13.

Comparison of the calculation models:
For smaller loading lengths, the calculation method given in EC5-1-1 will result in a larger total capacity for most of the cases in comparison with the model based on energy (Model 2). This is a result of the large contribution that the effective area, A_{ef}, gives for smaller section. The current regulations allow the applied load to be distributed over a loading length that is increased as much as 30 mm on each side. The additional length that the load is distributed over, $(2 \cdot \Delta l_i)$ is 2/3 of the original loading length for this example, and it will provide a significantly larger effect on the total capacity, than the strength factor will give in the new calculation model. The design load will converge towards a value that is 24% higher with the current regulations than with the model based on energy.

When comparing the results found from the model based on strains (Model 1) with the ones found with the model presented in EC5-1-1, it will give equal design loads for Case 1-7. This is because the capacities are only dependent on the pure compression strength for both models at these sill lengths, and the same definition is used for the effective area.

With a loading length equal to 50 mm, the condition based on the ratio between the loading length and the total deformation will not be satisfied.

$$\frac{l}{\Delta h} = \frac{50}{2.72} = 18.4 < 30$$

This will give a capacity that only relies on the pure compressive strength for the cases with the new calculation model based on strains (Model 1). Contributions from additional effects such as the *Hammock effect* can not be included in the capacity calculations, since the condition is violated. This will lead to a capacity that is 33% smaller for longest sills with the new calculation model based on strains compared to the current regulations.

	EC5-1-1	**Model 2**	**Model 1**
Case	$F_{c,90}$ [kN]	$F_{c,90}$ [kN]	$F_{c,90}$ [kN]
1	9.8	9.8	9.8
2	17.7	9.8	17.7
3	21.7	17.4	21.7
4	21.7	17.9	21.7
5	21.7	19.2	21.7
6	21.7	20.2	21.7
7	21.7	21.3	21.7
8	32.5	22.9	21.7
9	32.5	24.6	21.7
10	32.5	24.6	21.7

Table 8.14: Design load perpendicular to the grain for the different calculation models

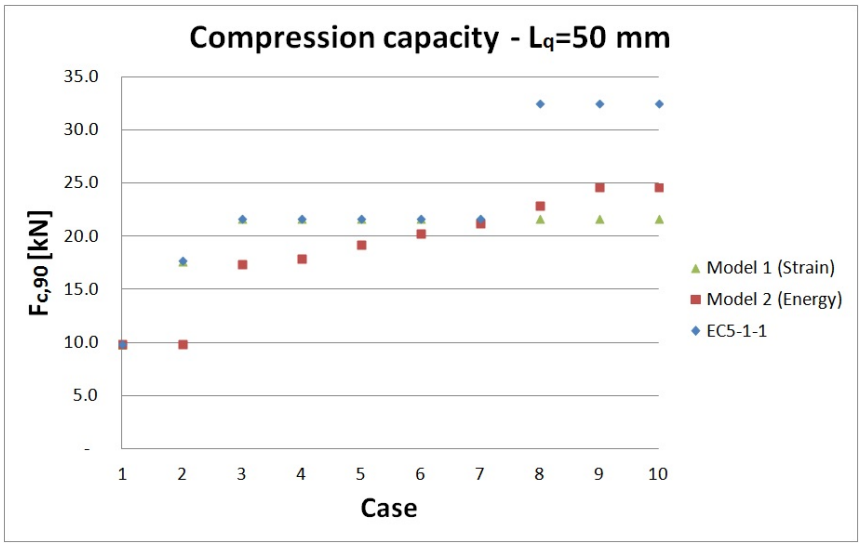

Figure 8.5: Design load perpendicular to the grain for the different calculation models

8.1.2 Custom regulations (3% plastic deformation)

The methods used to calculate the compression capacity for the different models will not change with a custom defined fracture criterion. The main difference is that the value of the compression strength, $f_{c,90}$, and the allowed total deformation underneath the loading area will receive different values. As defined in Section 7.2 the custom limits gives a characteristic compressive strength, $f_{c,90,k}$, equal to 3.43 MPa, and an allowed deformation of 4.62 mm.

The same examples (Example 1, 2 and 3) generated to calculate the capacity with the current regulation will be used in this section as well. Since the method of calculating the design loads, $F_{c,90}$, is identical as previously shown, only the final values of the different examples will be presented. In cases where the calculations methods change, this will be commented on.

Example 1

This example had a loading length, l (L_q), equal to 90 mm, and the following design load is calculated with the custom regulations:

	EC5-1-1	**Model 2**	**Model 1**
Case	$F_{c,90}$ [kN]	$F_{c,90}$ [kN]	$F_{c,90}$ [kN]
1	19.1	19.1	19.1
2	27.6	19.1	27.6
3	31.9	33.8	31.9
4	31.9	34.8	31.9
5	31.9	37.4	31.9
6	31.9	39.3	31.9
7	31.9	41.3	31.9
8	47.8	44.5	31.9
9	47.8	47.8	31.9
10	47.8	47.8	31.9

Table 8.15: Design load perpendicular to the grain for the different calculation models

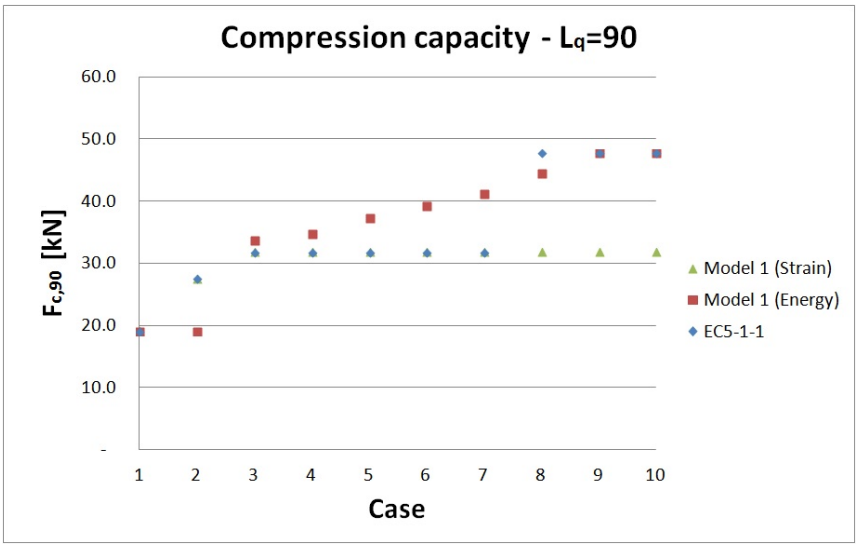

Figure 8.6: Design load perpendicular to the grain for the different calculation models

By looking at the comparison between the design values calculated with EC5-1-1 and the model based on energy (Model 2), the ratio between the two will not change. The only factor that changes with the custom regulations for the two models, is the value of the compressive strength, and this change is equal for both cases. The values of the design load perpendicular to the grain calculated for the two models, is 7.3% higher then the ones given in Table 8.10, as a result of the increased value of compressive strength, $f_{c,90}$.

The main change that comes from using the custom fracture limit, is the design values found with the calculation method based on strains (Model 1). Since the allowed deformation underneath the loading area has changed to 4.62 mm, it will generate a violation of the condition of the ratio between the loading length and deformation for this example.

$$\frac{l}{\Delta h} = \frac{90}{4.62} = 19.4 < 30$$

This leads to a total capacity where the load is carried only by the pure compressive strength of the cases. This will lead to values of the bearing capacity that are lower with the custom limits (3%), than with the current regulations (1%) for the model based on strains (Model 1).

Example 2

This example has a loading length, l (L_q) equal to 150 mm, and the calculation of the capacity leads to the following design loads for the different cases:

	EC5-1-1	**Model 2**	**Model 1**
Case	$F_{c,90}$ [kN]	$F_{c,90}$ [kN]	$F_{c,90}$ [kN]
1	31.9	31.9	31.9
2	40.3	31.9	40.3
3	44.6	56.3	44.6
4	44.6	57.9	54.8
5	44.6	62.3	54.8
6	44.6	65.5	54.8
7	44.6	68.8	71.7
8	66.9	74.2	71.7
9	66.9	79.6	71.7
10	66.9	79.6	71.7

Table 8.16: Design load perpendicular to the grain for the different calculation models

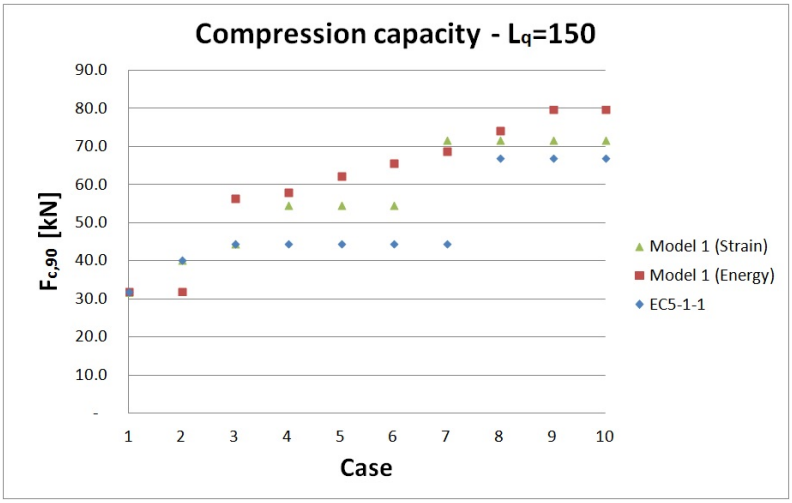

Figure 8.7: Design load perpendicular to the grain for the different calculation models

As described in Example 1 with the custom fracture limit, the ratio between the values found with EC5-1-1 and the model based on energy (Model 2) will not change. The main aspect that changes in this example, is the value of the design load calculated with the model based on strains (Model 1). With a loading length equal to 150 mm, the condition based on the ratio between the loading length and deformation will be satisfied.

$$\frac{l}{\Delta h} = \frac{150}{4.62} = 32.47 > 30$$

Since the condition given above is satisfied, the additional bearing capacity coming from the *Hammock effect* can be included. By allowing a total deformation underneath the loading area equal to 4.62 mm, it will change the value of the *Hammock constant*, C, that is included in the capacity model based on strains (Model 1).

$$C = 90 \cdot \sqrt{\frac{1}{16} \cdot (\frac{90}{4.62})^2 + 1} = 1227mm$$

By allowing a larger deformation, the factor C will take a smaller value, and the contribution from the *Hammock effect* will increase (see Equation 8.11). This will lead to a higher total capacity with the new calculation model based on strains compared to the model given in EC5-1-1.

Allowing larger deformations underneath the loading area it requires larger loading lengths to be able to include the additional capacity coming from the *Hammock effect*. This leads to an extra safety of the calculation of the bearing strength, if the custom limits should be allowed to be used instead of the current regulations. However, when the loading length has reached a certain size, and the ratio condition is satisfied, the capacity will be significantly larger with the custom regulations than with the current ones. This because the contribution from the additional capacity coming from the *Hammock effect* will increase with a less conservative deformation limit (will give a smaller value of the *Hammock constant*, which will result in a larger contribution from the additional term $f_{H,90}$).

Example 3

This example has a loading length, l (L_q) equal to 50 mm, and the calculated design values equals:

	EC5-1-1	**Model 2**	**Model 1**
Case	$F_{c,90}$ [kN]	$F_{c,90}$ [kN]	$F_{c,90}$ [kN]
1	10.6	10.6	10.6
2	19.1	10.6	19.1
3	23.4	18.8	23.4
4	23.4	19.3	23.4
5	23.4	20.8	23.4
6	23.4	21.8	23.4
7	23.4	22.9	23.4
8	35.0	24.7	23.4
9	35.0	26.5	23.4
10	35.0	26.5	23.4

Table 8.17: Design load perpendicular to the grain for the different calculation models

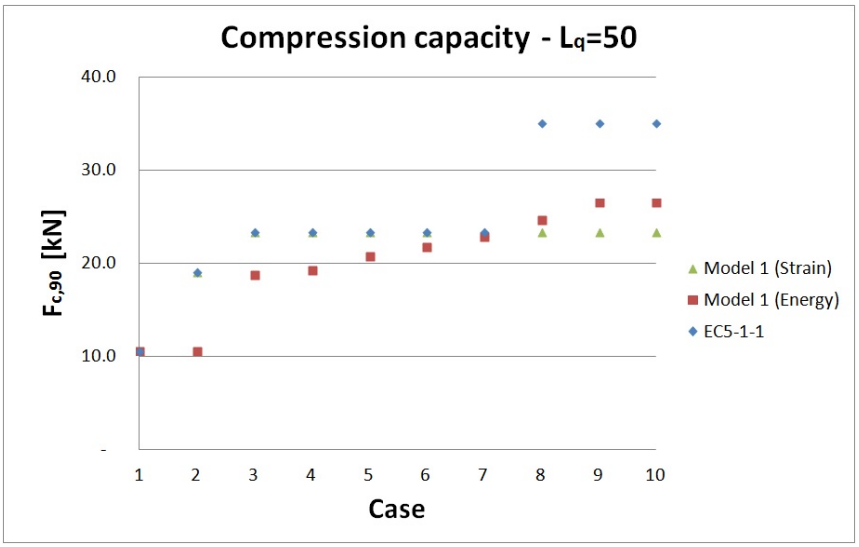

Figure 8.8: Design load perpendicular to the grain for the different calculation models

With a loading length equal to 50 mm, the ratio condition between the loading length and deformation will not be satisfied, and the additional capacity from the *Hammock effect* can not be included. This will lead to a total capacity that is only dependent on the compressive strength $f_{c,90,d}$, and values that are smaller for the new calculation model based on strains, compared with what the model in EC5-1-1 gives. The ratio between the model based on energy and the current model in the Eurocode, will stay the same.

8.2 Serviceability Limit State (SLS)

The new model for calculating in Serviceability Limit State will also be tested through constructed examples. This will provide an overview of the validity and usage of the model. The formula used in the calculations, is not dependent on the cross-section height, width or loading length, and the results change only by altering the amount of untouched timber, L_u and applied load $F_{c,90}$. The three examples will have the following values:

Example	a (L_u) [mm]	$F_{c,90}$ [kN]
1	100	10
2	200	26
3	500	60

Table 8.18: Geometry and applied load for the constructed examples

Example 1
This example will have an amount of untouched timber equal to 100 mm, which means that the *lower case* needs to be used in the serviceability calculations. By inserting the correct values from Table 7.19, into Equation 7.19, it results in the following deformation:

$$\Delta = -\frac{1}{0.71} ln(1 - \frac{10000}{28813}) = 0.57mm < \Delta_{max}$$

By applying a load perpendicular to the grain with magnitude 10 kN, it will produce deformations that is lower than the defined limit, Δ_{max}, found with both the current- and custom regulations, with values respectfully $\Delta_{max} = 2.72mm$ and $\Delta_{max} = 3.55mm$ (Table 7.19). Which means that the system can withstand the applied load of 10 kN, without violating the serviceability limits.

Example 2
In this example, the *lower case* given in Table 7.19 needs to be used, since L_u is less than 250 mm. By applying a compressive load perpendicular $F_{c,90} = 25kN$, it results in a deformation underneath the loading area equal to:

$$\Delta = -\frac{1}{0.71} ln(1 - \frac{26000}{28813}) = 3.10mm < \Delta_{max}$$

The deformation exceeds the limit that is defined with the current regulation, which is equal to 2.72 mm. By using the custom regulations, the deformation will be within the serviceability limit, and a load perpendicular to the grain equal to 28 kN can be applied to the system.

Example 3

For the last example the amount of untouched timber will be equal to 500 mm, which is above the critical limit of 250 mm. This means that the *upper case* in Table 7.20 can be used in the Serviceability Limit State calculations.

By applying a load equal to 60 kN, it gives the following deformation:

$$\Delta = -\frac{1}{0.32} ln(1 - \frac{60000}{72330}) = 5.53mm < \Delta_{max}$$

For the *upper case* the deformation limit equals $\Delta_{max} = 4.62mm$ with the current regulations, and 5.60 mm for the custom. This means that an applied load with magnitude 60 kN, violates the current regulations, but is within the given limit defined by the custom regulations.

Chapter 9

Discussion

Various parameters have been derived in this thesis, which have been used to calculate the compression capacity of timber sills loaded perpendicular to the grain. The values of the parameters used in the capacity calculations, are only meant to give an overview of the different sizes, and more research needs to be conducted to be able to ensure that the correct values have been found. Some of the strength factors have been determined by looking at the load-deformation curves from the different tests directly. Since only a few number of tests were conducted for each type of specimen, a certain degree of inaccuracy in the results must be expected. Increasing the amount of tests will result in more accurate parameters that represent the material behaviour better.

No test has been conducted with varying loading lengths or cross-sectional widths during this thesis. These two parameters can introduce other failure effects that have not been taken into account in the calculation models derived in this thesis. When the loading length is decreased to a very small area, it may lead to a failure where the load is cutting rapidly through the sill, which can lead to a significantly smaller capacity of the system. There may also be some problems stemming from the choice of cross-sectional width. When the width is decreasing, it can result in an instability, wherein the capacity is limited by failure mechanisms out of the plane, instead of just the deformations underneath the loading area.

Tests where the load is acting on the edges of the sill, have not been performed during this thesis. In the calculation model based on strains (Model 1), it has been introduced a load location factor that accounts for this configuration, but whether the right values and assumptions have been made should be verified through tests. In the new calculation model based on energy (Model 2), no factor accounting for this situation has been introduced. By assuming a value of the strength factor equal to 1 (Reference case), it will give quite conservative results of the capacity, and a new factor should therefore be derived for this type of configuration.

The different values of the factors derived from the image analysis in ARAMIS, also have some uncertainties. These are factors that make a significant contribution to the additional capacity coming from the *Hammock effect*, and are therefore important to determine accurately. To be able to get as accurate values of the tension height and strain concentrations as possible, all the

specimens were analysed. Many of the specimens showed a consistent result with equal values, and based on these results the parameters were determined. There are also uncertainties related to the chosen value of the Module of Elasticity. This parameter needs to be examined closer, so as to ensure that the correct value is used. A value twice the size of the value perpendicular to the grain was chosen in this paper.

The models derived in this thesis are mainly based on empirical assumptions, where factors have been multiplied with the pure compression strength, to represent the additional bearing capacity from variation in heights, sill lengths and loading lengths. For the capacity model based on strains (Model 1), a mechanical system based on equilibrium is introduced to describe the additional strength coming from the *Hammock effect*. By modelling this effect as a rope system, it will result in a large variation of the additional contribution, when factors such as the loading length is changed. This was taken into account by introducing a ratio condition. This prevented the capacity coming from the *Hammock effect* to converge towards unrealistic values.

The various factors derived in this thesis, were found by conducting compression tests on wood where the annual rings were arranged in a certain direction. From previous tests conducted, it shows how the strength varies with the annual direction [10]. Since the factors accounting for the additional capacities, coming from changes in load and specimens configurations, are scaled parameters, it will most probably lead to the same values as derived in this thesis. When it comes to the definition of the pure compressive strength, this might be a parameter that will change with the orientation of the annual rings, since the load-deformation curves changes. No explanations has been found as to how the Eurocode copes with effects such as these, and from which annual orientation the strength has been determined.

Chapter 10

Conclusion

Two new models have been introduced to calculate the compression capacity of wood perpendicular to the grain in this thesis. The two models have their origins in different approaches, which leads to some differences in the capacity calculations. The problem with the current regulations in the Eurocode, was the inability to describe the change in bearing capacity in an accurate way for different geometries and load configurations. With the current regulations, the capacity gets quite large compared to the new models when the loading length is small, since rules allow an increase of bearing length up to 30 mm on both sides of the loading area. For small loading lengths, this may result in an increase in the bearing length that is larger than the actual loading length. The model based on strains, uses this same definition of the bearing area, but the total capacity is regulated by the contribution from the additional factor $f_{H,90}$. Since the model based on energy (Model 2) does not include a larger bearing length in the capacity formula, it will give results that are not affected by effects like these. The increase in capacity coming from the distribution of the applied load was included directly in the strength factor, k_1, which is based on the total energy needed to get a certain deformation underneath the loading area. For both of the new calculation models, this will result in bearing capacities that are lower than the ones calculated with the Eurocode regulations for smaller loading lengths.

The results from the tests conducted to find the effects of different cross-sectional heights on the total bearing capacity, showed that the height did not contribute to the overall strength in any significant way for systems with height larger than 30 mm. This is in agreement with the conclusions drawn by Blass and Görlacher.

For larger loading lengths, the model based on energy (Model 2) will give a capacity that is higher than the ones calculated with the current regulations. With the current calculation model in Eurocode 5, the traditional building method here in Norway does not fulfil the requirements, which is odd since no major faults or problems have been recorded in these types of connections. It is therefore reasonable to believe that the new calculation model gives a more correct description of the bearing capacity of a timber sill loaded perpendicular to the grain, than the current model. One of the goals of this thesis, was also to derive a calculation method that in a better way included the different geometry and load configuration of sills. This is taken more into account by the new calculation model, which can be seen in the results from

the generated examples. The model based on energy provides a stable increase in the capacity for various amount of untouched timber, while the current model increases erratically when the additional factors are included.

This thesis suggests changing the fracture criterion by allowing a deformation that is three times larger than the current regulations. By allowing a tripling of the deformation limit, it resultes in an increase of the compression strength, $f_{c,90}$, equal to 7%. The reason for this small increase, is that wood loaded perpendicular to the grain has a material behaviour (load-deformation curve) that stabilizes quickly when entering the plastic domain. Indications have also been found that the compressive strength given in the documentation of the wood used in this thesis is quite conservative. The value calculated in this paper is 15% larger, and by allowing the custom limits as well, it will give a compressive strength that is 22% higher then what is used today. This may be one of the problems with the current calculation method, which leads to regulations that the Norwegian building methods are not currently satisfying.

The benefit of using the new failure criterion, is that it allows a greater deformation underneath the loading area. From the analysis of the material behaviour generated from the compression test, it was shown how the material can withstand deformation up to 8-9 mm without any failure mechanisms occurring. The current regulations allow a deformation in the range of 2-3 mm, which is quite conservative, taken the material behaviour into account. The same result was also found by Riberholt [10], and he suggested that the limits should be increased by a factor of 10. This is a little higher than the value found in this thesis (a factor of 3 was found in this thesis, which could be used and still be within the deformation limits where the first failure mechanisms occurred). By allowing a deformation three times larger, it will give more tolerance when calculating in Serviceability Limit State, but the contribution to the bearing capacity in Ultimate Limit State will be less significant. The factors taking the system configurations into account, derived in the new calculation models, were not affected in any significant way by the change in deformation limit.

The model derived for Serviceability Limit State calculations has its limitations, but it provides the opportunity for a designer to chose a desired deformation and load in a connection, and check if it is within the valid limits. In today's regulations, there are no distinct formulas to use in serviceability state calculations, and this state is only accounted for by changing some parameters in the Ultimate Limit State equation. The calculation model derived in this thesis in serviceability state will provide results that are not violating the bearing capacity of the timber, and the calculated deformations will always be on the safe side of the fracture limit.

10.1 Further work

In order to determine more accurate values for the different parameters in the new calculation models, a larger number of compression tests should be conducted. Tests should also be performed where the load is acting on the edges, to verify if the assumptions made in this thesis are correct for this type of configuration.

Different wood types should be tested, so as to see if the suspicion regarding the compressive strength given in the current regulations being too conservative is true, which was found to be the case for Norwegian CE G40C (GL32c) in this thesis.

It should also be verified if the new capacity models derived in this thesis are applicable for other systems than continuously supported timber sills, such as systems with compressive forces acting on both sides.

Large amounts of data describing the behaviour of a timber sill loaded perpendicular to the grain have been generated during this thesis, which can be used in further research. This data is stored at the Department of Structural Engineering (KT) at the Norwegian University of Science and Technology (NTNU).

Bibliography

[1] Signe Kierkeaard Cain, Moelven Industrier ASA - Gode Rom Magasin: *Det som bærer huset*, http://torebodalimtra.org/no/Tema/Det-som-barer-huset/, 2010

[2] Hans Larsen and Vanhik Enjily: *Practical design of timber structures to Eurocode 5*, Thomas Telford Limited, 40 Marsh Wall, London, 2009

[3] Eivind Skaug, FOKUS på tre Nr. 40: *Trevirkets oppbygning og egenskaper*, Trefokus AS og Treteknisk, ISSN 1501-7427 Opplag 3000/04/07

[4] Leijten, Jorissen and Leijer: *The local bearing capacity perpendicular to grain of structural timber elements*, University of Technology Eindhoven, Faculty of Architecture, 2011

[5] L. Bleron, L. Denaud, R. Collet and R. Marchal: *Experimental study of locally loaded timber in compression perpendicular to the grain*, P21A - Commitee of technical and construction equipment standardization office (BNTEC).

[6] A. Leijten and Dennis Schoemakers : *Bearing strength perpendicular to grain of timber*, University of technology Eidenhoven, Netherlands.

[7] van Der Put: *Derivation of the bearing strength perpendicular to the grain of locally loaded timber blocks*, Faculty of Civil Engineering and Geo-sciences. Timber structures and wood technology. Netherlands, Juli 2008

[8] K. Steen: *Changes around holed in Glulam beam strengthened with self-tapping screws*, Department of Structural Engineering. Norwegian University of Science and Technology (NTNU) . Norway, Trondheim, 2012

[9] A. Hardeng: *The bearing capacity of locally loaded beams and sills for compression perpendicular to the grain*, Universitetet for Miljø- og Biovitenskap. Instituttet for matematiske realfag og teknologi. Ås, Norway, 2011

[10] J. Persson: *Numerical analyses of compression perpendicular to the grain in Glulam beams with and without reinforcement*, Department of Construction Science. Structural Mechanics. Lund University. Sweden, 2011

[11] K. A. Malo, J. Siem og P. Ellingsbø: *Quantifying ductility in timer structures*, Department of Structural Engineering and Department of Architecture design, History and Technology. Norwegian University of Science and Technology (NTNU), Trondheim, Norway, 2011

[12] A. J. M. Leijten, S. Franke, P. Quenneville og R. Gupta: *Bearing Strength Capacity of Countinous Supported Timer Beams: Unified Approach of Test Methods and Structural Design Codes*, Journal of Structural Engineering Vol. 138 Nr. 2, Eindhoven Univ. of Technology, Eindhoved Netherlands, Februar 2012

[13] Eurocode 5, part 1-1 - Norsk Standard - *Design of timber structures - General Common rules and rules for buildings*: NS-EN 1995-1-1:2004+A1:2008+NA:2010, November 2004

[14] Norsk Standard -*Timber structures - Glue laminated timber - Strength classes and determination of characteristic values.* NS-EN 1194, 1st issue, September 1999

[15] Norsk Standard -*Structural timber -Strength classes.* NS-EN 338:2009, September 2009

[16] Norsk Standard - *Timber structures - Structural and glue laminated timber - Determination of some physical and mechanical properties.* NS-EN 408:2010+A1:2012. June 2012

[17] Fridtjov Irgens - *Formelsamling - Mekanikk.* 3rd issue, Trondheim, January 2003

Chapter 11

Appendix

Written appendix

Appendix A - Test set-up
Appendix B - *Stages* used for the different specimens in ARAMIS
Appendix C - Strength properties for Norwegian CE L40C

Electronic appendix

CD with PDF version of the thesis, test data, calculations, figures and pictures.

11.1 Appendix A - Test set-up

Based on the new capacity models derived in this thesis, several parameters needed to be determined. At the Department of Construction Engineering at NTNU, it has during this thesis been conducted compression tests of timber sills in full-scale. The cross-section geometry of the specimens, has been chosen based on earlier research, and from own assumptions to be able to determine the various parameters need in the new capacity models

Large amounts of data on the behaviour of timber sills loaded in compression perpendicular to the grain was generated during this thesis. This data consists of strains, stresses and deformations patterns in x-,y-,z-direction during different load steps, and found by using ARAMIS, which is an analysing tool that uses images to describe the material behaviour. Data describing the material behaviour was generated both underneath and on the side of the loading area.

The notations of the axes used in the analysis of the specimens is chosen so the x-axes follows the longitudinal direction for the wood, y-axes the traverse and z-axes the direction of the width of the specimens. The duration of the tests is chosen so that the fracture limit is reached within 300 seconds (5 min), a value recommended in NS-EN 408:2010+A1:2012 [16].

Material:
Wood type: GL32c (Norwegian CE L40C)
Temperature: 20°C
Relative humidity: 65%

Equipment:
Compression machine: INSTRON 5900 Series (100 kN)
Image analysis: ARAMIS - Optical 3D Deformation Analysis
Spray paint: White: CRC Crick 130, Black: Hard Hat Rust-Oleum 750°C

Execution:
Reference block
Duration:10 min
Total deformation: 20 mm
Deformation speed: 2 mm/min
Images recorded: 120
Image intervals: 1 image each 5 seconds

Sill
Duration: 15 min
Total deformation: 30 mm
Deformation speed: 2 mm/min
Images recorded: 150
Image intervals: 1 image each 7 seconds

Specimens:

(All lengths in the following tables are given in millimetre [mm])

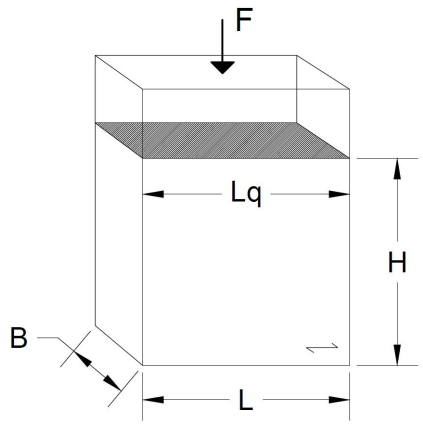

Specimen	H	L_q	L_u	L	B	Amount
R30-i	30	0	90	90	89	4
R60-i	60	0	90	90	89	4
R90-i	90	0	90	90	89	5
R120-i	120	0	90	90	89	4
R150-i	150	0	90	90	89	4

Total amount of tests: 21

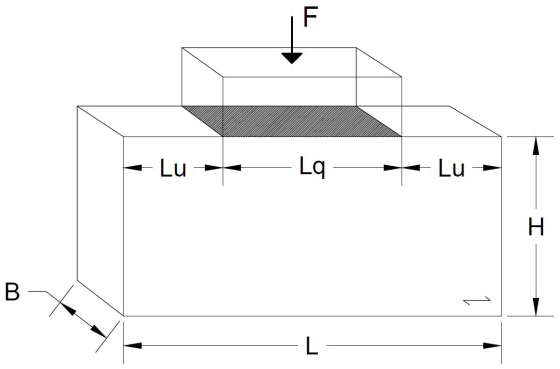

Specimen	H	L_q	L_u	L	B	Amount
Lu30-i	90	90	30	150	89	3
Lu50-i	90	90	50	190	89	5
Lu70-i	90	90	70	230	89	3
Lu100-i	90	90	100	290	89	3
Lu150-i	90	90	150	390	89	3
Lu200-i	90	90	200	490	89	3

Total amount of tests: 20

11.2 Appendix B - *Stages* (ARAMIS)

To be able to find the correct values of the different parameters used in the new capacity model based on strains (Model 1), it was defined *stages* where the allowed total deformation underneath the loading area was generated for the different specimens. The *stages* used for the different specimens are summarized in the table underneath.

	Current regulations	**Custom regulations**
Lu	*Stage*	*Stage*
30-1	25	40
30-2	21	33
30-3	17	27
50-1	22	34
50-2	19	31
50-3	22	44
50-4	16	28
50-5	22	34
70-1	18	32
70-2	22	34
70-3	16	29
100-1	24	50
100-2	21	48
100-3	25	36
150-1	23	35
150-2	21	32
150-3	no result	no result
200-1	24	36
200-2	21	33
200-3	21	32

11.3 Appendix C - Norwegian CE L40C

The type of timber used in this thesis is Norwegian CE L40C, which has approximately the same strength properties as GL32c given in NS-EN 1194 [14].

MOELVEN

KARAKTERISTISKE FASTHETER
LIMTRE OG SMALT LIMTRE

	Egenskap/enhet		Limtre CE L40C	Smalt Limtre - splittet i to deler	Smalt Limtre - splittet i tre deler
Bøyning	$f_{m,k}$	N/mm²	30,8	28	24
Strekk	$f_{t,0,k}$	N/mm²	17,6	17,6	17,6
	$f_{t,90,k}$	N/mm²	0,4	0,4	0,4
Trykk	$f_{c,0,k}$	N/mm²	25,4	25,4	25,4
	$f_{c,90,k}$	N/mm²	2.7 (5.7*)	2.7 (5.7*)	2.7 (5.7*)
Skjær	$f_{v,k}$	N/mm²	3.5 **	3.5 **	3.5 **
Elastisitetsmodul	$E_{0,\text{mean}}$ deformasjonsberegning	N/mm²	13 000	12 500	12 500
	$E_{0,05}$ stabilitetsberegning	N/mm²	10 500	10 000	10 000
	$E_{90,\text{mean}}$ deformasjonsberegning	N/mm²	410	410	410
Skjærmodul	$G_{0,\text{mean}}$	N/mm²	760	760	760
Densitet	ρ_k styrkeberegning	kg/m³	400	400	400
	ρ_{mean} lastberegning	kg/m³	470	470	470

*) skal KUN benyttes sammen med NS3470-1:1999/A1:2008 pkt. 12.1.4 Trykk på tvers av fiberretning. Dette som alternativ metode til EK5 pkt. 6.1.5

**) sprekkfaktor k_{cr} iht EK5 pkt 6.1.7 settes lik 0.80

For fasthetsverdier for våre øvrige produkter; Moelven S-bjelken og Kerto henviser vi til gjeldende Tekniske Godkjenninger:

S-bjelken **TG 20040**

Kerto-S **TG 2142**

Versjon 2, november 2012

Gode rom